



BARION - BARION - POTENTIALS IN ONE - BOSON - EXCHANGE MODEL

DISSERTATION

SUBMITTED IN PARTIAL FULFILMENT OF THE REQUIREMENTS
FOR THE AWARD OF THE DEGREE OF

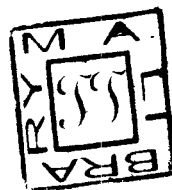
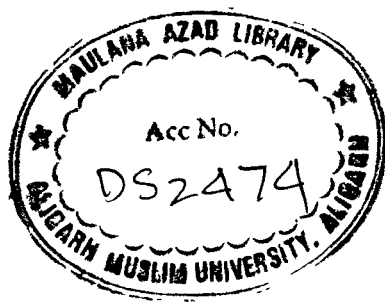
Master of Philosophy
IN
PHYSICS

BY

MOHAMMAD SAJJAD ATHAR

DEPARTMENT OF PHYSICS
ALIGARH MUSLIM UNIVERSITY
ALIGARH (INDIA)

1992



TO

MY

MUMMI & PAPA

PROFESSOR



DEPARTMENT OF PHYSICS

ALIGARH MUSLIM UNIVERSITY


ALIGARH 202002 (India)

Tele No. : 9001

Tel. No. : 564 230 AMU IN

C E R T I F I C A T E

Certified that Mr. Md. Sajjad Athar has carried out the research on 'Baryon-Baryon Potentials In One-Boson-Exchange Model' under my supervision and the work is suitable for submission for the award of the degree of Master of Philosophy.


(S.K. Singh)
Supervisor

A C K N O W L E D G E M E N T

I am greatly indebted to my Teacher and Supervisor Prof.S K. Singh who took tremendous pain to go through the every bit of my work and has been kind enough to share my agony during the whole period of the M.Phil incubation.

I feel immense pleasure to acknowledge the help given by Prof.M.Z. Rehman Khan, whose personality has also been a constant source of inspiration for me.

I am grateful to Dr.M.Shoeb for his co-operation. Thanks are also due to Ms.Nasira Neelofer and Ms.Najma Bano, my colleagues, for their constant encouragement.

It would be incomplete if I do not express my gratitude to my friends, Md.Parwaiz, Moshahid A Rizvi, Raashid Nehal and Iqbal, Rooshi and Kiki, my brother and sisters, who have been showering the sublime affection from where-ever they are.

Customarily, U.G.C. is acknowledged for the grant of Junior Research Fellowship.

Last but not the least, I am obliged to the Chairman, department of Physics for providing me the basic facilities to carry out the M.Phil. work.

Md. Sajjad Athar/13-11-82
MOHAMMAD SAJJAD ATHAR

C O N T E N T S

Page Nos.

CHAPTER - 1

Introduction

1

1.1 . The Nucleon - Nucleon Interactions

1.2 . Hypernuclei

1.3 . Production of Hypernuclei

1.4 . Hyperon - Nucleon Interaction

(a) Λ N Interaction

(b) Σ N Interaction

(c) Ξ - N and Λ - Λ Interaction

Tables

Figures

References

CHAPTER - 2

Nucleon - Nucleon Potential

37

Introduction

2.1 . Brief review of some older

N - N potentials

2.2 . Hamada and Johnston Potential

2.3 . Reid Hard and Soft Core Potentials

2.4 . Argonne Potential

Figure

References

CHAPTER - 3 Field Theoretical Approach

68

Introduction

3.1 . Yukawa Potential

3.2 . Post Yukawa field Theoretic approaches

3.3 . The Bonn Potential

Figures

References

CHAPTER - 4 Experimental Studies on Λ - N interaction

96

Introduction

4.1 . Binding Energy of the Λ particle in
Nuclear Matter

4.2 . Λ - N Scattering

(a) Scattering Length and Effective range

(b) Phase shifts

4.3 . Hypernuclear Decays

4.3.1 . Weak hypernuclear decays

4.3.2 . Electromagnetic decays

CHAPTER - 5 Λ - N - Interaction

143

Introduction

5.1 . Model of Gal , Soper and Dalitz

5.2 . Model of Nijmegen group

5.3 . Model of Bodmer et.al.

5.4. Model of Rahman Khan et.al.

Chapter - 6 $\Sigma - N$, $\Xi - N$ and $\Lambda - \Lambda$ Potentials

183

Introduction

6.1 . Σ - Nucleon Interaction

6.2 . Ξ - Nucleon Interaction

6.3 . $\Lambda - \Lambda$ Interaction

CHAPTER - 7

Summary and Conclusions

201

CHAPTER - 1

Introduction :-

In this dissertation we have discussed the Baryon - Baryon interaction in One- Boson - Exchange potential model. The term Baryon - Baryon interaction is used here to mean the nucleon - nucleon, hyperon - nucleon, and hyperon-hyperon interactions. The properties of the nucleons and the hyperons have been tabulated in Table - 1.

In the nucleon - nucleon case the data originate from the study of nuclei as well as from the scattering experiments on nucleons. However, in the hyperon - nucleon case the investigations based on scattering experiments are hampered due to the short life - time of the hyperons. Therefore, the information about the hyperon - hyperon interaction and hyperon - nucleon interaction is obtained from the study of the hypernuclear properties. Initially due to the lack of the experimental data, the study of hypernuclei was at slow pace. With the discovery of hypernuclear resonances and hypernuclear gamma rays, a new era in the study of hyperon - nucleon interaction or hyperon - hyperon interaction started.

In this chapter, we shall present a discussion of the nucleon - nucleon interactions and an introduction to hypernuclei. In the hypernuclear study, the production mechanism and a brief introduction to predictions of the different hyperon - nucleon interactions will be given.

In Chapter - 2, the various proposed phenomenological potentials for the nucleon - nucleon interactions will be discussed. The predictions of the different different potentials will be compared with

the experimental data on the deuteron and nucleon - nucleon phase shifts. Specifically we will discuss the various phenomenological nucleon - nucleon potentials viz. Hamada -Johnston, Reid Hard and Soft core, Paris and Argonne potentials.

In Chapter - 3, the field theoretical model of nucleon - nucleon potential better known as "The Bonn Potential" will be discussed in some detail.

In Chapter - 4, the various experimental data on hypernuclei e.g. binding energy, decays and Λ - N scattering are presented and the information about Λ - Nucleon interaction obtained from these data is discussed.

In chapter - 5, we discuss the Λ -nucleon potential. The various phenomenological Λ -Nucleon potentials of Gal et.al., Nagels et.al., Bodmer et.al. and Khan et.al. are discussed.

In Chapter-6 other hyperon - nucleon potentials viz. Λ - Λ , Σ - N, Ξ - N potentials are discussed in some detail., where the experimental and phenomenological analyses of these potentials have been made .

In Chapter - 7, a summary of the present study and the conclusions that can be deduced from this work are given .

1.1 The Nucleon - Nucleon Interactions

It is now well known that the nucleus is made up of nucleons and the pions mediate the interaction between the nucleons. Yukawa⁽¹⁾ suggested that the range of the nuclear force could be identified with the mass of a particle exchanged by a pair of interacting nucleons. If two interacting particles exchange a meson of mass m , then the maximum range of the force

associated with that particle will be of order \hbar/mc . Therefore, he concluded that the mass of the exchanged meson could be inferred from the known range of the nucleon - nucleon force. The discovery of the π -meson and its role in the nucleon - nucleon force, led, ultimately, to the One-boson-exchange nucleon-nucleon force, or the one - boson -exchange potential. Neglecting the neutron-proton mass difference, the neutron and the proton can be treated as the two possible charge states of the same particle, the nucleon⁽²⁾. We write the nucleon N as a two-component vector in isospin space i.e.

$$N = \begin{pmatrix} \alpha \\ \beta \end{pmatrix}$$

$$\text{with } p = \begin{pmatrix} 1 \\ 0 \end{pmatrix} \quad \text{and } n = \begin{pmatrix} 0 \\ 1 \end{pmatrix}$$

By direct analogy with spin, \vec{S} , the isospin \vec{T} is introduced. The nucleon carries isospin $\frac{1}{2}$, and the third component, T_3 has the eigenvalues $+\frac{1}{2}$ (the proton) and $-\frac{1}{2}$ (the neutron):

$$p = \left| \frac{1}{2} \frac{1}{2} \right\rangle, \quad n = \left| \frac{1}{2} -\frac{1}{2} \right\rangle$$

Thus the proton is "isospin up" and the neutron is "isospin down". Therefore, the total isotopic spin for two nucleons can then either be $T = 0$ (antisymmetric under the exchange of the two nucleons) or $T = 1$ (symmetric under interchange) (Table 2).^(3,4)

According to Pauli principle an allowed state of two nucleons must be antisymmetric under the simultaneous exchange of space, spin and isotopic spin. There is enough evidence that the strength of nuclear forces is same in nn, np and pp states.

Therefore, for the interaction potential there are two basic

criteria which should be fulfilled:

(a) the charge independence requires that the interaction potential $V(\vec{r})$ should be the same in all states of the same space - spin symmetry;

(b) the interaction potential $V(\vec{r})$ must be a scalar in isotopic spin . It is conveniently written as

$$V = V_0 P_0 + V_1 P_1 ,$$

where P_0 and P_1 are the projection operators onto the two - nucleon states with $T = 0$ and $T = 1$ respectively . For two nucleons,

$$P_0 = \frac{1 - \vec{\tau}_1 \cdot \vec{\tau}_2}{4}$$

$$P_1 = \frac{3 + \vec{\tau}_1 \cdot \vec{\tau}_2}{4}$$

where $\vec{\tau}_i$ is the isotopic spin operator for the i^{th} nucleon, the operators $\vec{\tau}$ are simply the Pauli spin matrices in isotopic - spin.

The original idea of Yukawa of a scalar field interacting with nucleons was extended to vector field by Proca⁽⁵⁾ and then to pseudoscalar and pseudovector fields by Kemmer⁽⁶⁾.

In the 1950s ,the one-pion-exchange potential became well established for the long range part ($r \geq 2$ fm, r is the distance between the centres of the two nucleons) of the nuclear force, the evidence of which came from small - angle NN scattering experiments and the deuteron properties⁽⁸⁾. The different pieces of evidence for the one - pion - exchange have been re-examined by Ericson and Rosa-Clot⁽⁹⁾.

For the intermediate ($1\text{fm} < r < 2\text{fm}$) and the short ($r < 1\text{ fm}$) range multipion exchanges and the exchange of heavier mesons have been considered. In the intermediate range the two - pion exchange is most important, although heavier meson exchange (like ω) also becomes relevant^(10,11). The three - pion - exchange has not been found to be very significant due to the short range ($\sim \frac{h}{3m_{\pi}c} \sim 0.47\text{fm.}$) *

This region is masked by a repulsive core which is introduced phenomenologically⁽¹²⁾. After the discovery of several heavier mesons and resonances, the study of nucleon- nucleon interaction entered into the modern era. Breit⁽¹³⁾ and Sakurai⁽¹⁴⁾ have independently suggested that a meson of spin 1 could explain the repulsive core in the nucleon - nucleon potentials. The ρ - meson ($T = 1$) and the ω - meson ($T = 0$) have $J = 1$ and decay into two and three π - mesons, respectively. A third meson, the η - meson, has $T = 0$, $J = 0$. The contribution of the two π - meson exchange corresponds to two uncorrelated π - meson, whereas that from ρ, ω, η , etc., correspond to bound pion state contribution,. The properties of the different mesons have been tabulated in Table - 3.

Various studies on the energy level structure of nuclei shows the presence of spin - orbit force in the nucleon- nucleon interaction. Tzoar et.al.⁽¹⁵⁾ were the first, who gave a favourable spin - orbit interaction from the meson - theoretical description. Later Breit and Sakurai⁽¹³⁾ have also suggested that a meson of spin 1 could explain the spin - orbit interaction in the nucleon - nucleon potentials . A schematic figure of nucleon - nucleon potentials is presented in fig. 1.

1.2 Hypernuclei

Strange particles including the Λ - hyperons participate in the strong interaction. If at low energies this interaction is of attractive nature, we can expect the formation of a nucleus containing a Λ -hyperon (also Σ -hyperon, Ξ -hyperon and Λ - Λ hyperon). Such nuclei are called hypernuclei. The first hypernuclei was found in 1953 by the Polish scientist Danysz and Pniewski⁽¹⁶⁾ who observed the decay of hypernucleus in nuclear emulsions. The event observed by them has been schematically shown in fig. (2). In fig (2), from the point A where a fast proton has reacted with Ag or Br nuclei, which were present in the emulsion, besides the normal tracks of protons and α -particles, a thick track is tapering towards the end and corresponds to a hypernucleus⁽¹⁷⁾. From the parameters of this track it was established that it belonged to a Boron-nucleus having atomic number 5. Due to the large ionization losses this nucleus decelerated rapidly and came to halt in about 10^{-12} sec at the point B. After the halt the nucleus splitted into a proton, an α -particle and a π -meson with a total kinetic energy $Q > 40\text{Mev}$.

At present a large number of hypernuclei are known which have been shown in fig.(3).⁽¹⁸⁾

The discovery of Λ hypernuclei was followed by the calculations of the charge, mass, lifetime, decay energy and the energy of separation⁽¹⁹⁾.

The charge of the hypernuclei is calculated from the ionization and life time τ by a comparison with time during which the ionization losses occur for the nuclei which decay in flight. The lifetime

τ of the hypernuclei was to be lying in the interval $10^{-11} < \tau < 10^{-12}$ sec.⁽²⁰⁾

From the known masses of particles M_i and their kinetic energy T_i , the mass of the hypernucleus can be calculated. The expression for the mass is given by

$$M_{HY} = \sum_i (M_i + T_i)$$

The binding energy of Λ in the ground is given by⁽¹⁹⁾

$$B_{\Lambda} (g.s.) = (M_{core} + M_{\Lambda} - M_{HY}),$$

where M_{core} is the mass of the nucleus in the ground-state after the removal of the Λ -particle.

The kinetic energy E_{kin} of the $1s$ - state for $A \gg 1$ and $R = 1.2 A^{1/3}$ fm using a square well potential is given by⁽²¹⁾

$$E_{kin} = \left[V - B_{\Lambda} (g.s.) \right] \frac{\pi^2 \hbar^2}{2MR^2} = 118 A^{-2/3} \text{ MeV.}$$

The decay energy is calculated from the kinetic energy of the decay products, which in turn is calculated with the help of range energy formula :

$$T_x = \alpha \left[\frac{m_x}{m_p} \right]^{1-n} Z_x^{2n} R_x^n,$$

where T_x is in MeV, R_x is in micron, α and n have values 0.25 and 0.58 respectively. It has been found out that the decay energy/accompanied by the escape of π -meson is about 40 Mev.

1.3 Production of Hypernuclei

After the initial discovery of hypernuclei many hypernuclei have been

proposed and studied at various laboratories. The main processes, by which these hypernuclei are produced are given below:

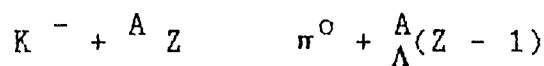
(a) Strangeness Exchange Reaction

(b) Electromagnetic Production

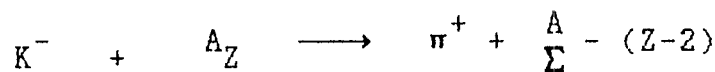
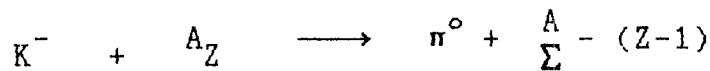
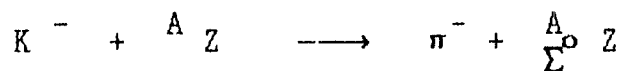
(c) Associated Production

(a) Strangeness Exchange Reaction using Kaon beams ⁽²²⁾

(a) The examples of formation of Λ hypernuclei are :



(b) The examples of formation of Σ hypernuclei are :



(c) The examples of formation of Ξ hypernuclei are :



the strangeness exchange reactions further can be categorized into two, the

first one is " Recoilless Λ production" and the other is "Quasi-free production"⁽²⁰⁾. For example the reaction $K^- + n \longrightarrow \pi^- + \Lambda$ on a neutron inside the nucleus has been extensively used for the hypernucleus formation. When the pions are emitted at 0° , the recoil momentum (longitudinal) depends on the K^- momentum as has been tabulated in Table (4). As it is clear from the table (4) that for the Kaon momentum between 300 and 1000 MeV/c, the recoil of the Λ particle is less than 100 MeV/c, where as the Fermi momentum of nucleon is of the order of 250 MeV/c. Therefore, we can say that there exists a greater probability of forming a hypernucleus.

For the Kaon momenta of more than 500 MeV/c with small reaction angles the transverse recoil momentum of the Λ particle is given by

$$q_T \approx 2\vec{p} \sin \frac{\alpha}{2},$$

where α is the small value of the reaction angle, \vec{p} is the momentum of the Kaon and the emitted pion i.e. $\vec{p} \approx \vec{p}_K \approx \vec{p}_\pi$. We have depicted the reaction in fig (4).

In the (K^-, π^-) reaction there exist a greater probability that a neutron in the nucleus will be replaced by the Λ particle without changing the wavefunction. This type of reaction is known as "Recoilless Λ production", which is a coherent or, say, elastic process. States populated by recoilless Λ production are known as strangeness exchange resonances, which are very much excited and are fixed in a continuum. The recoilless Λ - production has been schematically shown in fig (5a).

However, the greater contribution to the strangeness exchange

reaction comes from the incoherent or, say inelastic processes due to the fact that the total cross-section for kaons and pions at momenta larger than 500 MeV/c is only 30 millibarns which leads to stronger absorption. This helps in the recoilless production from a small portion of the nuclear surface.

However, from the many possible incoherent processes the reaction of our interest will be only those in which the strangeness exchange is accompanied by the neighbouring orbits without any additional interaction of kaons or pions with the nucleus. This is known as quasifree production and has been illustrated in fig. (5b).

(b) Electromagnetic - Production of Hypernuclei

As discussed earlier most of the informations on hypernuclei are obtained from $A(K^-, \pi^-)_{\Lambda}A$ reaction. But there are certain disadvantages of the (K^-, π^-) reaction viz⁽¹³⁾:

- (i) It excites strongly only the natural parity hypernuclear states.
- (ii) Due to the absorption of K^- as well π^- strongly in the nucleus there arise many complexities when reaction mechanism and the absorption are considered.
- (iii) Since, the low spin states (natural parity) dominate the spectrum at forward angles, therefore, the reaction emphasizes the spectroscopy of such states.
- (iv) A limited information on the structure of the hypernucleus is obtained from (K^-, π^-) reaction.

Therefore, there was need of an alternative approach. Consequently, various reaction have been proposed⁽²⁴⁻²⁸⁾ and two of them

have been studied in detail :

(i) the (π^+, K^+) and (ii) the (γ, K^+) & $(e, e' K^+)$.

First of all the electromagnetic production of hypernuclei will be discussed which are $A(\gamma, K)_{\Lambda}A$ and $A(e, e' K)_{\Lambda}A$ reaction involving nuclear targets A and final - state hypernucleus $_{\Lambda}A$. These have been schematically shown in fig (6).

The electromagnetic production of hypernuclei through (γ, K^+) and $(e, e' K^+)$ reaction has been proposed at the new generation of electron accelerators such as CEBAF. The study of the (γ, K^+) reaction at CEBAF is expected to enhance significantly our understanding of processes involving strange hadrons and coupling of photon to the baryon.

Two possible experimental scenarios have been found to be suitable for hypernuclear studies at Continuous Electron Beam Accelerator Facility (CEBAF):

(i) the $(e, e' K^+)$ at finite (but small) outgoing electron and K or angles, and

(ii) the (γ, K^+) or $(e, e' K^+)$ at a 0° outgoing electron angle.

It has also been proposed to get an associated high resolution K^+ spectrometer to have the electromagnetic production of hypernuclei⁽³⁰⁾. The Bates electron accelerator, when extended to 1 GeV could also be used to explore the (γ, K^+) process near its threshold of $k_{lab} = 909.6$ MeV/c.

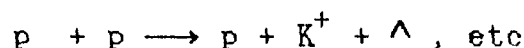
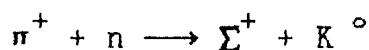
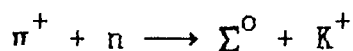
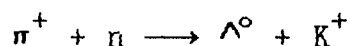
The $A(e, e' K^+)_{\Lambda}A$ reaction excites both the natural and un-natural parity, low and high spin hypernuclear states with comparable strength. Since, the electron and the K^+ meson are weakly absorbed in the nucleus, therefore, the complexity of the nuclear reaction is less.

In the $\gamma + p \longrightarrow K^+ + \Lambda$ reaction or $\pi^+ + n \longrightarrow K^+ + \Lambda$ the transferred momenta to the nucleus is very high (larger than the Fermi momentum). Therefore, for these reactions probable bound hypernuclear states are expected in high spin configurations.

A schematic representation of possible states involved in the reaction $^{12}\text{C} (\gamma, K^+) ^{12}\text{B}$, has been shown in figure (7). This representation shows how a nucleus - to - hypernucleus transition occurs. Here in fig (7), proton in the target nucleus (^{12}C) is replaced by a lambda in its effective potential well.

There are advantages of the $(e, e'K^+)$ reaction over the (γ, K^+) reaction like the information obtained from photon reaction is limited due to the same photon energy and momentum whereas it is not the case with $(e, e'K^+)$ reactions. However there is no experimental data available to us on $(e, e'K^+)$ reaction. We are mentioning the plots for some of the experimental data on (γ, K^+) reaction which is available to us and shown in fig (8,9,10) (31).

(c) Associated Production The examples of such type of reaction is



The associated production in most of the cases is denoted by (π^+, K^+) reaction due to its extensively usefulness in the hypernuclear production. After the theoretical studies of Dover et. al. (32) the Associated production of Λ hypernuclei by the (π^+, K^+) reaction was

proposed. Now a days it is widely studied⁽³³⁻³⁶⁾. The first experimental work was started at AGS., with the Moby Dick spectrometer. At PILAC (LOS ALAMOS) and also at KEK the work is in progress to get an intense beam of pions to study the hypernuclear production through (π^+, K^+) reaction. There are certain advantages of (π^+, K^+) reaction over the $(K^-, \bar{\pi})$ reaction like the high spin state is favoured by the form factor of the (π^+, K^+) reaction.

As far as the associated production is concerned there is no magic momentum and $q > 350$ MeV/c and the elementary cross-section is maximum near $p \approx 1050$ MeV/c. Due to the longer mean free path for K^+ in the nuclear matter the distortion for the outgoing wave is reduced and the reaction is less peripheral in nature. In the BNL experiment a series of Λ single - particle states in light - to - heavy hypernuclei have been obtained. Till now the achieved experimental energy resolution is 3 MeV. The efforts are going on at KEK to reduce the resolution to 1 MeV.

At PILAC (LOS ALAMOS) attempt is going on to extract the precise spin - orbit splittings for Λ . Also from this facility the details of levels structures which reflect the various components of the $\Lambda - N$ interaction (like $\vec{\sigma}_N \cdot \vec{\sigma}_\Lambda$) can be obtained. The prediction of the existence of super-symmetric states which manifest a characteristic aspect of the nuclear many-body systems with Pauli-free hyperon can also be confirmed from the PILAC experiments.

The most important characteristic of the (π^+, K^+) reaction is that not only the highest spin state

$$\left[{}^0f_{7/2}^{-1}, {}^{\Lambda}f_{7/2} \right]_J = 6^+ \quad \text{but also}$$

other stretched states

$$\left[{}^0f_{7/2}^{-1} (nl)^{\Lambda} \right]_{J_{\max}} \quad \text{with } (nl)^{\Lambda}$$

being $0s_{\Lambda}$, $0p_{\Lambda}$ and $0d_{\Lambda}$ are preferentially populated and, therefore, the obtained spectrum shows all the bound Λ orbitals.

With this introduction of hypernuclei we shall now discuss in a little detail the interaction of Λ , Σ , and Ξ with the nucleon and the $\Lambda\Lambda$ interaction.

1.4 Hyperon - Nucleon Interaction

(a) Λ -N Interaction Λ -N interaction can not be described by the One Pion exchange diagram due to the violation of isospin conservation at the left vertex $\vec{T}_{\Lambda} = 0$ while $T_{\pi} = 1$ which has been depicted in fig (11). The lightest exchangeable mesons are K (496 MeV) and/or the scalar meson (500 MeV), which lead to the short range nature of the Λ -N interaction depicted in figure (12). (17,20)

It has been found out that the depth of the potential well V_0 in the Λ -N case (~ 18.5 MeV) is less than the depth of the well describing the bound (n-p) state in the case of a deuteron.

We compare the energy of separation of a Λ -hyperon from a Λ -nucleus [which is B_{Λ}], on the one hand, and the energy of separation of the nucleons from the corresponding normal nucleus [which is B_N], on the other, we can draw a conclusion similar to the one in the previous paragraph - that a Λ -N interaction is weaker than the N-N interaction.

This can be further illustrated by the fact that the Deuteron binding energy, as we know, is 2.225 MeV while the Λ - N binding energy for a two body system is supposed to be even negative also. Even in a three body system like ${}^3_{\Lambda}\text{H}$ (a Λ n p system), the binding energy is only 0.13 (\pm 0.05) MeV. Hence, the conclusion is that for the Λ - nucleus, $B_{\Lambda} < B_N$.

By assuming the singlet interaction (i.e. $S=0$) in which spins are aligned antiparallel to be stronger than the triplet interaction (i.e. $S=1$) in which spins are aligned parallel the calculation of B_{Λ} is in agreement, which can also be inferred from the fact that the ${}^4_{\Lambda}\text{H}$ and ${}^4_{\Lambda}\text{He}$ hypernuclei have $J^{\pi} = 0^{+}$ ground state and $J^{\pi} = 1^{+}$ excited states. We can understand the difference between the N - N interaction and Λ - N interaction by comparing the value of scattering length and effective ranges tabulated in Table (5). From the data of the effective range it is quite safe to conclude that the inner repulsive core cancels a large part of the outer attraction and makes the remaining attractive tail effectively to be of long range.

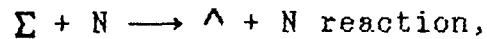
The forward to backward ratio of the Λ - N scattering cross section indicates that the strength of the P - state interaction is roughly half of the strength of the S- State interaction.

Λ particle can be converted to the Σ particle by emitting/absorbing a pion and, therefore, the OPE type interaction with a strong tensor component contributes to the Λ N - Σ N coupling.

B. Σ - N Interactions

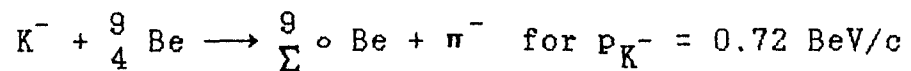
Now we shall come to the Σ - N interaction. Since it is well known

that Σ particles are not stable in nuclear matter and react strongly via the



the Q value for the decay is 80 MeV and it appears that the probability of a Σ hypernuclei formation is less. (37,38)

However, in 1980 the first Σ hypernuclei ${}^9_{\Sigma}\text{Be}$ were observed by proton synchrotron at CERN in the reaction



There is a width $= \Gamma < 8 \text{ MeV}$ at the peak of the energy spectrum of π^- - meson corresponding to the formation of the hypernucleus ${}^9_{\Sigma^0}\text{Be}$. This fact, then, goes on to suggest the presence of certain prohibition on a strong interaction between a Σ^0 - hyperon and the nucleus in the nucleus.

In the later years, more Σ - hypernuclei were formed which have already been referred in fig (3).

The Σ - hyperon has isospin $I = 1$ and couples with a nucleon such that $I = 1/2$ and $3/2$. Therefore, all the complexity of the NN system is present in the ΣN interaction.

C. Ξ -N and Λ - Λ Interaction

The Ξ particles interact in nuclear matter through $\Xi + N \longrightarrow 2\Lambda$ with Q value of 30 MeV and, therefore, it seems that, there exist a little more probability of Ξ - hypernucleus formation. There exist also a large probability of $\Lambda\Lambda$ hypernucleus formation due to the low value of Q and the decay of Ξ into two Λ s. Knowledge of the $\Lambda\Lambda$ interaction depends mainly on the three emulsion events identified with the double hypernuclei ${}^{10}_{\Lambda\Lambda}\text{Be}$, ${}^6_{\Lambda\Lambda}\text{He}$ and ${}^{13}_{\Lambda\Lambda}\text{B}$ respectively (39,40).

The total separation energy of ${}_{\Lambda\Lambda}^{10}\text{Be}$ and ${}_{\Lambda\Lambda}^6\text{He}$ is

$$B_{\Lambda\Lambda} ({}_{\Lambda\Lambda}^{10}\text{Be}) = 17.71 \pm 0.08 \text{ MeV}$$

$$B_{\Lambda\Lambda} ({}_{\Lambda\Lambda}^6\text{He}) = 10.92 \pm 0.6 \text{ MeV}.$$

In the case of Ω particle the interaction with nucleon via $\Omega + N \longrightarrow \Lambda +$ gives Q value of 175 MeV. Therefore, it seems very unlikely that a Ω - hypernucleus will be formed.

TABLE - 1 Properties of the Baryons

BARYONS (Spin $\frac{1}{2}$)

| Baryon | Quark content | Charg | Mass (MeV) | Lifetime (seconds) | Principal decays |
|--------------------------------------|---------------|---------|--------------------|------------------------|------------------------|
| $N \begin{cases} p \\ n \end{cases}$ | uud udd | +1 0 | 938.280 939.573 | ∞ 900 | $p \bar{\nu}_e, \dots$ |
| Λ | uds | 0 | 1115.6 | 2.63×10^{-10} | $p \pi^-, n \pi^0$ |
| Σ^+ | uus | +1 | 1189.4 | 0.80×10^{-10} | $p \pi^0, n \pi^+$ |
| Σ^0 | uds | 0 | 1192.5 | 6×10^{-20} | $\Lambda \gamma$ |
| Σ^- | dds | -1 | 1197.3 | 1.48×10^{-10} | $n \pi^-$ |
| Ξ^0 | uss | 0 | 1314.9 | 2.90×10^{-10} | $\Lambda \pi^0$ |
| Ξ^- | dss | -1 | 1321.3 | 1.64×10^{-10} | $\Lambda \pi^-$ |
| Λ_c^+ | udc | +1 | 2281 | 2×10^{-13} | not established |

BARYONS (Spin 3/2)

| Baryon | Quark content | Charge | Mass | Lifetime | Principal decays |
|------------|--------------------|---------------|------|------------------------|---|
| Λ | uuu, uud, udd, ddd | +2, +1, 0, -1 | 1232 | 0.6×10^{-23} | $N \pi$ |
| Σ^* | uus, uds, dds | +1, 0, -1 | 1385 | 2×10^{-23} | $\Lambda \pi, \Sigma \pi$ |
| Ξ^* | uss, dss | 0, -1 | 1533 | 7×10^{-23} | $\Xi \pi$ |
| Ω^- | sss | -1 | 1672 | 0.82×10^{-10} | $\Lambda K^-, \Xi^0 \pi^-, \Xi^- \pi^0$ |

TABLE 2 : Relation between the Isotopic - Spin and Space - Spin Symmetries
for states of the Two - Nucleon System.

| | $T_z = -1 \left\{ \begin{array}{l} (p,p) \end{array} \right\}$ | $T_z = 0 \left\{ \begin{array}{l} (p,n) \end{array} \right\}$ | $T_z = 1 \left\{ \begin{array}{l} (n,n) \end{array} \right\}$ |
|---------|--|---|---|
| $T = 1$ | Space - Spin Antisym. (I - spin sym) | (Space - Spin Antisym) (I - spin sym) | (Space - Spin Antisym) (I - spin sym) |
| $T = 0$ | — | (Space - Spin Sym.) (I-spin Antisym) | — |

Table 3 : Properties of the Mesons

PSEUDOSCALAR MESONS (spin 0)

| Meson | Quark content | Charge | Mass | Lifetime | Principal decays |
|--------------------------|--|----------|---------|---|---|
| π^\pm | $u\bar{d}, d\bar{u}$ | $+1, -1$ | 139.569 | 2.60×10^{-8} | $\mu\nu_\mu$ |
| π^0 | $(u\bar{u} - d\bar{d})/\sqrt{2}$ | 0 | 134.964 | 8.7×10^{-17} | $\gamma \gamma$ |
| K^\pm | $u\bar{s}, s\bar{u}$ | $+1, -1$ | 493.67 | 1.24×10^{-8} | $\mu\nu_\mu, \pi^\pm \pi^0, \pi^\pm \pi^\pm \pi^\pm$ |
| K^0, \bar{K}^0 | $d\bar{s}, s\bar{d}$ | 0, 0 | 497.72 | $\left\{ \begin{array}{l} K_S^0 \ 0.892 \times 10^{-10} \\ K_L^0 \ 5.18 \times 10^{-8} \end{array} \right.$ | $\pi^+ \pi^-, \pi^0 \pi^0$ $\pi e \nu_e, \pi \mu \nu_\mu, \pi \pi \pi$ |
| η | $(u\bar{u} + d\bar{d} - 2s\bar{s})/\sqrt{6}$ | 0 | 548.8 | 7×10^{-19} | $\gamma\gamma, \pi^0 \pi^0 \pi^0, \pi^+ \pi^- \pi^0$ |
| η' | $(u\bar{u} + d\bar{d} + s\bar{s})/\sqrt{3}$ | 0 | 957.6 | 3×10^{-21} | $\eta \pi \pi, \rho^0 \gamma$ |
| D^\pm | $c\bar{d}, d\bar{c}$ | $1, -1$ | 1869 | 9×10^{-13} | $K \pi \pi$ |
| D^0, \bar{D}^0 | $c\bar{u}, u\bar{c}$ | 0, 0 | 1865 | 4×10^{-13} | $K \pi \pi$ |
| F^\pm (now D_s^\pm) | $c\bar{s}, s\bar{c}$ | $+1, -1$ | 1971 | 3×10^{-13} | not established |
| B^\pm | $u\bar{b}, b\bar{u}$ | $+1, -1$ | 5271 | $\left\{ \begin{array}{l} 14 \times 10^{-13} \\ 6 \times 10^{-23} \end{array} \right.$ | $D + ?$ |
| B^0, \bar{B}^0 | $d\bar{b}, b\bar{d}$ | 0, 0 | 5275 | | |
| η_c | $c\bar{c}$ | 0 | 2981 | | $KK\pi, \eta \pi \pi, \eta' \pi \pi$ |

VECTOR MESONS (Spin 1)

| Meson | Quark content | Charge | Mass | Lifetime | Principal decays |
|------------|---|--------------|------|-----------------------|---------------------------------------|
| ρ | $u\bar{d}, d\bar{u},$ $(u\bar{u} - d\bar{d})/\sqrt{2}$ | +1, -1, 0 | 770 | 0.4×10^{-23} | $\pi^+ \pi^-$ |
| K^* | $u\bar{s}, s\bar{u}, d\bar{s}, s\bar{d}$ | +1, -1, 0, 0 | 892 | 1×10^{-23} | $K \pi$ |
| ω | $(u\bar{u} + d\bar{d})/\sqrt{2}$ | 0 | 783 | 7×10^{-23} | $\pi^+ \pi^- \pi^0, \pi^0 \gamma$ |
| ϕ | $s\bar{s}$ | 0 | 1020 | 20×10^{-23} | $K^+ K^-, K^0 \bar{K}^0$ |
| J/ψ | $c\bar{c}$ | 0 | 3097 | 1×10^{-20} | $e^+ e^-, \mu^+ \mu^-, 5\pi, 7\pi$ |
| D^* | $c\bar{d}, d\bar{c}, c\bar{u}, u\bar{c}$ | +1, -1, 0, 0 | 2010 | $> 1 \times 10^{-22}$ | $D\pi, D\gamma$ |
| Υ | | 0 | 9460 | 2×10^{-20} | $\tau^+ \tau^-, \mu^+ \mu^-, e^+ e^-$ |

Table 4 : The dependence of the recoil momentum (longitudinal)
on the K^- - momentum at 0° .

| | | | | | | |
|----------------------------|-----|-----|-----|-----|-----|-----|
| K^- momentum (MeV/c) | 0 | 100 | 300 | 500 | 700 | 900 |
| Λ Momentum (MeV/c) | 250 | 190 | 70 | 0 | 40 | 80 |

Table 5 : The value of scattering length and Effective range in the case
of $\Lambda - N$ and $N - N$ interaction

| | $^1 S_0$ | | $^3 S_1$ | |
|----------------------------------|---------------|---------|---------------|---------|
| | $\Lambda - N$ | $N - N$ | $\Lambda - N$ | $N - N$ |
| Scattering length (a) (in fm) | -2.3 | -23.7 | -1.9 | 5.42 |
| Effective range (r) (in fm) | 3.2 | 2.74 | 3.4 | 1.77 |

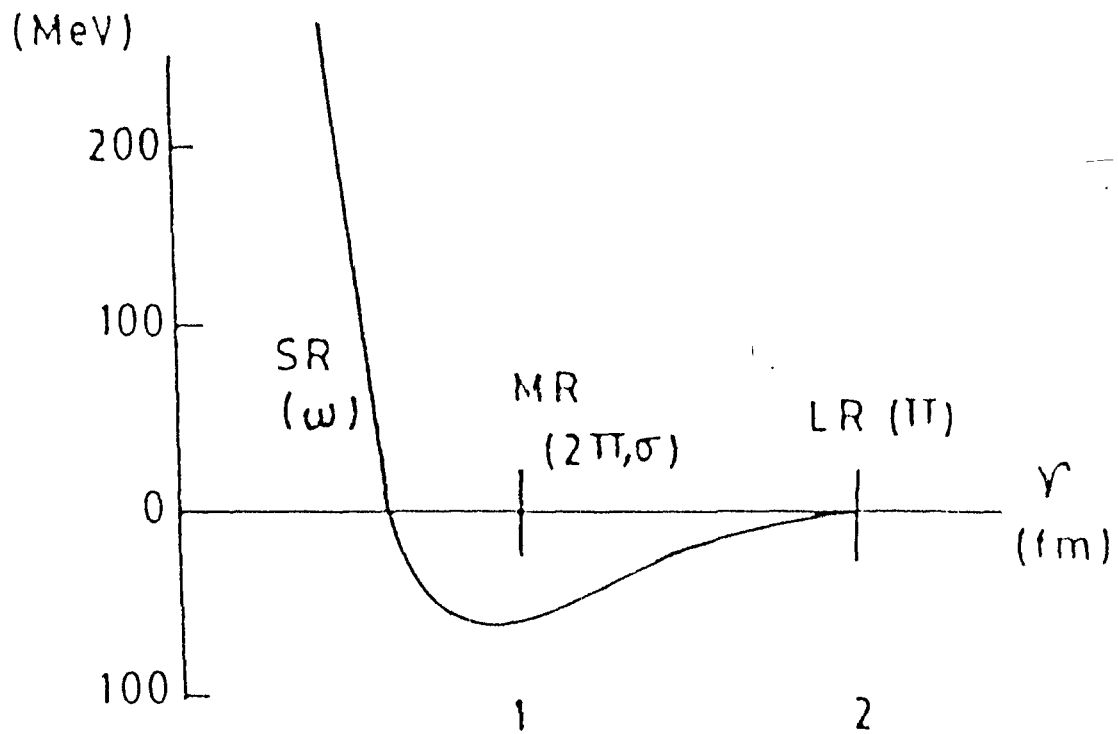


Figure 1: Shape of the central force for the 1S_0 NN State. The long-range, intermediate-range, and short-range parts of the potential are identified, along with the important mesons in each region.

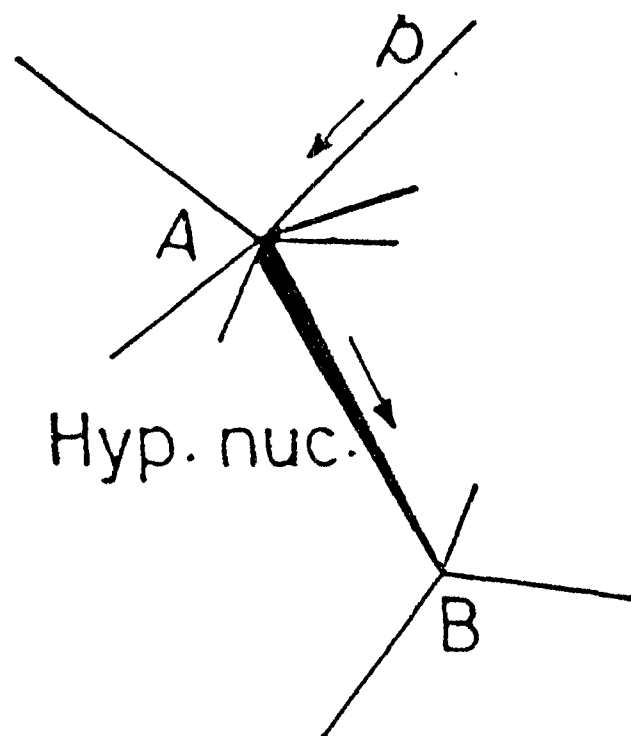
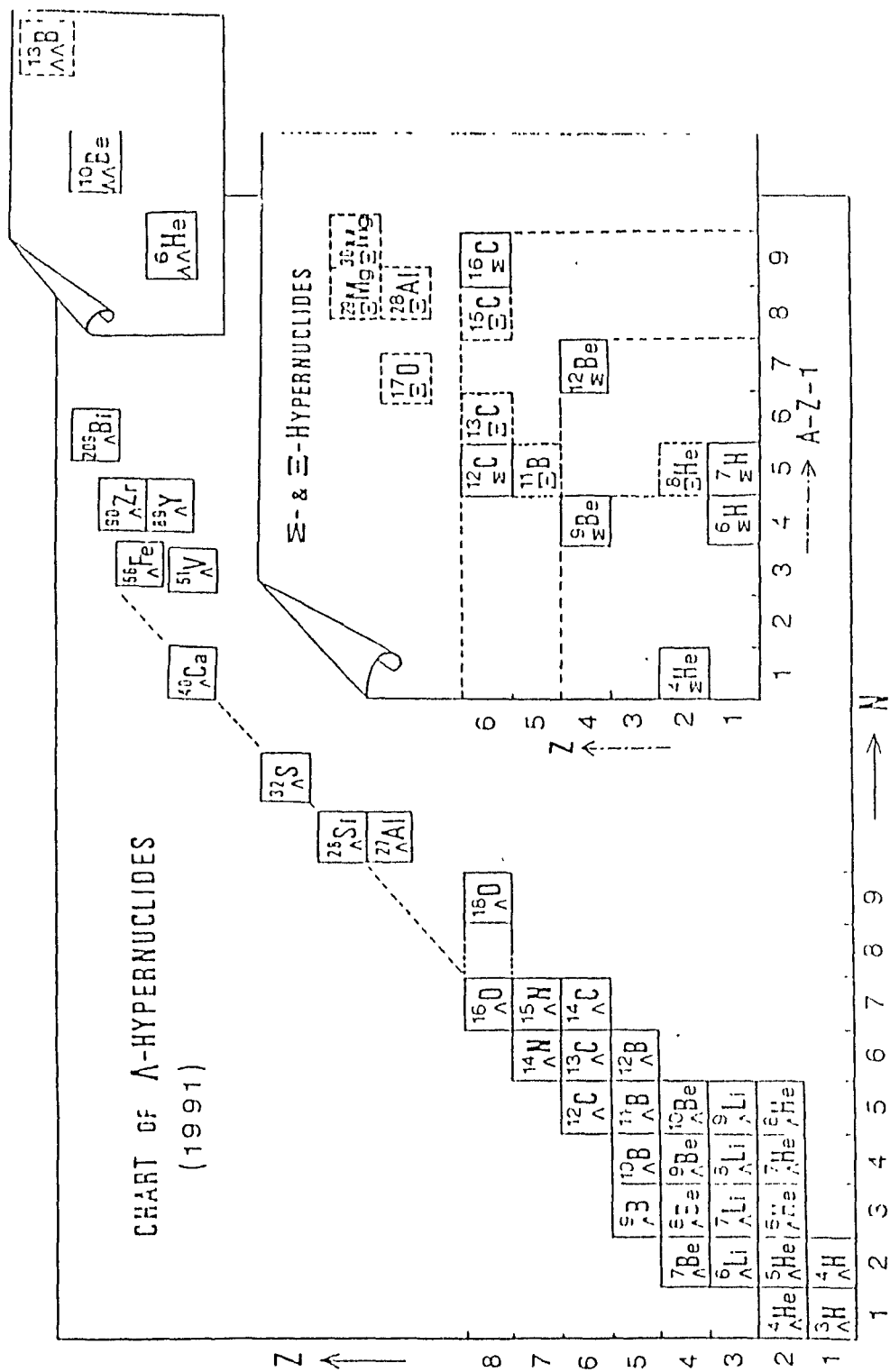


Figure 2: Schematic representation of the event observed by Danysz and Pniewshi.



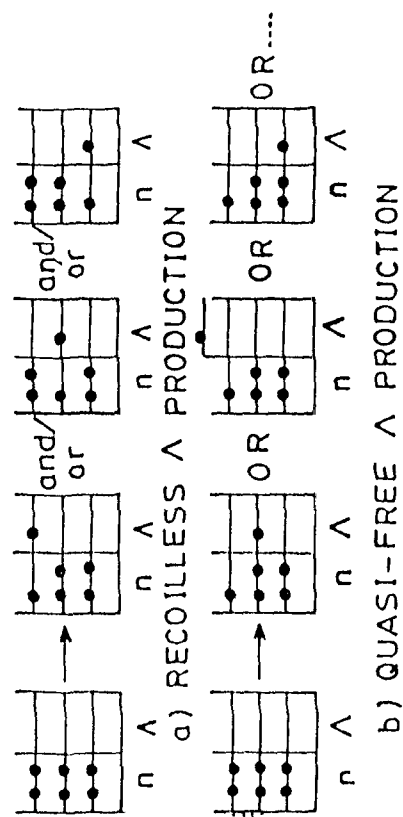


Figure 5a,b) Recoilless and quasifree production is shown schematically.

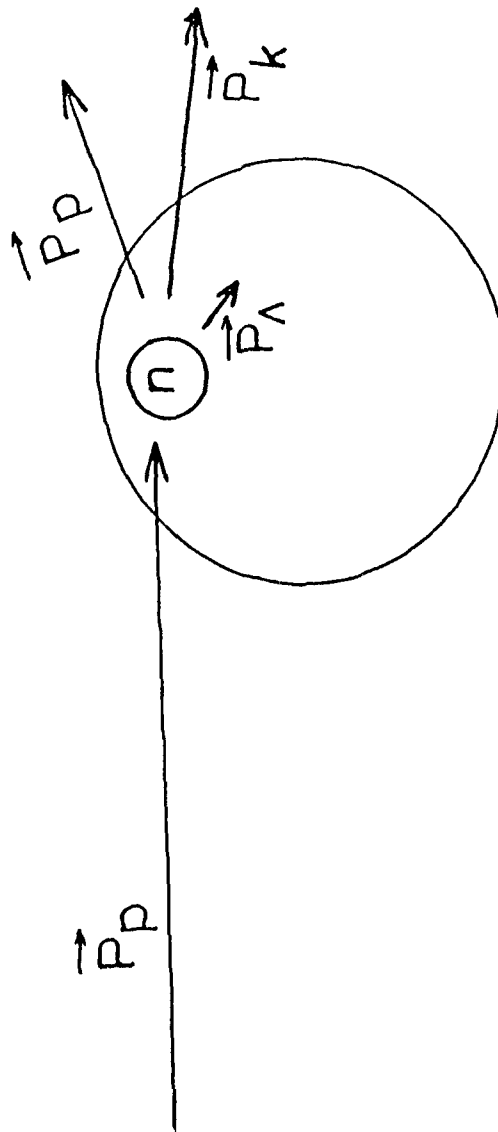


Figure 4: In the associated production the momenta of the proton and K^+ have to be measured in order to determine the Λ recoil.

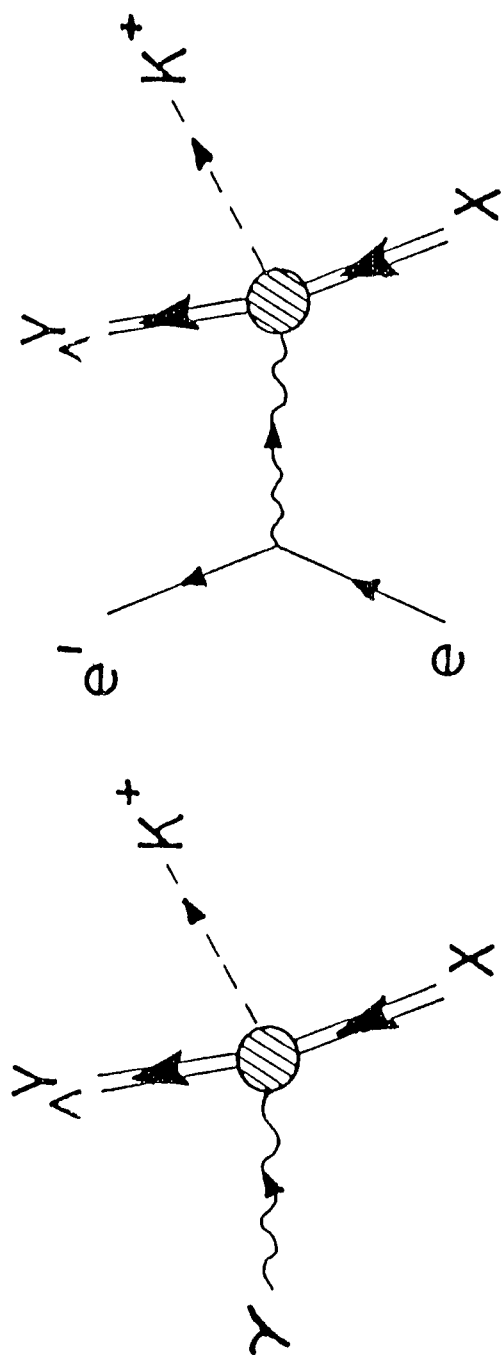


Figure 6: Diagrams for photo $^-$ and electro-production of Λ^Y .
Kaons from nuclei (X) leading to hypernuclei (Λ^Y).

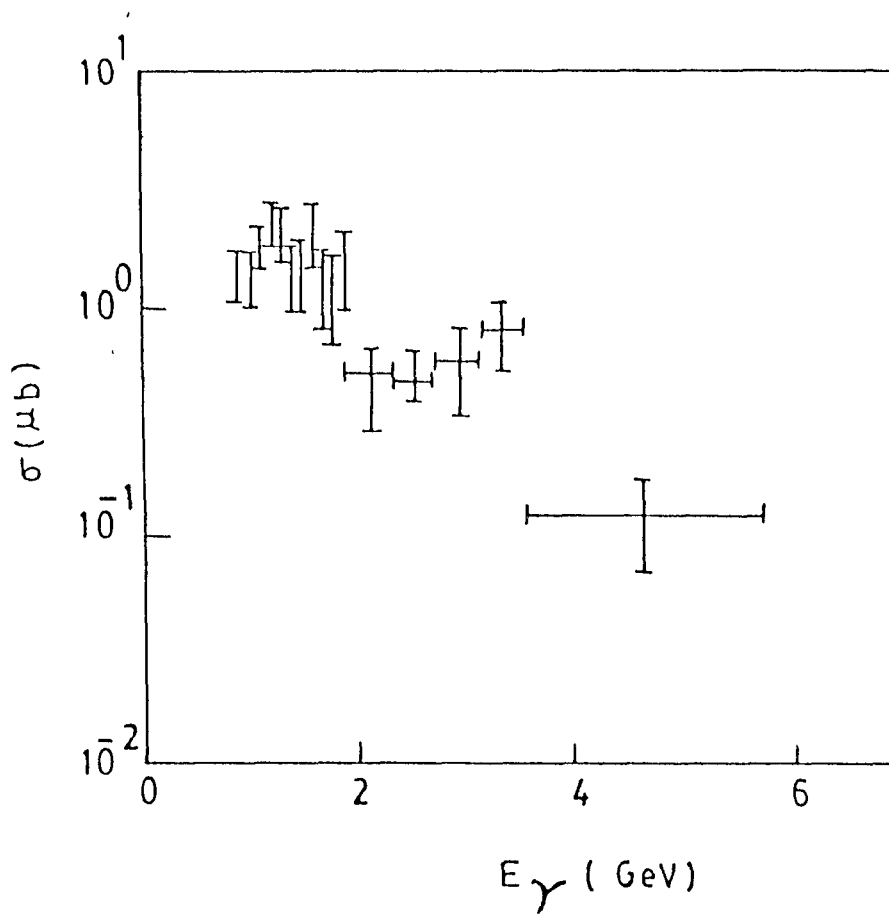


Figure 8: Total $\gamma p \rightarrow \Lambda^0 K^+$ cross-section as a function of laboratory photon energy E_γ .

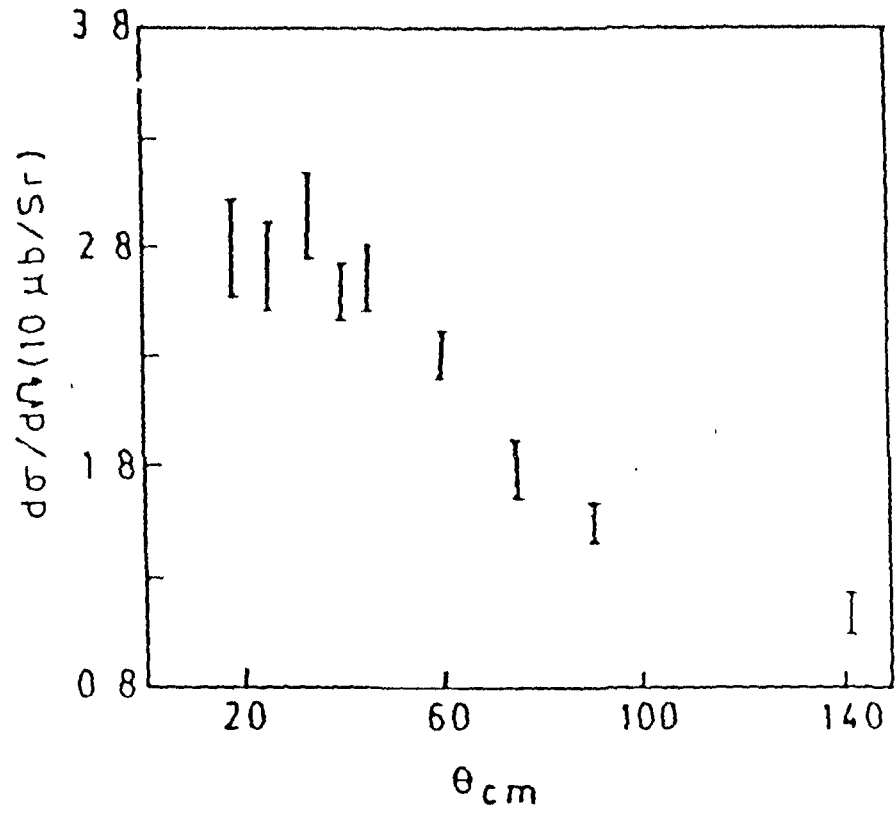


Figure 10: $\Xi^0 + p \longrightarrow K^+ + \Lambda$ cross sections at $k_L = 1.4 \text{ GeV}/c$.

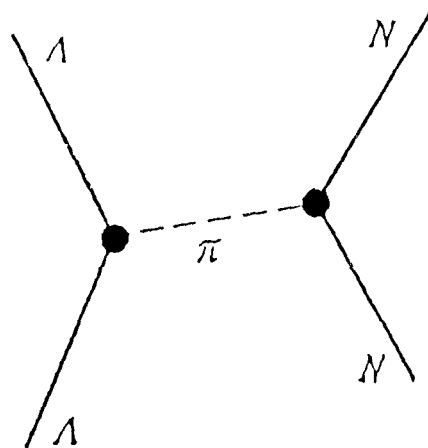


Figure 11: ΛN interaction cannot be described by a one-pion diagram of the type shown here.

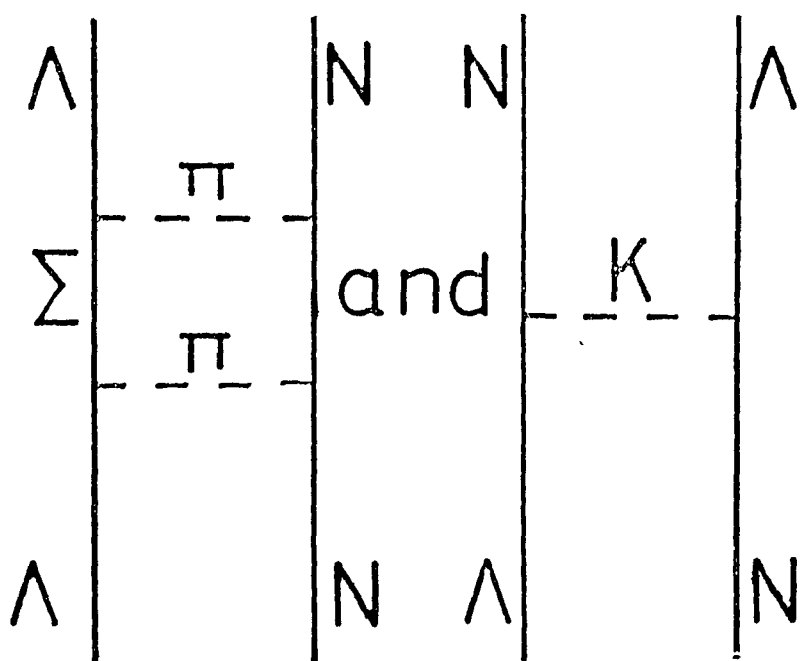


Figure 12: The most important contributions to the Λ - N potential.

References

1. H. Yukawa, Proc. Phys. Math. Soc. (Japan) 17, 48 (1935).
2. W. Heisenberg, Z. Phys. 77, 1 (1932).
3. D. Griffiths, Introduction to elementary particles.
New York : John Wiley & Sons, 1987.
4. J.T.Londergan and A.Macfarlane , SERC School Series
(Nuclear Physics, Sep 28-Oct 11, 1987).
5. A. Proca, J. Phys. Radium 7, 347 (1936).
6. N. Kemmer , Proc. Roy. Soc. (London) A 1166, 127 (1938)
Proc. Cambridge Phil Soc. 34, 354 (1938)
Proc . Roy. Soc. (London) A 173, 91 (1939)
7. G.Breit et.al., Phys. Rev. 120, 2227 (1960)
Rev. Mod. Phys. 34, 766 (1962)
8. J.Iwadare et. al., Prog. Theor. Phys. (Kyoto) 15, 86 (1956);
16, 455 (1956).
N.K.Glendenning and G.Kramer, Phys. Rev. 126, 2159 (1962)
9. T.E.O.Ericson and M.Rosa - Clot, Nucl. Phys. A405, 497 (1983)
T.E.O.Ericson and M.Rosa-Clot, Ann. Rev. Nucl. Part. Sci.
35, 271 (1985).
10. M.Taketani et. al., Prog. Theor. Phys. (Kyoto) 7, 45 (1952)
11. K.A.Brueckner and K.M.Watson, Phys. Rev. 90, 699 (1953);
92, 1023 (1953).
12. R.Machleidt et.al., Phys. Rep. 149, No.1, (1987)
13. G. Breit, Phys. Rev. 51, 248 (1962)
14. J.J. Sakurai Ann. Phys. (N.Y.) 11, 1 (1960)

- Phys. Rev. 119, 1784 (1960)
- Nuovo Cim. 16, 338 (1960)
15. N.Tzoar et. al. Phys.Rev.Letts. 2,433(1959)
 16. M.Danysz and J.Pniewski, Phil. Mag. 44, 348 (1953)
 17. N. Mukhin, Experimental Nuclear Physics (Vol II)
Moscow : Mir Publishers (1987)
 18. H.Bando et.al., Strangeness Nuclear Physics
OECU - 1991 - 10
 19. B. Povh, Z. Phys. A 279, 159 (1976)
 20. B. Povh, Ann. Rev. Nucl. Part. Sci. 28, (1978)
 21. B. Povh, Prog. Part. Nucl-Phys., (ed. D. Wilkinson) 5,(1981)
 22. B. Povh, Hyperons in Nuclei,
European Organization for Nuclear Research Geneva
25 May 1976.
 23. J. Cohen, Int. Journal of Mod. Phys. A , 4 , No.1 (1989).
 24. N.N.Fetisov et.al., Phys. Lett. 38 B, 129 (1972)
 25. A.K.Kerman and B.Povh, Phys. Lett. 40 B, 628 (1972)
 26. C.B.Dover et. al. , Phys. Rev. C 22, 2073 (1980)
 27. A.M. Bernstin , Proc. of the Int. Conf. on Hyper - Nuclear and Kao
Physics, Heidelberg , 1982, ed. B. Povh
 28. A.M.Bernstein et. al. , Nucl. Phys. A 358, 195c (1981).
 29. S.S.Hsiao and C.R.Cotanch , Phys. Rev. C 28, 1668 (1983).
 30. A. M. Bernstein , Bates Proposal , 1987.
 31. T.W. Donnelly , Lecture Notes in Physics
234, Springer - Verlag New York (1985).

intermediate range parts completely determined from πN and $\pi\pi$ interaction. ; for practical many-body calculations it is frequently used in its parametrized form .

Argonne group⁽⁴⁾ has presented nucleon - nucleon potentials with and without Δ (1232) degrees of freedom. The two models give excellent and almost identical fits to the deuteron properties and np scattering below 330 MeV. Recently the Δ degrees of freedom has been incorporated in the Paris potential in Graz potential and the two body phenomenology has been done. (30)

In this chapter we shall discuss the various phenomenological potentials: viz. Hamada - Johnston potential, Reid Hard and Soft core potential, Paris potential and Argonne potential.

However, before going into the details of these potentials we shall discuss in brief about some older N - N potentials.

2.1 Brief review of some older N - N potentials:

In 1957, Gammel and Thaler⁽²¹⁾ were the first who constructed a quantitative NN potential. This potential used a hard core (infinite repulsion) at small distances ($r \leq 0.4$ fm) to account for the trend of 1S_0 phase - shift turning negative for lab energies about 250 MeV.

Another semi - quantitative, potential was constructed by Signell and Marshak⁽²²⁾ who used some input from the pion theoretic potential derived by Gartenhaus⁽²³⁾. Signell and Marshak observed that even though several meson-theoretic two-nucleon potentials give a good fit of the data at low energies, yet all of these potentials fail to fit the 100 and 150 MeV p-p scattering data. (23,24). Signell and Marshak based on the

modification of Ohnuma and Feldman⁽²⁵⁾, conceived to include a spin-orbit term to the Gartenhaus potential.

The following is the form of the Signell and Marshak potential:⁽²²⁾

$$V = V_G + \vec{L} \cdot \vec{S} \frac{V_o}{X_c} \frac{d}{dx} \left(\frac{e^{-x}}{x} \right) \Big|_{r=r_c} \quad \text{for } r < r_c$$

$$V = V_G + \vec{L} \cdot \vec{S} \frac{V_o}{X_c} \frac{d}{dx} \left(\frac{e^{-x}}{x} \right) \quad , \quad \text{for } r > r_c$$

where V_G is the Gartenhaus potential which has the central part plus tensor part, and $x = r/r_o$, $x_c = r_c/r_o$, $r_c = \frac{1}{M} = 0.21 \text{ fm}$, $r_o = 1.07 \text{ fm}$ $V_o = 30 \text{ MeV}$.

This potential was found to be in accordance with the experimental data upto 150 MeV.

Later in the work Signell, Zim and Marshak⁽²⁶⁾ modified the spin - orbit part of the SM potential so that the spin - orbit potential has a range of $(2\mu)^{-1}$ corresponding to the exchange of two mesons by the nucleons.

This is known as SM1 potential⁽²⁶⁾

$$V_{LS} = \frac{V_o}{x} \frac{d}{dx} \left(\frac{e^{-2x}}{x} \right) ,$$

with $x = \mu r$ and $V_o = 21 \text{ MeV}$.

From the SM1 potential the data were in agreement with the experimental results upto 150 MeV.

Bryan⁽²⁷⁾ obtained an improved fit to the high - energy p - p scattering data from the 40 to 310 MeV range by considering the static potential (central, tensor, and spin - orbit) of the form:

$$V = \sum_{n=2}^5 A_n x^{-n} e^{-2x} + V_2 \text{ (OPEP)}$$

together with infinite repulsive cores for the central potential with $x = h/\mu c$, V_2 (OPEP) is the OPE potential, and A_n are constants which are fitted from the scattering data.

Later Saylor, Bryan and Marshak⁽²⁸⁾ after realizing that the Bryan potential is weak in the outside region, developed a boundary condition model with potential tails outside. These modified forms were found to be more appreciable.

Yale group⁽²⁹⁾ expressed the phase shifts as some function of energy, containing-

-parameters which can be varied to obtain a fit of the data at several energies. The data was fitted over the whole energy range upto 345 MeV.

2.2 Hamada and Johnston Potential

Hamada and Johnston⁽¹¹⁾ described an energy independent nucleon - nucleon potential which represents the nucleon data (n - p and p - p both below 315 MeV). Apart from the usual central and tensor parts, the model is characterized by a short range strong linear LS potential in the triplet even state. The latter potential is also present in the single states. The phase shifts calculated from the model are in fair agreement with the Yale solutions for $T=1$ and $T=0$. Hamada - Johnston potential has proved to be popular in nuclear-structure calculations because it has relatively a simple form.

The H.J. potential contains the four terms-central (C), tensor (T), spin-orbit (LS), and quadratic spin-orbit (LL) terms:

$$V = V_C + V_T S_{12} + V_{LS} \vec{L} \cdot \vec{S} + V_{LL} L_{12} , \quad \dots\dots\dots 1)$$

where L_{12} is the operator defined by

$$L_{12} = (\vec{\sigma}_1 \cdot \vec{\sigma}_2) \vec{L}^2 - \frac{1}{2} \left\{ (\vec{\sigma}_1 \cdot \vec{L}) (\vec{\sigma}_2 \cdot \vec{L}) + (\vec{\sigma}_1 \cdot \vec{L}) (\vec{\sigma}_1 \cdot \vec{L}) \right\}$$

$$= \left\{ \sigma_{LJ} + (\vec{\sigma}_1 \cdot \vec{\sigma}_2) \right\} \vec{L}^2 - (\vec{L} \cdot \vec{S})^2$$

The V_i ($i = C, T, LS, LL$) are allowed to be spin parity dependent.

They are give by

$$V_C = 0.08 \left(\frac{1}{3} \mu \right) (\vec{\tau}_1 \cdot \vec{\tau}_2) (\vec{\sigma}_1 \cdot \vec{\sigma}_2) y(x)$$

$$\left[1 + a_C y(x) + b_C y^2(x) \right]$$

$$V_T = 0.08 \left(\frac{1}{3} \mu \right) (\vec{\tau}_1 \cdot \vec{\tau}_2) Z(x) [1 + a_T y(x) + b_T y^2(x)]$$

$$V_{LS} = \mu G_{LS} y^2(x) [1 + b_{LS} y(x)]$$

$$V_{LL} = \mu G_{LL} \frac{1}{x^2} Z(x) [1 + a_{LL} y(x) + b_{LL} y^2(x)] ,$$

where μ is the pion mass , x is the internucleon distance measured in μ^{-1}

and $y(x) = e^{-x/x}$

$$Z(x) = \left(1 + \frac{3}{x} + \frac{3}{x^2} \right) y(x)$$

The coefficients a_C, b_C, a_T and b_T determines the deviation of the potentia from OPEP at smaller x , and V_{LS} represents a short-range linear LS potential whose strength G_{LS} depends on the parity of the state concerned

The presence of hard cores in all states has been assumed . The hard core radius is $x_0 = 0.343$ (all states).

The parameters of H.J. used in equation 2) are given in table 1 and the results of H.J. group has been given in Table 2.

Table 1

| State | a_c | b_c | a_T | b_T | G_{LS} | b_{LS} | G_L | a_{LL} | b_{LL} |
|--------------|-------|-------|-------|-------|----------|----------|-----------|----------|----------|
| Singlet-even | +8.7 | +10.6 | — | | | | -0.000891 | +0.2 | -0.2 |
| triplet-odd | -9.07 | +3.48 | -1.29 | +0.55 | +0.1961 | -7.12 | -0.000891 | -7.26 | +6.92 |
| triplet-even | +6.0 | -1.0 | -0.5 | +0.2 | +0.0743 | -0.1 | +0.000267 | +1.8 | -0.4 |
| Singlet-odd | -8.0 | +12.0 | — | — | — | — | -0.00267 | +2.0 | +6.0 |

Table 2

Low energy properties of some NN potential

| Potential | H-J ⁽¹¹⁾ | RSC ⁽¹⁸⁾ | Experimental Values |
|------------------------|---------------------|---------------------|---------------------|
| E_B (MeV) | 2.269 | 2.22460 | 2.22463(3) |
| P_D (%) | 6.97 | 6.470 | 4-7 |
| Q (fm ²) | 0.285 | 0.2796 | 0.2860 (15) |

| | | | |
|--------------|---------|--------|---------------------|
| η (D/S) | 0.02656 | 0.2622 | 0.0265 \pm 0.0004 |
| 3S_1 | | | |
| $a(fm)$ | - | 5.390 | 5.424 (4) |
| $r(fm)$ | 1.77 | 1.72 | 1.748 (6) |
| P_t | | -0.027 | |
| $1S_0$ | | | |
| $a_{pp}(fm)$ | - | - | -7.823 |
| $r_{pp}(fm)$ | - | - | 2.794 |
| $a_{nn}(fm)$ | -17.0 | -17.1 | -16.4 |
| $r_{nn}(fm)$ | -2.83 | 2.80 | - |

2.3. Reid Hard and Soft Core Potentials

The potential of Reid⁽¹²⁾ belongs to the group in which potentials are constructed separately for each set of partial waves. This procedure has the technical advantage that the potentials in each set can be adjusted independently of each other. Reid constructed three set of potentials one with hard cores, two with soft repulsive cores.⁽¹⁾

Isotopic Spin One $T = 1$ phase shifts can be obtained from pp scattering data alone. The $T = 1$ phase shifts was calculated by integrating the Schrodinger equation whose potential is the sum of the Coulomb and NN potential. At a large radius where NN potential is negligible the solution was fitted to Coulomb wave function to get the phase.

Hardcore $T = 1$ potentials are given in equation (1) through (5) where $h = 10.463$ MeV , from OPEP. The hardcore radius x_c is 0.29614 in the 1S state and 0.3 in the others.

$$V(^1S_0) = -h (e^{-x} + 39.633 e^{-3x}) / x \quad (1)$$

$$V(^1D_2) = -h (e^{-x} + 4.939 e^{-2x} + 154.7 e^{-6x}) / x \quad (2)$$

$$V(^3P_0) = -h (G_1 + 16.2 e^{-2x} - 55.6 e^{-3x} - 545 e^{-6x}) / x \quad (3) ,$$

where

$$G_1 = (1 + \frac{4}{x} + \frac{4}{x^2}) e^{-x} + (\frac{24}{x} + \frac{4}{x^2}) e^{-6x}$$

$$V(^3P_1) = h (G_2 - 1.1553 e^{-2x} - 8.722 e^{-3x} + 175.1 e^{-6x}) / x \quad (4) ,$$

$$\text{where } G_2 = (1 + \frac{2}{x} + \frac{2}{x^2}) e^{-x} - (\frac{12}{x} + \frac{2}{x^2}) e^{-6x}$$

$$V(^3P_2 - ^3F_2) = V_c + V_T S_{12} + V_{LS} \vec{L} \cdot \vec{S} , \quad (5)$$

where

$$V_c = h (e^{-x/3} - 13.8 e^{-3x} + 138 e^{-6x}) / x$$

$$V_T = h [(\frac{1}{3} + \frac{1}{x} + \frac{1}{2}) e^{-x} - (\frac{6}{x} + \frac{1}{2}) e^{-6x} - 5.688 e^{-3x}] / x$$

$$V_{LS} = -250.9 h e^{-6x/x}$$

$$x = \mu r, \mu = 0.7 F^{-1}.$$

The hardcore radius was allowed to vary only in the 1S state. An alternate 1D potential with the 1S core, $x_c = 0.29614$ is

$$V(^1D_2, \text{alternate}) = -h (e^{-x} + 25.86 e^{-3x})/x \quad (6)$$

Softcore $T = 1$ potentials in MeV are given in (7) through (11), h is 10.463 MeV and $x = \mu r$, where $\mu = 0.7 F^{-1}$.

$$V(^1S) = -h \frac{e^{-x}}{x} - 1650.6 \frac{e^{-4x}}{x} + 6484.2 \frac{e^{-7x}}{x} \quad (7)$$

$$V(^1D_2) = -h \frac{e^{-x}}{x} - 12.322 \frac{e^{-2x}}{x} - 1112.6 e^{-4x/x} + 6484.2 e^{-7x/x} \quad (8)$$

$$V(^3P_0) = -h \left[\left(1 + \frac{4}{x} + \frac{4}{x^2} \right) e^{-x} - \left(\frac{16}{x} + \frac{4}{x^2} \right) e^{-4x} \right] / x \\ + 27.133 e^{-2x/x} - 790.74 e^{-4x/x} + 20662 e^{-7x/x} \quad (9)$$

$$V(^3P_1) = h \left[\left(1 + \frac{2}{x} + \frac{2}{x^2} \right) e^{-x} - \left(\frac{8}{x} + \frac{2}{x^2} \right) e^{-4x} \right] / x \\ - 135.25 e^{-2x/x} + 472.81 e^{-3x/x} \quad (10)$$

$$V(^3P_2 - ^3F_2) = V_c + V_T S_{12} + V_{LS} \vec{L} \cdot \vec{S}, \quad (11)$$

$$\text{where } V_c = \frac{h}{3} \frac{e^{-x}}{x} - 933.48 \frac{e^{-4x}}{x} + 4152.1 \frac{e^{-6x}}{x}$$

$$V_T = h \left[\left(\frac{1}{3} + \frac{1}{x} + \frac{1}{x^2} \right) e^{-x} - \left(\frac{4}{x} + \frac{1}{x^2} \right) e^{-4x} \right] / x - 34.925 e^{-3x}/x$$

$$V_{LS} = - 2074.1 e^{-6x}/x$$

Two alternate potentials are

$$V ({}^1S , \text{alternate}) = - h \frac{e^{-x}}{x} + 105.32 \frac{e^{-3x}}{x} - 2401.9 e^{-4x}/x + 5598.2 e^{-6x}/x \quad (12)$$

$$V ({}^1D , \text{alternate}) = - h \frac{e^{-x}}{x} - 318.64 e^{-3x}/x + 526.27 e^{-5x}/x \quad (13)$$

Isotopic Spin Zero

Hardcore T = 0 potential are given in (14) through (16) . The hard core radius x_c is 0.38383 in the 3S_1 - 3D_1 state and 0.3 in the others. It was allowed to vary only in the 3S_1 - 3D_1 state.

$$V ({}^1P) = 3h (e^{-x} - 11.08 e^{-2x} + 20.3 e^{-3x} + 465 e^{-6x}) / x \quad (14)$$

$$V ({}^3D_2) = -h (G_3 + 28.45 e^{-2x} - 93.6 e^{-3x}) / x , \quad (15)$$

$$\text{where } G_3 = \left(3 + \frac{6}{x} + \frac{6}{x^2} \right) e^{-x} - \left(\frac{18}{x} + \frac{6}{x^2} \right) e^{-3x}$$

$$V ({}^3S_1 - {}^3D_1) = V_c + V_T S_{12} + V_{LS} \vec{L} \cdot \vec{S} , \quad (16)$$

$$\text{where } V_c = - h (e^{-x} + 387.4 e^{-6x}) / x$$

$$V_T = -h \left[\left(1 + \frac{3}{x} + \frac{3}{x^2} \right) e^{-x} - \left(59.968 + \frac{18}{x} + \frac{3}{x^3} \right) e^{-6x} - 5.33 e^{-3x} \right] / x$$

$$V_{LS} = 1181.2 e^{-6x}/x$$

Soft core T = 0 potential are given in (17) through (19),

$$V(1P_1) = 3h \frac{e^{-x}}{x} - 634.39 e^{-2x}/x + 2163.4 \frac{e^{-3x}}{x} \quad (17)$$

$$V(3D_2) = -3h \left[\left(1 + \frac{2}{x} + \frac{2}{x^2} \right) e^{-x} - \left(\frac{8}{x} + \frac{2}{x^2} \right) e^{-4x} \right] / x$$

$$- 220.12 e^{-2x}/x + 871 e^{-3x}/x \quad (18)$$

$$V(3S_1 - 3D_1) = V_c + V_T S_{12} + V_{LS} \vec{L} \cdot \vec{S}, \quad (19)$$

where

$$V_c = -\frac{he^{-x}}{x} + 105.468 \frac{e^{-2x}}{x} - 3187.8 e^{-4x}/x + 9924.3 e^{-6x}/x$$

$$V_T = -h \left[\left(1 + \frac{3}{x} + \frac{3}{x^2} \right) e^{-x} - \left(\frac{12}{x} + \frac{3}{x^2} \right) e^{-4x} \right] / x$$

$$+ 351.77 e^{-4x}/x - 1673.5 e^{-6x}/x$$

$$V_{LS} = 708.91 e^{-4x}/x - 2713.1 e^{-6x}/x$$

Two alternate potentials are

$$V ({}^3S_1 - {}^3D_1 , \text{ alternate }) = V_C + V_T S_{12} + V_{LS} \vec{L} \cdot \vec{S} , \quad (20)$$

$$\text{where} \quad V_C = -h \frac{e^{-x}}{x} + 102.012 \frac{e^{-2x}}{x} - 2915 \frac{e^{-4x}}{x} + 7800 \frac{e^{-6x}}{x}$$

$$V_T = -h \left[\left(1 + \frac{3}{x} + \frac{3}{x^2} \right) e^{-x} - \left(\frac{12}{x} + \frac{3}{x^2} \right) e^{-4x} \right] / x + 163 e^{-4x} / x$$

$$V_{LS} = 251.75 e^{-4x} / x$$

$$-V ({}^1P_1 , \text{ alternate }) = 3 h \frac{e^{-x}}{x} - 240 \frac{e^{-2x}}{x} + 17000 \frac{e^{-6x}}{x} \quad (21)$$

Properties of the deuteron calculated from the potentials are given in Table 3, where E is the binding energy, Q is the electric quadrupole moment, ${}^P D$ is the D - state probability and A_D/A_S is the asymptotic D to S wave ratio.

In the table 4 and 5, effective range parameters for 3S and 1S has been compared with the experimental value.

Table : 3
Properties of the Deuteron

| Potential | E (MeV) | Q (F^2) | Po (%) | A_D / A_S |
|-------------|----------------------------|------------------------|----------|------------------------|
| H C | 2.22464 | 0.2770 | 6.497 | 0.02590 |
| S C | 2.22460 | 0.2796 | 6.470 | 0.02622 |
| S C A | 2.22464 | 0.2762 | 6.217 | 0.02596 |
| Expt. Value | 2.224644 ± 0.000046 | 0.2860 ± 0.0015 | 4 - 7 | 0.0265 ± 0.0005 |

Table : 4
 3S effective range parameters

| Potential | a(F) | r_e (F) |
|---------------------|-----------|-------------|
| H C | 5.397 | 1.724 |
| S C | 5.390 | 1.720 |
| S C A | 5.390 | 1.720 |
| Experimental Values | 5.424 (4) | 1.748 (6) |

Table : 5

1_S Effective range parameters for no Coulomb potential present

| Potential | a (F) | r_e (F) |
|-----------|---------|-------------|
| H C | -16.7 | 2.87 |
| S C | -17.1 | 2.80 |
| S C A | -17.1 | 2.80 |
| Exp | -16.4 | - |

2.4 Paris Potential

The interaction region was divided by the Paris group into three domains : Long - range (L R), intermediate range (MR), and short range (SR). The view point for the short range is that the potential is largely unknown . The short - range part of the N - N interaction in the "Complete" Paris potential is parametrized and fit to the data. A theoretical mesons exchange potential is fashioned in the medium range and the long range parts of the interaction. The Paris group fixed up $r_0 = 0.8 \text{ fm}$ as the perimeter between the short range and the medium range part of the potential⁽¹⁶⁻²⁰⁾.

The N - N potential based on these ideas took about a decade to come into a complete form . The work can be divided into three different stages :

(i) First of all the "theoretical" Paris potential was constructed which was able to describe the long range and medium - range part of the N - N

potential . Then this model was fitted to those parts of the $N - N$ interaction which are most sensitive to the long - range and medium - range interaction. (16-17)

(ii) The next stage was to get a "complete" Paris potential by incorporating a phenomenological short range part and fitting its part to NN phase shifts. (18)

(iii) Last stage was to get a parametrized Paris potential . This is useful for many - body calculations. (19)

The "Theoretical" Paris Potential

The contribution from the mesons exchange is divided into three different types.

(a) π - exchange

(b) Resonant and non- resonant two - pion exchange

(c) 3 - pion exchange , mediated primarily by ω - exchange

The evaluation of two - pion exchange is the key - stone of the theoretical Paris potential which has been computed from the cognizant of pion - nucleon phase - shift and pion - pion interaction which are made use as inputs in the dispersion relations with the subtraction requisited by Regge asymptotic behaviour.

The following are the key principles. Firstly, this method depends upon the fact that the scattering matrix is an analytic function of the relativistic variables which characterizes the scattering e.g. we can jot down a dispersion relation which consociate the scattering amplitude to an integral over the discontinuity of this amplitude.

Secondly, the property of the scattering amplitude is that of crossing

symmetry , for the NN problem, which states that the scattering amplitude which describes the NN elastic scattering , when analytically continued or in the S - matrix variables , gives the amplitude for the $N - \bar{N}$ elastic scattering . In terms of Mandelstam variables (s, t, u) it can be stated that the S-matrix element which describes $N - N$ elastic scattering is related to the $N - \bar{N}$ elastic scattering.

The use of crossing symmetry and analyticity signifies that the two - pion t - channel exchange amplitude which occurs in elastic $N - N$ interaction can be related to the process $N + \bar{N} \longrightarrow \pi + \pi \longrightarrow N + \bar{N}$.

By extrapolating the $\pi - N$ amplitude which in theory includes all $\pi - N$ resonances , S - wave , $\pi - \pi$ resonances as well as non - resonant backgrounds, the TPE box - diagram for NN scattering can be obtained.

The Paris group made use of two different $\pi - N$ phase shifts , labelled C and C', and the use of two different sets of S - wave $\pi - \pi$ phase shifts, labelled R (for "resonant") and NR (for "non-resonant") is also made.

The derived potential which is not much dependent on the choice of $\pi - N$ or $\pi - \pi$ phase , in this way agrees well with the phenomenological potential leaving besides central potential which is strongly dependent upon both of these phase shift sets.

In this way the theoretical - Paris potential is obtained and is then used to obtain the peripheral $N - N$ phase shifts. The centrifugal barriers masks the short distance behaviour of the interaction for such phase shifts and hence, these phases are sensitive only to the medium range and short range parts of the $N - N$ interaction.

$V_{\text{phen}} (r, E)$ is assumed to be constant with respect to r and , therefore , only the function of energy.

It is given as

$$V_{\text{phen}} (r, E) = V_{\text{phen}} (r) + E \bar{V}_{\text{phen}} (r) ,$$

where \bar{V}_{phen} was set to zero for the SS , SO, T and SO2.

Therefore, the potential becomes

$$V (r, E) = [U_{\text{theor}} (r) + E W_{\text{theor}} (r)] f (r) \\ + [1 - f (r)] V_{\text{phen}} (E)$$

It has been found out that $V_{\text{phen}} (E)$ is a linear function of E for the central component and almost constants for the SS , SO, T and SO2 components.

Therefore , $V_{\text{phen}} (E)$ was taken to be of the form $C + C'E$ for the central component and constant for the SS, SO, T and SO2 terms , so that the complete potential $V (r, E)$ can be written as

$$V (r, E) = U (r) + E W (r) ,$$

$$\text{where} \quad U (r) = U_{\text{theor}} (r) f (r) + C [1 - f (r)] \\ \cdot \quad W (r) = W_{\text{theor}} (r) f (r) + C' [1 - f (r)] ,$$

C' being zero for the SS, T, SO, and SO2 component and $V (r, E)$ contains six free parameters for each isospin state , $T = 0$, or $T = 1$, namely C_c , C_{ss} , C_{so} , C_T , C_{so2} and C'_c .

The resulting "complete" Paris potential provides an excellent fit to the properties of the deuteron . The resulting potential has the following qualitative properties.

i) For $J > 2$, it is dominated by the theoretical components

- ii) The phenomenological short range part is of soft - core form.
- iii) $V(r, E)$ obtained from the dispersion integrals is energy dependent. The energy dependence is linearized in constructing the complete Paris potential.
- iv) The two pion exchange contribution, including the ρ - exchange, and any contribution from two - pion S - wave phase shifts enters via the dispersion relation.

Parametrization of Paris Potential

The complete Paris potential, with its dispersion integrals and energy dependence is not particularly convenient to handle.

Therefore, parametrization were constructed in \bar{r} and \bar{p} space. With this parametrization the changes were made in the basic potential.

- i) The effect of the A_1 meson which is a pseudovector meson of mass ~ 1200 MeV has been added to V_{theor} .
- ii) In redetermining the parameters of the phenomenological component V_{phen} not only phase shifts but also other N - N observable were included in the fitting procedure.
- iii) A unique analytical expression for the complete potential is adopted,

namely a discrete sum of Yukawa type terms which has the advantage that their forms are simple in both in configuration and momentum space.

The linear energy dependence is transformed into a p^2 - dependence which can be handled without ambiguity.

For the two isospin values $T = 1$ and $T = 0$ the potential is expressed in terms of the usual non - relativistic in-variants

$$V(\vec{r}, p^2) = V_0(r, p^2) \Omega_0 + V_1(r, p^2) \Omega_1 + V_{LS}(r) \Omega_{LS} \\ + V_T(r) \Omega_T + V_{SO2}(r) \Omega_{SO2},$$

where

$$\Omega_0 = \frac{1 - \vec{\sigma}_1 \cdot \vec{\sigma}_2}{4}$$

$$\Omega_1 = \frac{3 + \vec{\sigma}_1 \cdot \vec{\sigma}_2}{4}$$

$$\Omega_{LS} = \vec{L} \cdot \vec{S}$$

$$\Omega_T = \frac{3 \vec{\sigma}_1 \cdot \vec{r} \vec{\sigma}_2 \cdot \vec{r}}{r^2} - \vec{\sigma}_1 \cdot \vec{\sigma}_2$$

$$\Omega_{SO2} = \frac{1}{2} (\vec{\sigma}_1 \cdot \vec{L} \vec{\sigma}_2 \cdot \vec{L} + \vec{\sigma}_2 \cdot \vec{L} \vec{\sigma}_1 \cdot \vec{L})$$

The central component contains a velocity dependent part and V_0 , V_1 are defined as

$$V(r, p^2) = V^a(r) + \left(\frac{p^2}{m}\right) V^b(r) + V^b(r) \left(p^2/m\right)$$

with
$$p^2 = -\hbar^2 \left[\frac{1}{r} \frac{d^2}{dr^2} - \frac{\vec{L}^2}{r^2} \right]$$

$$m = 938.2592 \text{ MeV for } T = 1,$$

$$\text{and } 938.9055 \text{ MeV for } T = 0$$

For each component $V(r)$ the following parametrization is used :

$$V(r) = \sum_{j=1}^n g_j F(m_j r) \frac{e^{-m_j r}}{m_j},$$

where

$$F (m_j r) = 1 \text{ for } V_o^a, V_o^b, V_1^a \text{ and } V_1^b$$

$$F (m_j r) = \frac{1}{m_j r} + \frac{1}{(m_j r)^2} \text{ for } V_{LS}$$

$$F (m_j r) = 1 + \frac{3}{m_j r} + \frac{3}{(m_j r)^2} \text{ for } V_T$$

$$F (m_j r) = \frac{1}{(m_j r^2)} \left[1 + \frac{3}{m_j r} + \frac{3}{(m_j r)^2} \right] \text{ for } V_{SO2}$$

The masses m_j are the same for all components , the first term ($j = 1$) corresponds to the OPE and appears only in V_o , V_1 and V_T .The potential is regularized at the origin $r = 0$.

The deuteron and low energy N - N properties obtained from this potential has been tabulated in Table (6) . S - and P- wave phase shifts of the parametrized Paris potential has been shown in fig (1) .

2.5. Argonne potential

Wiringa et al⁽⁴⁾ gave two sets of nucleon - nucleon potentials ;

i) a V_{14} model which is a conventional NN potential, and ii) a V_{28} model with explicit Δ (1232) degrees of freedom . The V_{14} model has 14 operator components describing NN - channel, while V_{28} model has 14 additional operators , including 12 transition operators for all possible $\pi N\Delta$ and $\pi\Delta\Delta$ couplings and two central operators for $N\Delta$ and $\Delta\Delta$ channels. They have obtained the deuteron properties and np scattering data below 330 MeV.

The V_{14} Potential Model

The V_{14} potential is written as a sum of 14 operators components

$$V_{14} = \sum_{p=1,14} \left[V_{\pi}^p(r_{ij}) + V_I^p(r_{ij}) + V_S^p(r_{ij}) \right] O_{ij}^p, \quad (1)$$

where the operators are

$$O_{ij}^p = 1, \vec{\tau}_i \cdot \vec{\tau}_j, \vec{\sigma}_i \cdot \vec{\sigma}_j, (\vec{\sigma}_i \cdot \vec{\sigma}_j) (\vec{\tau}_i \cdot \vec{\tau}_j), S_{ij}, S_{ij} (\vec{\tau}_i \cdot \vec{\tau}_j)$$

$$(\vec{L} \cdot \vec{S}), (\vec{L} \cdot \vec{S}) (\vec{\tau}_i \cdot \vec{\tau}_j), \vec{L}^2, \vec{L}^2 (\vec{\tau}_i \cdot \vec{\tau}_j),$$

$$\vec{L}^2 (\vec{\sigma}_i \cdot \vec{\sigma}_j), \vec{L}^2 (\vec{\sigma}_i \cdot \vec{\sigma}_j) (\vec{\tau}_i \cdot \vec{\tau}_j), (\vec{L} \cdot \vec{S})^2,$$

$$(\vec{L} \cdot \vec{S})^2 (\vec{\tau}_i \cdot \vec{\tau}_j), \quad (2)$$

where

$$S_{ij} = \frac{1}{3} (\vec{\sigma}_i \cdot \vec{r}_{ij}) (\vec{\sigma}_j \cdot \vec{r}_{ij}) - \vec{\sigma}_i \cdot \vec{\sigma}_j$$

is the tensor operator, \vec{L} is the relative orbital angular momentum, and \vec{S} is the total spin of the pair. The three radial components include the long-range OPE part $V_{\pi}^p(r)$, and phenomenological intermediate range and short range parts $V_I^p(r)$, $V_S^p(r)$, whose shapes were taken from the Urbane model. The $V_{\pi}^p(r)$ contributes only with the $\sigma\sigma$, $\tau\tau$ operators:

$$V_{\pi}^{\sigma\tau}(r) = \left[\frac{f_{\pi NN}^2}{4\pi} \cdot \frac{m_{\pi}}{3} \right] \frac{e^{-\mu r}}{\mu r} (1 - e^{-cr^2})$$

$$= (3.72681) Y_{\pi} (r) \quad \text{-----} \quad 3)$$

$$\text{and } V_{\pi}^{tr} (r) = \left[\frac{f_{\pi NN}^2}{4\pi} \cdot \frac{m_{\pi}}{3} \right] \left[1 + \frac{3^2}{\mu r} + \frac{3}{(\mu r)^2} \right] \\ \frac{1}{\mu r} (e^{-\mu r} - e^{-cr^2})^2 = (3.72681) T_{\pi}(r) ,$$

where $Y_{\pi} (r)$ and $T_{\pi} (r)$ are the usual Yukawa and tensor functions with smooth Gaussian cutoffs that makes them vanishing at $r = 0$. The values of m_{π} , c and $(\frac{f_{\pi NN}^2}{4\pi})$ were 138.03 MeV, 2 fm^{-2} and 0.081 respectively.

The intermediate range part $V_I^P(r)$ is taken from TPE processes which is dominated by the tensor interaction. The chosen phenomenological shape

$$V_I^P (r) = I^P T_{\pi}^2 (r) \quad \text{-----} \quad 4)$$

The short range part is described by taking Woods - Saxon shape

$$V_S^P (r) = S^P \{ 1 + \exp [(r - R)/a] \}^{-1} = S^P W (r) \quad \text{-----} \quad 5)$$

where $R = \frac{1}{2} \text{ fm}$, $a = 0.2 \text{ fm}$,

and I^P and S^P were the parameters determined by fitting data.

The V_{28} Potential Model In this they have started with a V_{14} part for NN channels , and then added operators to represent all possible processes with $\pi N \Delta$ or $\pi \Delta \Delta$ vertices , plus central operators in the $N \Delta$ and $\Delta \Delta$ channels.

The potential is written as

$$V_{28} ,_{ij} = \sum_{p=1,28} \left[V_{\pi}^P (r_{ij}) + V_I^P (r_{ij}) + V_S^P (r_{ij}) \right] O_{ij}^P \quad \text{-----} \quad 6)$$

where the $O_{ij}^{p=1,14}$ are given by eqn.2) and the remaining operators are the following

$$O_{ij}^{p=15} = (\vec{\sigma}_i \cdot \vec{S}_j) (\vec{\tau}_i \cdot \vec{T}_j) + (\vec{S}_i \cdot \vec{\sigma}_j) (\vec{T}_i \cdot \vec{\tau}_j) + \text{Hermitian Conjugate (H.C.)}$$

$$O_{ij}^{16} = S_{ij}^{II} (\vec{\tau}_i \cdot \vec{T}_j) + S_{ji}^{II} (\vec{T}_i \cdot \vec{\tau}_j) + \text{H.C.}$$

$$O_{ij}^{17} = (\vec{S}_i \cdot \vec{S}_j) (\vec{T}_i \cdot \vec{T}_j) + \text{H.C.}$$

$$O_{ij}^{18} = S_{ij}^{III} (\vec{T}_i \cdot \vec{T}_j) + \text{H.C.}$$

$$O_{ij}^{19} = (\vec{S}_i \cdot \vec{S}_j^\dagger) (\vec{T}_i \cdot \vec{T}_j^\dagger) + \text{H.C.}$$

$$O_{ij}^{20} = S_{ij}^{iv} (\vec{T}_i \cdot \vec{T}_j^\dagger) + \text{H.C.}$$

$$O_{ij}^{21} = \Lambda_{Ni} \cdot \Lambda_{\Delta j} + \Lambda_{\Delta i} \cdot \Lambda_{Nj}$$

$$O_{ij}^{22} = (\vec{\sigma}_i \cdot \vec{\Sigma}_j) (\vec{\tau}_i \cdot \vec{\Theta}_j) + (\vec{\Sigma}_i \cdot \vec{\sigma}_j) (\vec{\Theta}_i \cdot \vec{\tau}_j)$$

$$O_{ij}^{23} = S_{ij}^v (\vec{\tau}_i \cdot \vec{\Theta}_j) + S_{ij}^v (\vec{\Theta}_i \cdot \vec{\tau}_j)$$

$$O_{ij}^{24} = (\vec{S}_i \cdot \vec{\Sigma}_j) (\vec{T}_i \cdot \vec{\Theta}_j) + (\vec{\Sigma}_i \cdot \vec{S}_j) (\vec{\Theta}_i \cdot \vec{T}_j) + \text{H.C.}$$

$$O_{ij}^{25} = S_{ij}^{vi} (\vec{T}_i \cdot \vec{\Theta}_j) + S_{ji}^{vi} (\vec{\Theta}_i \cdot \vec{T}_j) + \text{H.C.}$$

$$O_{ij}^{26} = \hat{1}_{\Delta i} \cdot \hat{1}_{\Delta j}$$

$$O_{ij}^{27} = (\vec{\Sigma}_i \cdot \vec{\Sigma}_j) (\vec{\sigma}_i \cdot \vec{\sigma}_j)$$

$$O_{ij}^{28} = S_{ij}^{vii} (\vec{\sigma}_i \cdot \vec{\sigma}_j) ,$$

where the $\vec{\sigma}_i$ is the transition spin operator for particle i that changes a spin $\frac{1}{2}$ state to a $\frac{3}{2}$ state, \vec{T}_i is the transition isospin operator for that changes a isospin $\frac{1}{2}$ state to a $\frac{3}{2}$ state,

$\vec{\Sigma}_i$ is the Pauli isospin operator for a $\frac{3}{2}$ state 1_{N_i} is the unit operator in N space and 1_{Δ_i} is the unit operator in Δ space.

The various generalization of the tensor operator S_{ij} are the following.

$$S_{ij}^{II} = 3 (\vec{\sigma}_i \cdot \overset{\Delta}{r}_{ij}) (\vec{\sigma}_j \cdot \overset{\Delta}{r}_{ij}) - \vec{\sigma}_i \cdot \vec{\sigma}_j$$

$$S_{ij}^{III} = 3 (\vec{\Sigma}_i \cdot \overset{\Delta}{r}_{ij}) (\vec{\Sigma}_j \cdot \overset{\Delta}{r}_{ij}) - \vec{\Sigma}_i \cdot \vec{\Sigma}_j$$

$$S_{ij}^{iv} = 3 (\vec{\Sigma}_i \cdot \overset{\Delta}{r}_{ij}) (\vec{\sigma}_j \cdot \overset{\Delta}{r}_{ij}) - \vec{\Sigma}_i \cdot \vec{\sigma}_j$$

$$S_{ij}^v = 3 (\vec{\sigma}_i \cdot \overset{\Delta}{r}_{ij}) (\vec{\Sigma}_j \cdot \overset{\Delta}{r}_{ij}) - \vec{\sigma}_i \cdot \vec{\Sigma}_j$$

$$S_{ij}^{vi} = 3 (\vec{\Sigma}_i \cdot \overset{\Delta}{r}_{ij}) (\vec{\Sigma}_j \cdot \overset{\Delta}{r}_{ij}) - \vec{\Sigma}_i \cdot \vec{\Sigma}_j$$

$$S_{ij}^{vii} = 3 (\vec{\Sigma}_i \cdot \overset{\Delta}{r}_{ij}) (\vec{\Sigma}_i \cdot \overset{\Delta}{r}_j) - \vec{\Sigma}_i \cdot \vec{\Sigma}_j .$$

The full Hamiltonian is the sum of rest - mass and kinetic energy operators and the interaction is given by equation 1 and equation 6 .

Therefore , the Schrodinger equation may be written as

$$\sum_j H_{ij} \psi_j = E \psi_i ,$$

where in the centre of mass frame

$$H_{ij} = (M_i + m_j - 2m_N) + \frac{\hbar^2 (m_i + m_j)}{2m_i m_j} \nabla_{ij}^2 + V_{ij}$$

The calculated deuteron and low energy parameters obtained by the Argonne group has been tabulated in Table 6 .

Table 6 : The Calculated deuteron and low-energy parameters.

| Deuteron Properties | V_{14} | V_{28} | Paris | Experimental |
|-----------------------|----------|----------|---------|--------------|
| $E_d(\text{MeV})$ | -2.2250 | -2.2250 | -2.2249 | -2.22463(3) |
| $Q_d(\text{fm}^2)$ | 0.286 | 0.286 | 0.279 | 0.2860(15) |
| η_d | 0.0266 | 0.0265 | 0.0261 | 0.0265(5) |
| $\mu_d(\mu_n)$ | 0.845 | 0.846 | 0.853 | 0.857441(2) |
| $P_D(\%)$ | 6.08 | 6.13 | 5.77 | 4 - 7 |
| $P_\Delta(\%)$ | 0 | 0.52 | 0 | ? |
| Scattering parameters | | | | |
| $^3a_{np}(\text{fm})$ | 5.45 | 5.46 | 5.427 | 5.424(4) |
| $^3r_{np}(\text{fm})$ | 1.80 | 1.81 | 1.766 | 1.748(6) |
| $^1a_{np}(\text{fm})$ | -23.67 | -23.70 | | -23.715 |
| $^1r_{np}(\text{fm})$ | 2.77 | 2.78 | | 2.73(3) |

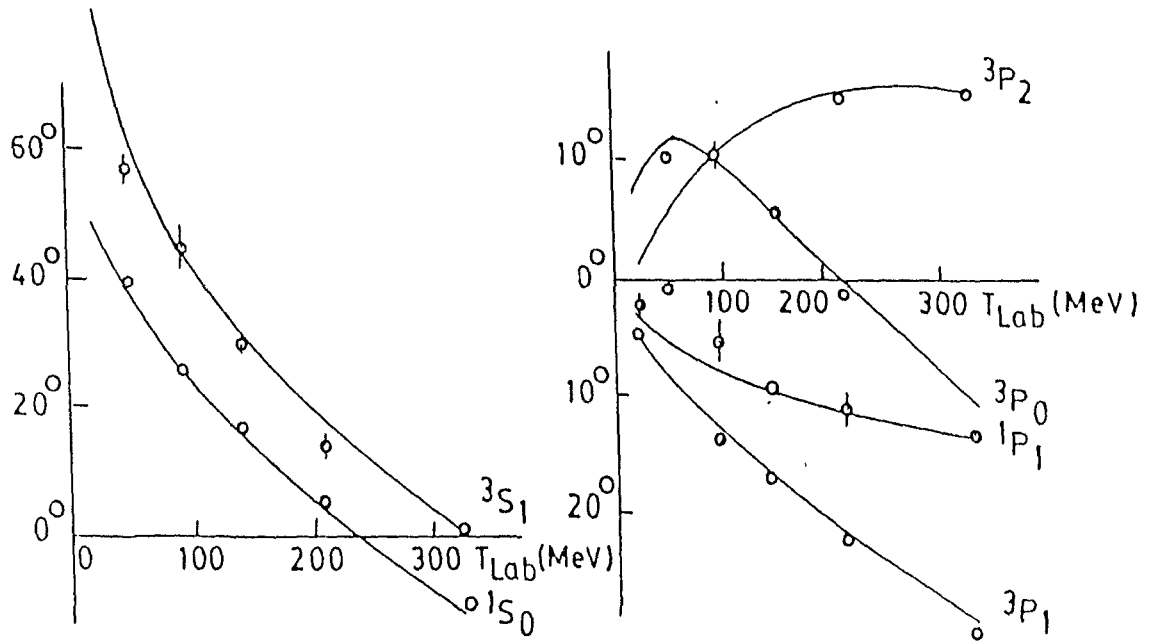


Figure 1: S- and P- wave phase shifts of the parameterized Paris potential.

References

1. Lecture Notes in Physics , (Chapter-1), 144, Springer-Verlag, Berlin
(1981)
2. N.Mukhin , Experimental Nuclear Physics (Vol II)
Moscow : Mir Publishers (1987)
3. H.Yukawa, Proc. Phys. Math. Soc. (Japan) 17, 48 (1935)
4. R.B.Wiringa et.al., Phys. Rev. C 29, 4, 1207 (1984)
5. F.E. Close , An Introduction to Quarks and Partons,
Academic Press (London) 1979.
6. C.De Tar , Phys. Rev. D17, 302 (1978) : 17, 323(1978)
7. C.S.Warke and R.Shanker , Phys. Rev. C21, 2463 (1980)
8. M.Harvey , Nucl. Phys. A352, 326 (1981)
9. O.Chamberlain et.al. , Phys. Rev 105 , 288 (1957)
10. H.P. Stapp et.al. , Phys. Rev. 105 , 302 (1957)
11. T.Hamada and I.O.Johnston, Nucl. Phys. 34, 382 (1962)
12. R.V.Reid , Ann of Phys. 50, 411 (1968)
13. R.Machleidt et.al. , Phys. Reports 149,1(1987)
14. I.E. Lagaris and V.Pandharipande, Nucl. Phys. A359, 331 (1981)
15. A.D. Jackson et.al., Nucl. Phys. A249, 397 (1975)
16. R.Vinh Mau et.al. , Phys. Lett. 44B, 1(1973)
17. W.N.Cottingham et.al. , Phys. Rev. D8 , 800(1973)
18. M.Lacombe et.al., Phys. Rev. D12 , 1495(1975)
19. M.Lacombe et.al. , Phys. Rev. C21, 861(1981)
20. M.Lacombe et.al. , Phys. Rev. C23, 2405(1981)
21. J.L.Gammel and R.M.Thaler , Phys. Rev. 107, 291 (1957)

- 22. P.S.Signell and R.E.Marshak , Phys. Rev. 106, 832 (1957) ;
109, 1229 (1958)
- 23. S.Gartenhaus , Phys. Rev. 100, 900(1955)
- 24. M.Levy, Phys. Rev. 88, 725 (1952)
- 25. S.Ohnuma and D.Feldman , Phys. Rev. 102, 1641 (1956)
- 26. P.S.Signell et.al. , Phys. Rev. Lett. 1, 416 (1958)
- 27. R.A.Bryan, Nuovo Cim. 16, 895 (1960)
- 28. D.P.Saylor et.al., Phys. Rev. Letts 5, 266 (1960)
- 29. K.E.Lassila et.al., Phys. Rev. 126, 881 (1962)

Chapter - 3

Field Theoretical Approach

Introduction :

As mentioned earlier in chapter 1 and 2, the Yukawa's arguments are being presented as follows .

According to quantum mechanics there exists the uncertainty relation for energy - time observables :

$$\Delta E \cdot \Delta t \sim h$$

$$\implies \Delta E \sim \frac{h}{\Delta t}$$

This energy may be accountable for creating virtual meson with mass ,

$$m = \frac{\Delta E}{c^2} = \frac{h}{c^2 \Delta t} \text{ for a short time } \Delta t.$$

The virtual particles exist only for a short span of time Δt during which they are separated from the nucleon by a distance 'a' not surpassing $a = c\Delta t$. After the passage of time Δt , the virtual particle is "captured" again by a nucleon. It can be tacited that the nucleon is encircled by a cloud of virtual mesons which are continuously being created and annihilated.

The radius of the meson - cloud is given by

$$a = \frac{ch}{\Delta E} = \frac{ch}{mc^2} = \frac{h}{mc}$$

It is the transfer of a virtual mesons form one nucleon to another which is responsible for the nuclear interaction.

Yukawa obtained the nuclear interaction time :

$$\tau_{\text{nucl}} = \Delta t = \frac{h}{\Delta E} = \frac{ha}{hc} = \frac{a}{c} = 0.7 \times 10^{-23} \text{ seconds}$$

$$\text{and } \Delta E \simeq \frac{h}{\Delta t} \simeq \frac{1.1 \times 10^{-34} \text{ J-sec}}{0.7 \times 10^{-23} \text{ sec}} \simeq 100 \text{ MeV} = 200 m_e$$

This is how Yukawa meson was predicted.

In 1938, μ - mesons were discovered in cosmic rays. It was speculated that it is the quanta of nuclear interaction. The mass of μ - meson was determined to be $\sim 207 m_e$. However, it was soon realized that muons do not participate in strong nuclear interactions.

3.1 Yukawa potential

The energy - momentum relation for a freely moving particle is given by (2-4)

$$E^2 = p^2 c^2 + m^2 c^4, \quad (\text{for particle with } m \neq 0)$$

———— (1)

where E is the total energy, including the rest mass energy.

Applying the quantum mechanical operators in equation 1),

$$\vec{p} \longrightarrow -i\hbar \vec{\nabla}$$

$$\text{and } E \longrightarrow i\hbar \frac{\partial}{\partial t},$$

gives

$$-\hbar^2 \frac{\partial^2}{\partial t^2} = -\hbar^2 c^2 \nabla^2 + m^2 c^4 \quad \text{———— (2)}$$

By operating on $\phi(\vec{r}, t)$, the operator equation (2) gives the following relativistic equation for the free particle :

$$-\hbar^2 \frac{\partial^2 \phi(\vec{r}, t)}{\partial t^2} = -\hbar^2 c^2 \nabla^2 \phi(\vec{r}, t) + m^2 c^4 \phi(\vec{r}, t)$$

$$\text{or } (\hbar^2 c^2 \nabla^2 - \hbar^2 \frac{\partial^2}{\partial t^2} - m^2 c^4) \phi(\vec{r}, t) = 0$$

$$\text{or } (\nabla^2 - \frac{1}{c^2} \frac{\partial^2}{\partial t^2} - \frac{m^2 c^2}{\hbar^2}) \phi(\vec{r}, t) = 0 \quad \text{--- (3)}$$

Incorporating interaction also , the equation 3) becomes

$$\nabla^2 \phi - \frac{1}{c^2} \frac{\partial^2 \phi}{\partial t^2} - \frac{m^2 c^2}{\hbar^2} \phi = 4\pi g_N , \quad \text{--- (4)}$$

where g_N is the density of meson charge of the nucleon.

The solution of the above equation for the time - independent case is of the form

$$\phi = - g_N \frac{e^{-r/\lambda}}{r} , \quad \text{where } \lambda = \hbar/mc.$$

Therefore, the interaction of a nucleon with the meson field is given by

$$V = g_N \phi = - g_N^2 \frac{e^{-r/\lambda}}{r}$$

This is the Yukawa potential for the exchange of pions between the nucleons.

Here the negative sign shows the attractive character of nuclear potential.

3.2 Post Yukawa field theoretic approaches

After the detection of pions more methodical work was started to study the nuclear forces . The nuclear forces were divided into three regions , a "classical" (long range , $r \geq 2$ fm , where r denotes the distance between the centres of two nucleons) , a "dynamical" (intermediate range , $1 \text{ fm} < r < 2 \text{ fm}$), and a "core" region (short range $r < 1 \text{ fm}$). The classical region is dominated by one - pion exchange. The

two pion exchange is the keystone in the intermediate range although heavier mesons exchanges (like ρ , ω , etc) also have their relevance. Finally many different processes play role in the core region, like the multiplication exchanges, heavy mesons of various kinds and quark - gluon exchange.⁽⁵⁾

In the 1950s the one pion exchange was ascertained as the long range part of the nuclear force, the evidence of which came from the analysis of Nucleon - Nucleon scattering data and the deuteron properties. In the case of the deuteron, the quadropole moment can be well explained by the one pion exchange potential⁽⁶⁾.

Also, the asymptotic D/S state ratio of the deuteron wave functions provides convinicing evidence for the dominance of one pion exchange in the tail region ($r > 2$) fm.⁽⁷⁾

Now after one pion exchange the two pion exchange contribution to the nucleon-nucleon interaction was first tried. A lot of problems occurred when the 2π - exchange contribution to the NN interaction was first (in 1950s) tried. The various efforts of pion-theoretical potential are broadly divided into two groups: The Taketani-Machida-Onuma⁽⁸⁾ and the Bruckner-Watson⁽⁹⁾ type.

The main difference between the two approaches were that the box - diagrams (i.e. fig 1a) and pair terms (i.e. fig 1c) and 1d) were always included in the Taketani - Machida - Onuma, approach whereas Bruckner - Watson excluded the box diagram from the begining and can also at will drop out the pair terms. BW found almost an exact cancellation of one - pair (fig 1c) and two-pair contribution (fig 1d) to the NN

nucleons in the framework of the relativistic three-dimensional reduction of the Bethe - Salpeter⁽¹⁷⁾ equation suggested by Blankenbecler and Sugar⁽¹⁶⁾. In the following work⁽¹⁷⁾, the correlated 2π - S - Wave contribution was also studied. Nutt and Wilets⁽¹⁸⁾ developed a similar field - theoretical model with a difference that antiparticle contributions were ignored.

Recently Bonn group⁽¹⁹⁻³⁰⁾ has developed a program that includes all relevant diagrams in a field theoretical model.

3.3 The Bonn Potential

Bonn potential is a field theoretic attempt to obtain the NN potential from one - boson exchange. Bonn potential has gone through various stages of development and many versions of it are available in r - space and momentum space for use in various calculations. In the following we sketch the basic approach to calculate this potential from NN in a semirelativistic field theoretic way, using Feynman diagrams. We are mentioning this approach in some detail.

The respective Feynman diagram has been shown in fig 2). We are looking in the centre of mass system of two interacting nucleons, the momenta of the two incoming particles are \vec{q} and $-\vec{q}$, the outgoing momenta are \vec{q}' and $-\vec{q}'$ respectively. The nucleons have been treated on their mass shell" i.e.,

$$E = \sqrt{M^2 + \vec{q}^2} \quad \text{and} \quad E' = \sqrt{M^2 + \vec{q}'^2},$$

where M is the nucleon mass

Machleidt group have further assumed that the process takes place "on the energy shell" i.e. $E' = E$.

$$\frac{P_\alpha}{q^2 - m_\alpha^2} \approx \frac{P_\alpha}{(E' - E)^2 - (\vec{q}' - \vec{q})^2 - m_\alpha^2}$$

" On the energy shell"

$$\frac{P_\alpha}{q^2 - m_\alpha^2} = \frac{P_\alpha}{-(\vec{q}' - \vec{q})^2 - m_\alpha^2} = - \frac{P_\alpha}{(\vec{q}' - \vec{q})^2 + m_\alpha^2}$$

The interaction Lagrangian for meson - nucleon system is given by

$$L_i = g_i \bar{\psi} \Gamma_i \psi \phi_\alpha ; \quad i = 1, 2 ,$$

where ψ is the nucleon Dirac field

$\bar{\psi}$ is the adjoint nucleon Dirac field

and ϕ_α is the meson field operator.

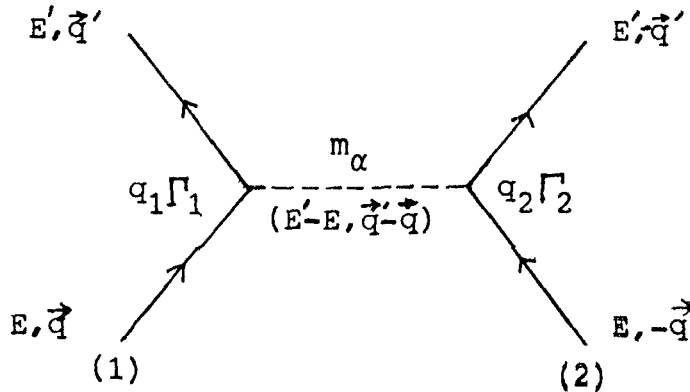


Figure 2: Feynman diagram representing a OBE exchange contribution to NN scattering in the centre of mass frame .Full lines denote nucleons ,the dashed line denote mesons.

Various Boson fields exchanges and their role in NN potential

(1) The pseudoscalar field (ps) Pseudoscalar mean that the field ϕ_{ps} switches sign in the case of either space or time reflection . Particles with negative intrinsic parity have this property e.g. π and η Lagrangian for the interaction is given by⁽²²⁾

$$L_{ps} = g_{ps} \bar{\psi} i\gamma_5 \psi \phi_{ps}$$

and OBE contribution (fig 2) for this interaction is given by

$$g_{ps}^2 \frac{\bar{u}_1(\vec{q}') i\gamma_5 u(\vec{q}) \bar{u}_2(-\vec{q}') i\gamma_5 u_2(-\vec{q})}{-(\vec{q}' - \vec{q})^2 - m_{ps}^2}$$

WE get for the whole diagram the following "momentum space potential"

$$\hat{V}_{ps}(\vec{k}) = - \frac{g_{ps}^2}{4M^2} \cdot \frac{\vec{\sigma}_1 \cdot \vec{k} \vec{\sigma}_2 \cdot \vec{k}}{\vec{k}^2 + m_{ps}^2}$$

where $\vec{k} = \vec{q}' - \vec{q}$ and $E = M$ has been assumed

$$\hat{V}_{ps}(\vec{k}) = - \frac{g_{ps}^2}{12M^2} \frac{3\vec{\sigma}_1 \cdot \vec{k} \vec{\sigma}_2 \cdot \vec{k}}{\vec{k}^2 + m_{ps}^2}$$

$$\hat{V}_{ps}(\vec{k}) = - \frac{g_{ps}^2}{12M^2} \frac{(\vec{\sigma}_1 \cdot \vec{\sigma}_2 + 3\vec{\sigma}_1 \cdot \vec{k} \vec{\sigma}_2 \cdot \vec{k} - \vec{\sigma}_1 \cdot \vec{\sigma}_2)}{\vec{k}^2 + m_{ps}^2}$$

$$S_{12}(\vec{k}) = 3\vec{\sigma}_1 \cdot \vec{k} \vec{\sigma}_2 \cdot \vec{k} - \vec{\sigma}_1 \cdot \vec{\sigma}_2 ,$$

where $\hat{k} = \vec{k} / |\vec{k}|$

$$\hat{V}_{ps}(\vec{k}) = -\frac{1}{12M^2} \cdot \frac{g_{ps}^2}{\vec{k}^2 + m_{ps}^2} \left\{ \vec{\sigma}_1 \cdot \vec{\sigma}_2 + S_{12}(\vec{k}) \right\}$$

By doing Fourier transformation into coordinate space

$$V_{ps}(\vec{x}) = \frac{1}{(2\pi)^3} \int d^3k e^{-i\vec{k} \cdot \vec{x}} V_{ps}(\vec{k})$$

$$= \frac{1}{(2\pi)^3} \cdot \frac{g_{ps}^2}{4M^2} (\vec{\sigma}_1 \cdot \vec{\nabla})(\vec{\sigma}_2 \cdot \vec{\nabla}) \int d^3k \frac{e^{i\vec{k} \cdot \vec{x}}}{\vec{k}^2 + m_{ps}^2}$$

$$= \frac{g_{ps}^2}{4\pi} \cdot \frac{1}{4M^2} (\vec{\sigma}_1 \cdot \vec{\nabla})(\vec{\sigma}_2 \cdot \vec{\nabla}) \frac{e^{-m_{ps}r}}{r}$$



where $r = |\vec{x}|$

$$= \frac{g_{ps}^2}{4\pi} \cdot \frac{m_{ps}^2}{12M^2} \left\{ \vec{\sigma}_1 \cdot \vec{\sigma}_2 + S_{12}(\hat{x}) \left[1 + \frac{3}{m_{ps}r} + \frac{3}{(m_{ps}r)^2} \right] \right\} \times \frac{e^{-m_{ps}r}}{r}$$

where $S_{12}(\hat{x})$ is the tensor operator

$$= 3 \vec{\sigma}_1 \cdot \hat{x} \vec{\sigma}_2 \cdot \hat{x} - \vec{\sigma}_1 \cdot \vec{\sigma}_2 \quad \text{and} \quad \hat{x} = \frac{\vec{x}}{r}$$

Since we know that the best known pseudoscalar field is the pion

There exists three charge states of the pion : + , - , neutral

Therefore, the Lagrangian is

$$L_{ps} = g_{ps} \bar{\psi} i \gamma_5 \vec{\tau} \psi \cdot \vec{\phi}_{ps},$$

where the three components of $\vec{\phi}_{ps}$ are now three charged states. $\vec{\tau}$ is the isospin operator for spin $\frac{1}{2}$ particles. $\vec{\tau} \cdot \vec{\phi}_{ps}$ is an invariant in isospin space.

The Scalar field Interaction Lagrangian for the scalar field is given as⁽²²⁾ $L_s = g_s \bar{\psi} \psi \phi$

The One - scalar - boson exchange contribution is

$$g_s^2 \frac{\bar{u}_1(\vec{q}') u_1(\vec{q}) \bar{u}_2(-\vec{q}') u_2(-\vec{q})}{(\vec{q}' - \vec{q})^2 - m_s^2}$$

We get for the whole diagram, the following "momentum space potential"

$$\hat{V}_{ps}(\vec{k}) = - \frac{g_s^2}{\vec{k}^2 + m_s^2} \left\{ 1 + \frac{\frac{1}{2}(\vec{\sigma}_1 + \vec{\sigma}_2) \cdot (-i)(\vec{k} \times \vec{p})}{2M^2} \right\},$$

where $\vec{k} = (\vec{q}' - \vec{q})$ and $\vec{p} = \frac{1}{2}(\vec{q} + \vec{q}')$

The first term on the right hand side is the strong attractive central force, the second a spin - orbit force.

Introducing the total spin $\vec{S} = \frac{1}{2}(\vec{\sigma}_1 + \vec{\sigma}_2)$

The Fourier transform of the previous equation is given by

$$\frac{1}{(2\pi)^3} \int d^3k \vec{S} \cdot (-i) (\vec{k} \times \vec{p}) \frac{e^{i\vec{k} \cdot \vec{x}}}{\vec{k}^2 + m_s^2}$$

$$= \vec{S} \cdot \vec{L} \frac{m_s^2}{4\pi r} \left\{ \frac{1}{m_s r} + \frac{1}{(m_s r)^2} \right\} \frac{e^{-m_s r}}{r}$$

where $\vec{L} = \vec{r} \times \vec{p}$

The full r - space scalar exchange potential will be

$$V_s(\vec{x}) = -\frac{g_s^2}{4\pi} \left\{ 1 + \vec{L} \cdot \vec{S} \frac{1}{(2M^2)} \frac{m_s^2}{m_s r} + \frac{1}{(m_s r)^2} \right\} \frac{e^{-m_s r}}{r}$$

The scalar meson exchange causes a strong attractive central force and a spin - orbit force.

iii) The Vector field (V) Interaction Lagrangian for the vector field is given as⁽²²⁾ $L_v = g_v \bar{\psi} \partial_\mu \psi \phi_\mu^v$

The one - vector - boson exchange contribution is

$$g_v^2 \frac{\bar{u}_1(\vec{q}') \gamma_\mu u_1(\vec{q}) (-g^{\mu\nu}) \bar{u}_2(-\vec{q}') \gamma_\nu u_2(\vec{q})}{-(\vec{q}' - \vec{q})^2 - m_v^2}$$

We get for the whole diagram the following "momentum space potential"

$$\hat{V}_v(\vec{k}) = \frac{g_v^2}{\vec{k}^2 + m_v^2} \left\{ 1 - 3 \frac{\vec{S} \cdot (-i) (\vec{k} \times \vec{p})}{2M^2} \right\}$$

Therefore, with the help of Fourier transform

$$V_v(\vec{x}) = -\frac{g_v^2}{4\pi} \left\{ 1 - \vec{L} \cdot \vec{S} \frac{3m_v^2}{2M^2} \left[\frac{1}{(m_v r)} + \frac{1}{(m_v r)^2} \right] \right\} \frac{e^{-m_v r}}{r}$$

We find a strong repulsive central force and a spin - orbit force which has the same sign as in the scalar case.

(iv) The Tensor field Interaction Lagrangian for the field is given as

$$L_t = \frac{f_v}{2M} \bar{\psi} \sigma_{\mu\nu} \psi \partial^\mu \phi^\nu$$

$$\text{where } \sigma_{\mu\nu} = \frac{i}{2} [\gamma_\mu, \gamma_\nu] = \frac{i}{2} (\gamma_\mu \gamma_\nu - \gamma_\nu \gamma_\mu)$$

$$\text{the vertex is } \Gamma_{t,v} = -i \frac{f_v}{2M} \sigma_{\mu\nu} (q - q')^\mu$$

For the tensor coupling the corresponding expression is

$$\begin{aligned} \hat{V}_t(\vec{k}) &= -\frac{f_v^2}{4M^2} \frac{(\vec{\sigma}_1 \times \vec{k}) \cdot (\vec{\sigma}_2 \times \vec{k})}{\vec{k}^2 + m_v^2} \\ &= \frac{f_v^2}{12M^2} \left\{ 2 \vec{\sigma}_1 \cdot \vec{\sigma}_2 - 2 \vec{\sigma}_1 \cdot \vec{\sigma}_2 \frac{m_v^2}{\vec{k}^2 + m_v^2} - \frac{S_{12}(\vec{k})}{\vec{k}^2 + m_v^2} \right\} \end{aligned}$$

From the Fourier transform again, we have

$$V_t(\vec{x}) = \frac{f_v^2}{4\pi} \cdot \frac{m_v^2}{12M^2} \left\{ 2 \vec{\sigma}_1 \cdot \vec{\sigma}_2 \right.$$

$$- S_{12}(\hat{x}) \left[1 + \frac{3}{m_v r} + \frac{3}{(m_v r)^2} \right] \left\{ \frac{e^{-m_v r}}{r} \right.$$

The tensor force obtained has the opposite sign compared to the π case. We shall now look into physical manifestation of the field described theoretically so far. In the mass range below the nucleon mass, there are two pseudoscalar particles, namely π (138) and η (550) and two vector particles ρ (769) and ω (783). The various coupling constants $g_{NN\alpha}^2/4\pi$ for $\alpha = \pi, \eta, \rho, \omega$, etc are given in table 1 and 2.

The isoscalar ω has a strong vector coupling and the isovector ρ has a strong tensor coupling to the nucleon. There exist also an isovector scalar meson δ (983), which, due to its large mass and its small coupling constant, provides only a small contribution.

Compared to the (isovector) π , the contribution from the (isoscalar) η is very small because the coupling constant of the η is small, and second the mass of the η is substantially larger than the pion mass. The magnitude of One - meson exchange contribution is roughly proportional to $g_{\alpha}^2/m_{\alpha}^2$. Therefore, η is not important for the NN system. Providing as isospin - independent tensor force, the essential effect of the η are that it lowers the $3P_1$, raises the $3P_0$ phase shifts, and slightly reduces the $3S-3D$ tensor force. The η' due to larger mass (958) is not taken into account in boson - exchange model⁽³²⁾.

Therefore, the pion as the lightest particle provides the long range force and due to its pseudoscalar nature, the tensor force. This tensor force is reduced at short ranges by the ρ meson to a realistic size.

Since π and ρ are isovector particles , therefore , they imply a strong isospin dependence for spin - orbit force . The ω creates the short range repulsion and the spin - orbit force.

However , there are a few mesons of mass $\sim 1\text{GeV}$ e.g. ϕ (1020) and $S^*(975)$. These mesons have a considerable $S\bar{S}$ content ($S \rightarrow$ strange quark), their coupling to the nucleon is , therefore, suppressed according to the Zweig rule .(33)

There are many authentic reasons not to consider other mesons. First , their contribution is masked to a considerable extent by the strong short - range repulsion originating from ω -exchange . Then we have to apply the form factors (cutoffs) to each meson-nucleon vertex in the meson theory. In the figures 3,4 and 5) , the different potentials V_c , V_t and V_{LS} has been plotted for the different mesons.

The following operator structure is assumed to each spin - isospin state :

$$V(r) = V_c(r) + V_T(r) S_{12} + V_{LS}(r) \vec{L} \cdot \vec{S} ,$$

where on the right hand side we have the central, tensor and spin orbit force, S_{12} is the r - space tensor operator which is given as

$$S_{12} = \frac{(\vec{\sigma}_1 \cdot \vec{r})(\vec{\sigma}_2 \cdot \vec{r})}{r^2} - \vec{\sigma}_1 \cdot \vec{\sigma}_2$$

and the total isospin of the two nucleon system is denoted by T .

Till now we have not mentioned about the intermediate range attraction . We have to consider plural meson exchange and we shall see how that provides us with the missing parts.

The 2π exchange

The essential features of the model (fig 6) are that it takes the effects from nucleon resonances (isobars) and direct $\pi\pi$ - interaction into account. The effect of other resonances have been found out to be negligible .

Machleidt group have considered the various crossed box diagrams which were first neglected in the calculation due to the extreme complexity. However , it was found that they are non - negligible and help to provide on isoscalar character for the 2π - exchange contributions.

Macheleidt group checked their 2π - exchange model on high partial waves , then they proceeded to state of lower angular momentum , which showed that a model consisting of one - meson exchange and 2π - exchange only is unable to describe the empirical NN data.

The $\pi\rho$ exchange From OBE it is known that the π - and ρ - mesons play the role of opponents because their tensor forces have opposite sign . It is , therefore , tempting to include next to the π and ρ , the two - boson exchange diagrams expecting them to counterbalance the corresponding 2π contributions . Fig 7) displays the processes to be considered in analogy to the diagrams of uncorrelated 2π - exchange .

The effect of $\pi\rho$ contributions is to functions as a counterpart of the 2π exchange contributions . The 2π - exchange provides also rather short - ranged contributions which are sufficiently counterbalanced by the $\pi\rho$ exchange .

This group also gave a thought to 3π - and 4π exchanges in an approximate way. However, it turns out to be of little importance as they

cancel each other to a large extent. Here we are mentioning the deuteron properties and low energy NN parameters. The comparison has been made with the experimental values (Table 3).

A few phase-shifts of NN scattering has been shown in fig (8) .

Table 1 : Various meson - nucleon couplings and their contributions to the nuclear force as obtained by one - boson - exchange

| Coupling Bosons | | | Characterstics of Predicted forces | | | |
|-----------------|-------------------------|---|------------------------------------|------------------------------------|-------------------|------------------------------|
| | (Strength of Coupling | | | | | |
| | I = 0 | I = 1 | Central | Spin-Spin | Tensor | Spin-Orbit |
| | | | [1] | $[\vec{\sigma}_1, \vec{\sigma}_2]$ | $[S_{12}]$ | $(\vec{L} \cdot \vec{S})$ |
| ps | [1] η (weak) | $[\vec{\tau}_1, \vec{\tau}_2]$ π (strong) | - | weak coherent with v,t | strong | - |
| S | σ (strong) | δ (weak) | strong attractive | - | - | coherent with v |
| V | ω (strong) | ρ (weak) | strong repulsive | weak coherent with ps | opposite to ps | strong coherent with s |
| t | ω (weak) | ρ (strong) | - | weak coherent with ps | opposite to ps | - |

Table 2 : Meson-nucleon coupling constants used in full Bonn model .

| N N M couplings | Bonn |
|-----------------|---------------|
| NN π | 14.08 |
| NN η | 0 |
| NN ρ | 0.41 [6.1] |
| NN ω | 10.6 [0.0] |
| NN σ | 4.56 |
| NN δ | 1.62 |

For vector mesons , the $\left(\frac{\text{tensor}}{\text{vector}} \right)$ ratio is quoted in square brackets

Table 3 Deuteron and low energy parameters predicted
by BONN model

| Deuteron | Theory | Expt |
|---|---------|------------------------|
| Binding energy , E_B (MeV) | 2.22465 | 2.22463(3) |
| D-State probability, P_D (%) | 4.25 | 4 - 7 |
| Quadropole moment Q_d (fm ²) | .2807 | 0.2860 \pm 0.0015 |
| Asymptotic D/S - state | 0.0267 | 0.0271 \pm 0.0004 |
| R.M.S. radius (in fm) | 2.0016 | 1.9635 \pm 0.0045 |

| <u>n p low energy scattering</u> | | | |
|----------------------------------|--------------|---------|-------------------|
| Singlet | a_s (fm) | -23.740 | -23.715(15) |
| | r_s (fm) | 2.766 | 2.73(3) |
| Triplet | a_t (fm) | 5.427 | 5.424 \pm 0.004 |
| | r_t (fm) | 1.755 | 1.748 \pm 0.006 |

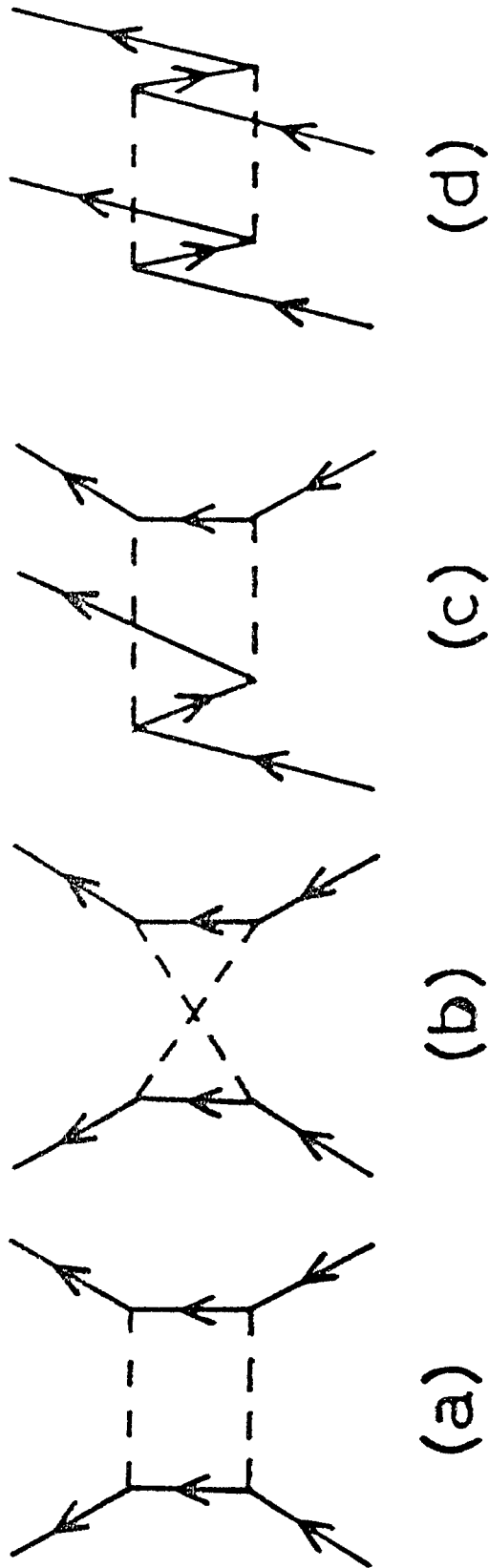


Figure 1 : Some two - pion - exchange contributions to the NN interaction.

- (a) is a box diagram,
- (b) a crossed box;
- (c) and (d) contain virtual pairs.

Full lines denote nucleons, dashed lines pions.

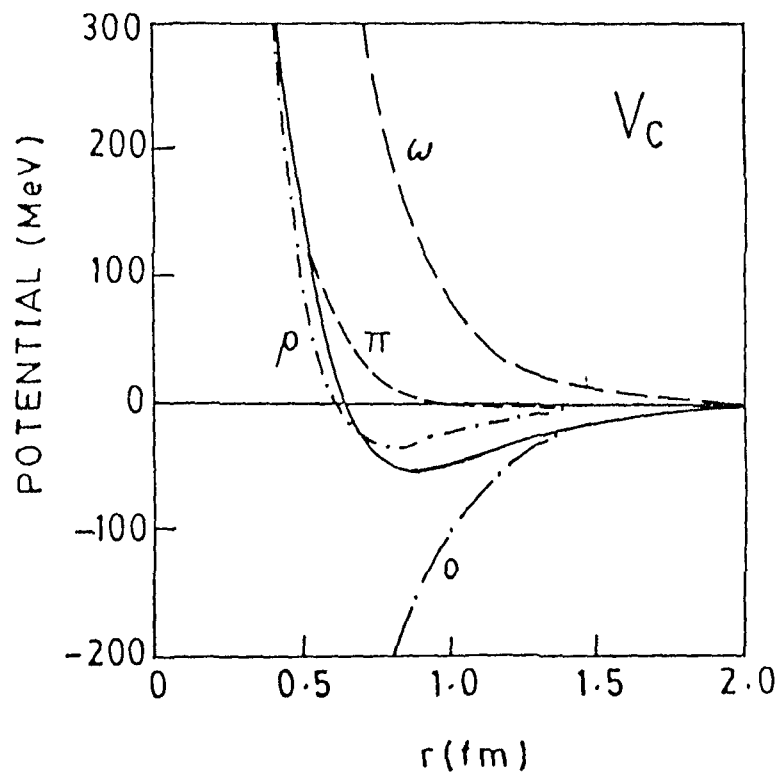


Figure 3 : Contributions from single mesons to the even-singlet central potential. The solid line represents the full potential.

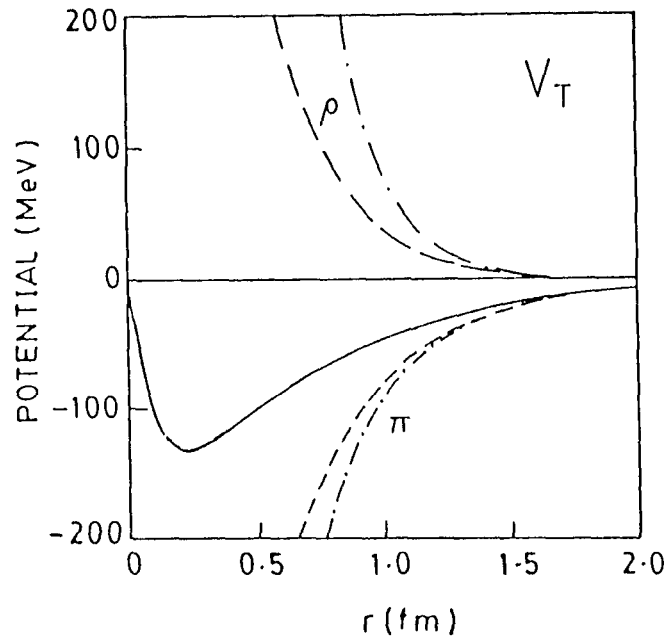


Figure 4 : The contributions from π and ρ (dashed) to the $T=0$ tensor potential. The solid line is the full potential. The dash-dot lines are obtained when the cutoff is omitted.

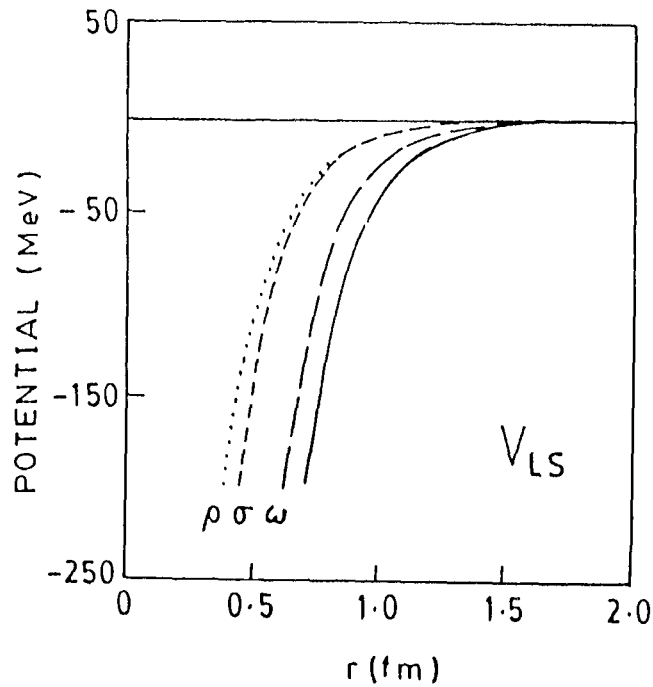


Figure 5 : The contributions from single meson to the $T=1$ spin-orbit potential, as denoted. The solid line is the full potential.

$$\begin{aligned}
& \text{Diagram: Two vertical lines with shaded ellipses at the ends, connected by two horizontal dashed lines labeled } \pi. \\
& = \begin{aligned} & \left[\text{Diagram: Two vertical lines connected by two horizontal dashed lines labeled } \pi \right] + \left[\text{Diagram: Two vertical lines connected by two crossed dashed lines labeled } \pi \right] & 2\pi NN \\ & + \left[\text{Diagram: Two vertical lines, the left one is double, connected by two horizontal dashed lines labeled } \pi \right] + \left[\text{Diagram: Two vertical lines, the left one is double, connected by two crossed dashed lines labeled } \pi \right] & 2\pi N\Lambda \\ & + \left[\text{Diagram: Two vertical lines, both are double, connected by two horizontal dashed lines labeled } \pi \right] + \left[\text{Diagram: Two vertical lines, both are double, connected by two crossed dashed lines labeled } \pi \right] & 2\pi\Delta\Delta \\ & + \left[\text{Diagram: Two vertical lines connected by two dashed lines that meet at a circle with an 'S' inside} \right] + \left[\text{Diagram: Two vertical lines, the left one is double, connected by two dashed lines that meet at a circle with an 'S' inside} \right] + \left[\text{Diagram: Two vertical lines, both are double, connected by two dashed lines that meet at a circle with an 'S' inside} \right] & \pi\pi\text{-}S_{\text{CORR}} \\ & + \left[\text{Diagram: Two vertical lines connected by a wavy line labeled } \rho \right] & \rho \end{aligned}
\end{aligned}$$

Figure 6 : Field - theoretic model for the 2π -exchange. Full lines represent nucleons, double lines isobars, and dashed lines pions. The circles are $\pi\pi$ correlations.

$$\begin{array}{c} \text{---} \pi \text{---} \\ | \quad \quad | \\ \text{~~~~} \rho \text{~~~~} \end{array} + \begin{array}{c} \text{---} \pi \text{---} \\ | \quad \quad | \\ \text{~~~~} \rho \text{~~~~} \end{array} \quad \pi \rho NN$$

$$\begin{array}{c} \text{---} \pi \text{---} \\ | \quad \quad | \\ \text{~~~~} \rho \text{~~~~} \end{array} + \begin{array}{c} \text{---} \pi \text{---} \\ | \quad \quad | \\ \text{~~~~} \rho \text{~~~~} \end{array} \quad \pi \rho N \Delta$$

$$\begin{array}{c} \text{---} \pi \text{---} \\ | \quad \quad | \\ \text{~~~~} \rho \text{~~~~} \end{array} + \begin{array}{c} \text{---} \pi \text{---} \\ | \quad \quad | \\ \text{~~~~} \rho \text{~~~~} \end{array} \quad \pi \rho \Delta \Delta$$

Figure 7 : $\pi\rho$ contributions to the NN interaction.

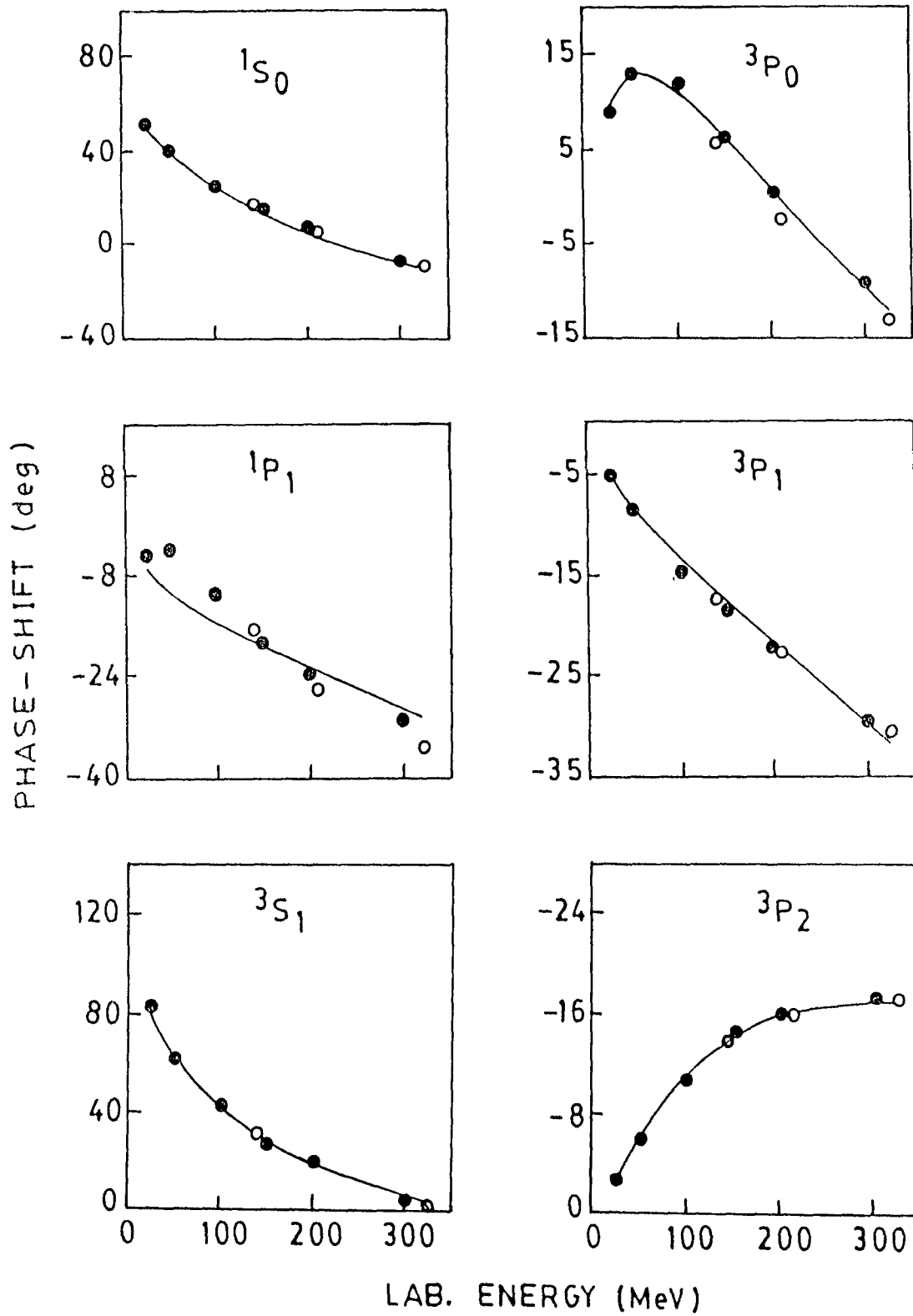


Figure 8 : A few phase shifts of NN scattering. The solid line represents the result predicted by full Bonn model.

References

1. Experimental Nuclear Physics Volume II
K.N.Mukhin , Mir Publishers - 1987 , Moscow.
2. H. Yukawa , Proc. Phys . Math . Soc. Japan 17 , 48 (1935)
3. H. Yukawa et.al., Proc . Phys. Math . Soc . Japan 20 , 319 (1938)
4. Introductory Nuclear Theory .
L.R.B. Elton , ELBS and SIR Isaac Pitman and Sons . Ltd,London (1959)
5. R. Machleidt et.al., Phys. Reports 149 , No.1 (1987)
M. Taketani et.al., Prog. Theor. Phys. (Kyoto) 6, 581 (1951)
6. N.K. Glendenning and G. Kramer , Phys. Rev. 126 , 2159 (1962)
J. Iwadare et.al., Prog. Theor . Phys. (Kyoto) 16 , 455 (1956)
7. D.Y.Wong, Phys. Rev.Lett 2 , 406 (1959).
8. M. Taketani et.al. , Prog. Theor. Phys. (Kyoto) 7 , 45 (1952)
9. K.A. Bruckner and K.M. Watson , Phys. Rev. 90 , 699 ; 92 , 1023 (1953)
10. N. Hoshizaki and S. Machida , Prog. Theor . Phys. (Kyoto) 27(1962) 288
11. R.J.N.Phillips , Rep. Prog. Phys. 22 562 (1959)
12. P.Signell , Advances in Nucl. Phys. 2 223 (1969)
13. M.H. Partovi and E.L. Lomon , Phys. Rev. D2, 1999 (1970)
14. M.H. Partovi and E.L. Lomon , Phys. Rev. D5, 1192(1972)
E.L.Lomon , phys. Rev. D14 2402 (1976)
15. E.E. Salpeter and H.A. Bethe , Phys. Rev. 84 , 1232 (1951)
16. R.Blankenbecler and R. Sugar , Phys. Rev. 142 , 1051 (1966)
17. E.L.Lomon, Phys. Rev. D22 , 229 (1981)
18. W.T. Nutt and L. Wilets Phys . Rev . D7 , 110 (1975)
19. K. Holinde and R. Machleidt , Nucl. Phys. A 372, 349 (1981)

20. K. Holinde and R. Machleidt Nucl. Phys. A 280 , 429 (1977)
21. R. Machleidt , Advances in Nuclear Physics , Vol 19
(J.W.Negele and E.Vogt , eds) ; Plenum Press . New York
22. R. Machleidt , "Relativistic Dynamics and Quark - Nuclear Physics"
(Johnson and Picklesimer eds) John Wiley and Sons , New York (1986)
23. K. Erkelenz et.al., Nucl. Phys. A 139 , 308 (1969)
24. K. Kotthoff et.al , Nucl . Phys. A 242, 429 (1975)
25. K. Holinde and R. Machleidt , Nucl. Phys A 247 , 495 (1975)
26. K. Holinde and R. Machleidt , Nucl. Phys. A 256, 479 (1976);
Nucl Phys A 264 , 484 (1976)
27. K. Holinde et.al., Phys. Rev. C , Vol 18, No.2 , 870 (1978);
Phys. Rev. C, Vol 19, No.3 , 948 (1979).
28. R. Machleidt and K. Holinde , Nucl. Phys. A 350, 396 (1980)
29. K. Holinde and R. Machleidt , Nucl. Phys. A 372, 349 (1981);
Holinde et.al. , Phys Rev. C, Vol 24, No.3 , 1159 (1981)
30. K.Holinde , Nucl. Phys. A 415, 477 (1984)
31. G.E. Brown and A.D. Jackson , The Nucleon - Nucleon Interacton,
North Holland , Asterdam (1976)
32. W. Grein and P. Kroll, Nucl. Phys. A 338, 332 (1980)
33. F.E.Close, Introduction to Quarks and Partons,
Academic Press , London (1979).

Chapter 4

Experimental studies on Λ - N interaction

Introduction :

The nuclear structure has always been an interesting subject of investigation using different probes. Unlike nucleon - nucleon interaction the Λ - nucleon interaction is still quite unknown. From the experimental data on binding energy of hypernuclei we know that Λ - nucleon interaction is weaker than the nucleon - nucleon interaction. The experimental information about Λ - nucleon interaction is obtained from the following sources :

- (1) Hyperon binding energy in hypernuclei
- (2) Λ - nucleon scattering experiment
- (3) Hypernuclear Decays
 - (3.1) Weak Decays
 - (3.2) Electromagnetic Decays

4.1 Binding Energy of the Λ particle in Nuclear Matter.

As discussed in the introductory chapter the binding energies of the Λ particle (B_Λ) in the nuclear ground states are the fundamental source of information on the Λ - nucleus interaction.

The binding energy of the Λ particle in the ground state (B_Λ) may be defined as the minimum energy needed to remove the Λ particle from the core of the hypernucleus iff it remains in the ground state. The kinematical analysis of decay fragments in nuclear emulsions is the most appropriate method for determining the binding energy of the Λ particle in the

hypernucleus. The binding energy of Λ hypernuclei, in other words may be defined as the difference in the Q value of its decay product and the Q value (37MeV) of free Λ - decay . It has been concluded on the basis of experiences that decays with charged mesons and all fragments producing visible tracks can only be taken into account with measuring binding energies. However , these can be realized only for the hypernuclei having mass number less than 16 ($A < 16$) . There is no reliable experimental data for $A > 16$, because the decay of heavy hypernucleus can not be identified uniquely⁽¹⁻³⁾. The various experimentally determined binding energies through emulsion techniques have been tabulated in Table 1 .

However , an upper limit B_Λ (ground state) for heavier hypernuclei has been estimated from the observed decays accompanied by pion emission .

The K^- interaction with Ag and Br nuclei in emulsion produces hypernuclei in the mass region $60 < A < 100$. The binding energy of $^{32}_{\Lambda}\text{S}$ is measured from its spectrum produced via the (K^- , π^-) strangeness exchange reaction ($B_\Lambda \simeq 17.5$ MeV) . Also the (K^- , π^-) reaction studies have yielded binding energy for $^{12}_{\Lambda}\text{C}$, $^{27}_{\Lambda}\text{Al}$, $^{32}_{\Lambda}\text{S}$, $^{40}_{\Lambda}\text{Ca}$, $^{209}_{\Lambda}\text{Bi}$. it has been shown in fig (1) .

The hypernuclei with $A \simeq 100$ are not expected to have a strong variation of B_Λ (ground state) with A. In fig (2) the variation of B_Λ with $A^{-2/3}$ has been shown for heavier hypernuclei with $r_0 = 1.1$ fm and 1.45 fm.

The B_Λ values obtained by extrapolating from the light hypernuclei agrees well with the theoretical estimations.⁽¹⁾

— At Brookhaven - LANL - Houston - Tohoku - TRIUMF - Vassar - CMU

-FSU - Mississippi collaboration has measured ⁽⁴⁾ the (π^+, K^+) cross sections on ^9Be , ^{12}C , ^{13}C , ^{16}O , ^{28}Si , ^{40}Ca , ^{51}V , and ^{89}Y target at P_π 1.05 GeV/c. ⁽⁷⁾

The data for $^{89}\text{Y}(\pi^+, K^+)\Lambda$ has been shown in fig (3). A series of sharp peaks has been observed. These peaks have been identified as s_Λ , p_Λ , d_Λ and f_Λ bound state of the Λ . The nodeless g_Λ has been predicted ⁽⁵⁾ to lie about 5 MeV in the continuum near $A = 90$ with an elastic width of approximately 900 keV. This width is small due to the relatively large l , of the state. The (π^+, K^+) data from emulsion studies ⁽⁶⁾ gives accurate values for S_Λ binding energies in light nuclei and upper limits on B_Λ for medium mass nuclei ⁽⁷⁾.

With the energy dependent local potential $V(r, E)$ of the form ⁽⁸⁾,

$$V(r, E) = \frac{m_\Lambda^*(r)}{m_\Lambda} U(r) + \left[\frac{1 - m_\Lambda^*(r)}{m_\Lambda} \right] E \quad \text{--- (1)}$$

$$U(r) = \tilde{t}_0 \rho(r) + \frac{3}{8} t_3 \rho^2(r) + \frac{1}{4} (t_1 + t_2) T(r)$$

$$T(r) = \frac{3}{5} \left(\frac{3}{2} \pi^2 \right)^{2/3} \rho^{5/3}(r)$$

$$\frac{\hbar^2}{2m_\Lambda^*(r)} = \frac{\hbar^2}{2m_\Lambda} + \frac{1}{4} (t_1 + t_2) \rho(r),$$

(where m_Λ is the free space Λ mass and $m_\Lambda^*(r)$ is the effective Λ mass in the nuclear medium of density $\rho(r)$) the Λ -binding energy is estimated.

Using equation (1) with the parameter

$$\tilde{t}_0 = -402.6 \text{ MeV fm}^3$$

$$t_3 = 3394.6 \text{ MeV fm}^6$$

$$t_1 + t_2 = 103.44 \text{ MeV fm}^5$$

gives an excellent fit to all the existing B_Λ data shown in fig (1).

These values correspond to an effective mass

$$\frac{m_\Lambda^*}{m_\Lambda}(0) = 0.8 \text{ in the interior of the hypernucleus and a well depth}$$

$$D_\Lambda \sim 27.5 \text{ MeV.}$$

It has been observed that a small fraction of heavy hypernuclei decays by emission of π^- . Since, most of the π^- are absorbed by the nucleus therefore, only less than 1 % of the decays are accompanied by a visible π^- track. By analyzing a large sample of data of hypernuclear decay the maximum π^- energy has been estimated.

The Q value for $\Lambda \longrightarrow p + \pi^-$ decay is 35.7 MeV. All proton states in the nucleus are occupied upto the Fermi surface. Due to the Pauli principle the proton produced in the Λ decay can not remain strongly bound in the nucleus and will jump at least to the lowest unoccupied level. In heavy nuclei the energetically lowest free levels are at the binding energy of Λ . The binding energy in heavy hypernuclei has been estimated to be $B_\Lambda \sim 22.7 \pm 0.4 \text{ MeV}$. From this value of B_Λ the depth of the potential well of the Λ particle in the nucleus has also been determined. ⁽⁷⁾

B_Λ (ground state) of hypernuclei can also be obtained by assuming that Λ feels a potential well of radius R approximately equal to that of the nuclear core and a depth D_Λ independent of the hypernuclear mass. Since the Λ particle in the hypernuclear ground state always remain in the 1s -

state , therefore , the binding energy increases with A .(9,10)

Among the various investigations for the phenomenological estimation of the Λ - well depth quite a number of them have been made under the simplified assumption of square well potential of depth D_Λ and radius $R = r_0 A^{1/3}$.

The binding energy of the Λ (in its ground state) is then given by the expression :

$$B_\Lambda = D_\Lambda - \frac{\hbar^2}{2m_\Lambda} \pi^2 \frac{1}{R^2}$$

D_Λ value was also calculated by Shoeb and Rahman Khan⁽¹¹⁾ , using the semi - empirical formula . The obtained value of D_Λ was 31.6 MeV. Ahmad et.al.⁽¹²⁾ have obtained the value of D_Λ by using a density dependent Λ N interaction in the framework of folding model . Recently Neelofer et.al.⁽¹³⁾ have obtained a one parameter, semi - empirical formula for Λ - binding energy of heavy hypernuclei in the inverse process of folding model . The value of D_Λ was 30.05 MeV and also the predicted value of B_Λ is in fairly good agreement with the experimental values.

Daskaloyannis et.al.⁽¹⁴⁾ have obtained B_Λ by using the following expressions :

$$B_\Lambda = D_\Lambda - (3\pi)^{2/3} D_\Lambda \left[(P+1)^{1/3} - (P-1)^{1/3} \right]^2,$$

$$\text{where } P = \left[1 + \frac{8}{(3\pi)^2} (1+S)^3 \right]^2$$

$$S = \left[\frac{2 \mu_{\Lambda A}}{\hbar^2} D_\Lambda \right]^{1/2} R .$$

The best obtained value for D_{Λ} is 29.50 MeV and r_0 is 1.035 fm.

However , the most quoted value of D_{Λ} is 30 ± 3 MeV.⁽¹⁵⁾

Recently, Kourtroulos et al.⁽¹⁶⁻¹⁹⁾ reported a phenomenological analysis of the ground and excited state binding energies and rms radii of p - shell and heavier hypernuclei which were determined by recent (π^+ , K^+) experiments . A Λ - nucleon potential including relativistic effects was used. It was found that the relativistic effects do not play any important role in determination of binding energy and r.m.s. radii.

TABLE 1 : Λ binding energies of hypernuclei identified uniquely

| | B_{Λ} (MeV) | | B_{Λ} (MeV) | | B_{Λ} (MeV) |
|-------------------------|---------------------|----------------------------|---------------------|---------------------------|---------------------|
| $^3_{\Lambda}\text{H}$ | 0.13 ± 0.005 | $^8_{\Lambda}\text{Li}$ | 6.80 ± 0.003 | $^{10}_{\Lambda}\text{B}$ | 8.88 ± 0.12 |
| $^4_{\Lambda}\text{H}$ | 2.04 ± 0.04 | $^9_{\Lambda}\text{Li}$ | 8.53 ± 0.15 | $^{11}_{\Lambda}\text{B}$ | 10.24 ± 0.05 |
| $^4_{\Lambda}\text{H}$ | 2.39 ± 0.03 | $^7_{\Lambda}\text{Be}$ | 5.16 ± 0.08 | $^{12}_{\Lambda}\text{B}$ | 11.37 ± 0.06 |
| $^5_{\Lambda}\text{He}$ | 3.12 ± 0.02 | $^9_{\Lambda}\text{Be}$ | 6.84 ± 0.05 | $^{12}_{\Lambda}\text{C}$ | 10.76 ± 0.19 |
| $^6_{\Lambda}\text{He}$ | 4.18 ± 0.10 | $^9_{\Lambda}\text{Be}$ | 6.71 ± 0.04 | $^{13}_{\Lambda}\text{C}$ | 11.69 ± 0.12 |
| $^8_{\Lambda}\text{He}$ | 7.16 ± 0.70 | $^{10}_{\Lambda}\text{Be}$ | 9.11 ± 0.22 | $^{14}_{\Lambda}\text{C}$ | 12.17 ± 0.33 |
| $^7_{\Lambda}\text{Li}$ | 5.58 ± 0.03 | $^9_{\Lambda}\text{B}$ | 7.88 ± 0.15 | $^{15}_{\Lambda}\text{N}$ | 13.59 ± 0.15 |

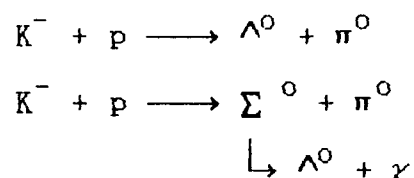
4.2 Λ - N scattering

A lot of effort has been made to procure Λ p scattering data with the ultimate aim of obtaining a realistic Λ N potential from the analysis . Due to the brief life - time of Λ particle , it is difficult to get a fine beam of hyperons. Therefore , even the available Λ p scattering data have

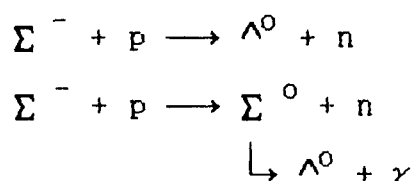
is comparatively poor statistics. The procured Λ - p scattering data consists of scattering cross section (σ_{tot}), forward to backward ratio (F/B) and polar to equatorial ratio (P/E). Still more reliable data are needed to get a lucid picture of Λ - N interaction. Here the results of Zorn et.al. (20) and Alexander et.al. (21) and also the various phenomenological analyses to predict the scattering length, the effective ranges, and the phase - shifts are given.

a. Scattering Length and Effective range

Zorn et.al. (20) measured the cross section for Λ - p elastic scattering with Λ momenta in the interval 110 - 330 MeV/c. The study was based upon the 10^5 pictures in which 95627 Λ hyperons were produced from the following direct K^- interaction :



and from the Σ^- interaction :



The geometrical criteria were applied and 224 scattering events were chosen.

The cross-sections for Λ - p elastic scattering as a function of incident Λ laboratory momentum have been tabulated in Table 2 (20) :

TABLE - 2

| Momentum interval P^{\wedge} (lab) | Aver.Momentum (MeV/c) | No.of accepted events | Cross - section (mb) |
|---|--------------------------|--------------------------|-------------------------|
| 120 - 150 | 135 | 14 | 209 ± 58 |
| 150 - 180 | 165 | 28 | 177 ± 38 |
| 180 - 210 | 194 | 49 | 153 ± 27 |
| 210 - 240 | 226 | 54 | 111 ± 18 |
| 240 - 270 | 252 | 59 | 87 ± 13 |
| 270 - 330 | 293 | 20 | 46 ± 11 |

The cross sections thus obtained were analyzed in terms of effective range theory . The cross section was written in terms of two singlet and two , triplet parameters . The singlet scattering length is denoted by a_s , the singlet effective range by r_{os} , the triplet scattering length a_t and the triplet effective range r_{ot} . Thus,

$$\sigma = \sigma_s + \sigma_t$$

$$\frac{\pi}{k^2 + \left(-\frac{1}{a_s} + \frac{1}{2} r_{os} k^2\right)^2} + \frac{3\pi}{\left(-\frac{1}{a_t} + \frac{1}{2} r_{ot} k^2\right)^2 + k^2} \quad (1)$$

Then the \wedge -p elastic scattering cross - sections data (Table :2) were used together with equation (1) and with the help of least square fitting (χ^2 - fitting) the following values of a_s , r_{os} , a_t and r_{ot} (in the energy range 110 - 330 MeV/c) were obtained :

$$a_s \simeq -2.0 F, \quad r_{os} \simeq 5.0 F$$

$$a_t \simeq -2.2 F, \quad r_{ot} \simeq 3.5 F$$

Alexander et al.⁽²¹⁾ performed the $\Lambda - p$ scattering experiments in a bubble chamber. Using the effective range approximation, they analyzed the experimental $\Lambda - p$ scattering data consisting of six data points in the c.m. energy range of about 2 to 20 MeV.

Their results were :

$$a_t^P = -1.6F, \quad r_{ot}^P = 3.3F$$

$$a_s^P = -1.8F, \quad r_{os}^P = 2.8F$$

Cline et al.⁽²²⁾ performed the experiment at a little higher momenta than Zorn⁽²⁰⁾ and Alexander⁽²¹⁾. The results have been shown in fig 4) and 5).

The validity of the expression for Λp cross section used in the fits rests on the assumption that the Λp elastic scattering takes place in pure s-wave. The fig (5) indicates that at least such is the case upto incident momenta of 200 - 240 MeV/c. Above this there are indication for some p-wave contribution. In fig (6), the cross-section for elastic scattering (mb) have been plotted against momentum of Λ (MeV/c). The triangles correspond to the previous reported cross-section values obtained in hydrogen bubble chamber experiments and the new values has been shown with closed circles.

Londergan and Dalitz⁽²³⁾ assumed the weak spin-dependence of Λp interaction, where the triplet term dominates the cross-section due to its statistical weight and, therefore, they took

$$a_s = a_t = a, \quad r_{os} = r_{ot} = r_o$$

so that

$$\sigma = \frac{4\pi}{\left[\left(-\frac{1}{a}\right) + \frac{1}{2r_0 k^2} \right]^2 + k^2} \quad (2)$$

The fit of the experimental data using equation (2) is shown in fig (7) yielding the values :

$$a = -1.80 \text{ fm} , r_0 = 3.16 \text{ fm}$$

Therefore, it was concluded that the Λp interaction is weaker than the N interaction and there is no Λp bound state.

Herndon and Tang⁽²⁴⁾ constructed an effective Λ - nucleon potential by examining the binding energy data of the s -shell hypernuclei and the Λ - proton scattering data with a number of effective central Λ - Nucleon potentials of various hard core radii (0-0.6 F) and intrinsic range (1.5 - 2.5 F). They obtained a good fit to these experimental data. The potential was found to be having an intrinsic range of 2.1 F , a hard core radius of 0.6 F, and an odd - parity state strength equal to 60% of even - parity strength. The Λ - proton effective range parameters have the following values :

$$\begin{array}{ll} a_t^p = 2.08 \text{ F} & r_{ot}^p = 3.40 \text{ F} \\ a_s^p = -2.25 \text{ F} & r_{os}^p = 3.29 \text{ F} \end{array}$$

Ali et.al.⁽²⁵⁾ made an analysis of the available Λp scattering data using Yukawa Λ - N interaction based on the effective range approximation. They included in their calculation purely attractive Yukawa potentials as well as the ones with hard cores.

The best fits to σ_{exp} helped in determining the Λ - N potentials

(1) Yukawa Λ -N potential (Purely attractive)

$$V_s \approx V_t = -U \left(\frac{\mu^3}{4\pi} \right) \exp(-\mu r) / \mu r ,$$

where $\mu = 1.024 \text{ fm}^{-1}$ corresponding to $b = 2.07 \text{ fm}$ and $U = 454 \text{ MeV fm}^3$ is the common volume integral of the singlet and triplet potentials and $S_s \approx S_t \approx 0.575$.

(2) Hard Core Yukawa Λ -N potential .

$$\begin{aligned} V_s &= \infty & r \leq r_c \\ V_s &= -W_s \exp(-\mu r) / \mu r & r > r_c \\ V_t &= \infty & r \leq r_c \\ V_t &= -W_t \exp(-\mu r) / \mu r & r > r_c \end{aligned}$$

For $r_c = 0.4 \text{ fm}$, $\mu = 2.12 \text{ fm}^{-1}$ corresponding to $b = 2.07 \text{ fm}$, $W_s = 1116 \text{ MeV}$, $S_s = 0.805$, $W_t = 929.4 \text{ MeV}$ and $S_t = 0.669$.

For $r_c = 0.6 \text{ fm}$, $\mu = 2.39 \text{ fm}^{-1}$ corresponding to $b = 2.4 \text{ fm}$, $W_s = 3095 \text{ MeV}$, $S_s = 0.758$, $W_t = 3095 \text{ MeV}$ and $S_t = 0.758$.

Fast et.al.⁽²⁶⁾ obtained the Σ^+_{-p} and Λ -p low energy scattering parameters using the experimental cross-section data. These low energy Σ^+_{-p} and Λ -p scattering parameter was used in a hyperon nucleon interaction model. The model is described by the one - boson - exchange (OBE)

potential which was used into a coupled channel Schrodinger equation. In the Λ p system the model has two free parameters which were the radii of the singlet and triplet repulsive hard cores of pure $I = \frac{1}{2}$ state. By assuming the extreme value of Λ p resonance and using both the Rehovoth, Heidelberg group(RH group)⁽²¹⁾ and Maryland⁽²⁰⁾ data for the Λ p case, Fast et.al. obtained the values for the effective range :

$$\begin{aligned} a_s &= -1.7 \pm 0.5 \text{ fm} , & r_s &= 2.5^{+1.0}_{-0.5} \text{ fm} \\ a_t &= -1.5 \pm 0.05 \text{ fm} , & r_t &= 2.0 \pm 0.05 \text{ fm} \end{aligned}$$

Shoeb et.al.⁽³⁾ used a phenomenological approach of getting the Λ N potential from low energy Λ p scattering data. An effective three body Λ NN force with the Λ N potential was used to account for the Λ binding in p - shell hypernuclei.

The results of a_s , a_t , r_{os} , r_{ot} for two different set of the potentials are the following :

$$\text{Set A : } a_s = a_t = -1.60 \text{ fm} , \quad r_{os} = r_{ot} = 2.4 \text{ fm}$$

$$\text{Set B : } a_s = -2.20 \text{ fm} , \quad a_t = 1.40 \text{ fm} , \quad r_{os} = 2.26 \text{ fm} , \quad r_{ot} = 2.55 \text{ fm}$$

However, from seeing the above discussion it can be said that still there is a need of many more reliable experimental data to get a lucid picture of Λ - N potential.

Phase shifts

Λ - proton scattering phase shifts analysis have been done by many groups like Herndon and Tang,⁽²⁴⁾ Rahman Khan and Shoeb⁽²⁷⁾, the Nijmegen group⁽²⁸⁾ etc. The analysis is based on the different potentials.. We are mentioning here in brief , the calculations & results of Rahman and Shoeb⁽²⁷⁾

along with the results of the Nijmegen group.⁽²⁸⁾

Rahman Khan and Shoeb have obtained the s-wave and p-wave phase shifts using the mean experimental low energy σ_{tot} and the Forward to Backward ratio which were given by Zorn etal and Alexander etal. . By assuming that at low energies δ_1 , and higher phase shifts make negligible contribution to σ_{tot} , they took

$$\sin^2 \delta_0 = \frac{k^2 \sigma_{\text{tot}}}{4\pi} \quad (3)$$

and for small δ , the approximated equation for the phase shift is

$$\delta_1 = \frac{x}{\sqrt{\frac{1}{\alpha^2(k)} - 1}} \quad (4)$$

$$\text{where } \alpha^2(k) = \frac{k^2 \sigma_{\text{tot}}}{4\pi}$$

$$\text{and } x = \left(\frac{F}{B} - 1 \right) / 3 \left(\frac{F}{B} + 1 \right)$$

The phase shifts calculated using equation(2) have been tabulated here in table 3.

Table - 3 . Phse shifts (in radians) calculated using equation (4)

| E_{cm} (MeV) | σ_{tot} (mb) | F/B | δ_0 (in radian) | δ_1 (in radian) |
|-----------------------|-------------------------------|------|---------------------------|---------------------------|
| 7.7 | 146 | 1.0 | 0.505 | ~ 0.0 |
| 10.3 | 101 | 1.28 | 0.484 | 0.008 |
| 17.1 | 52 | 1.80 | 0.445 | 0.030. |

The results of Nijmegen group in One boson exchange potential approach have been tabulated in Table 4 and 5). The potentials were found to be attractive in all partial waves. The different Nijmegen potentials will be discussed in Chapter - 5 in some detail.

Table 4 : Λp nuclear-bar phase shifts below the ΣN thresholds. The phase shifts of the not-displayed $L = 4$ waves are smaller than 0.20° everywhere and for $L = 5$ smaller 0.03° .

| p_Λ (MeV/c) | 100 | 200 | 300 | 400 | 500 | 600 | 633.3 |
|---------------------|-------|-------|-------|-------|-------|-------|-------|
| T_{lab} (MeV) | 4.5 | 17.8 | 39.6 | 69.5 | 106.9 | 151.1 | 167.5 |
| 1S_0 | 19.07 | 24.31 | 21.15 | 14.66 | 7.04 | -0.64 | -2.76 |
| 3S_1 | 21.97 | 28.48 | 26.54 | 21.70 | 16.57 | 15.35 | 38.15 |
| ϵ_1 | 0.17 | 0.86 | 1.96 | 3.41 | 5.46 | 10.35 | 25.86 |
| 3P_0 | 0.06 | 0.37 | 0.67 | 0.24 | -1.39 | -4.14 | -5.23 |
| 1P_1 | 0.12 | 0.92 | 2.76 | 5.55 | 9.03 | 13.37 | 15.38 |
| 3P_1 | 0.06 | 0.32 | 0.63 | 0.71 | 0.45 | 0.35 | 0.91 |
| 3P_2 | 0.18 | 1.27 | 3.50 | 6.27 | 8.72 | 10.30 | 10.63 |
| ϵ_2 | 0.00 | -0.00 | -0.04 | -0.13 | -0.24 | -0.25 | -0.17 |
| 3D_1 | 0.00 | 0.03 | 0.21 | 0.71 | 1.88 | 5.30 | 13.66 |
| 1D_2 | 0.00 | 0.05 | 0.33 | 1.08 | 2.39 | 4.16 | 4.81 |
| 3D_2 | 0.00 | 0.08 | 0.41 | 1.19 | 2.44 | 3.98 | 4.53 |
| 3D_3 | 0.00 | 0.05 | 0.28 | 0.86 | 1.85 | 3.13 | 3.58 |
| ϵ_3 | 0.00 | 0.00 | 0.02 | 0.05 | 0.13 | 0.25 | 0.31 |
| 3F_2 | 0.00 | 0.00 | 0.01 | 0.06 | 0.21 | 0.52 | 0.75 |
| 1F_3 | -0.00 | -0.00 | 0.00 | 0.03 | 0.10 | 0.24 | 0.30 |
| 3F_3 | 0.00 | 0.00 | 0.02 | 0.06 | 0.16 | 0.30 | 0.37 |

| | | | | | | | |
|----------------------------|-------|-------|------|------|------|------|------|
| 3F_4 | 0.00 | 0.00 | 0.02 | 0.08 | 0.25 | 0.56 | 0.71 |
| σ_{tot} (mb) | 309.6 | 126.7 | 50.7 | 22.3 | 13.1 | 14.4 | 39.0 |

Table 5 : Λn nuclear-bar phase shifts in degrees below ΣN thresholds.

| | | | | | | | | |
|----------------------------|-------|-------|-------|-------|-------|-------|-------|-------|
| p_{Λ} (MeV) | 100 | 200 | 300 | 400 | 500 | 600 | 641.7 | |
| T_{lab} (MeV) | 4.5 | 17.8 | 39.6 | 69.5 | 106.9 | 151.1 | 171.4 | |
| <hr/> | | | | | | | | |
| 1S_0 | 21.31 | 26.46 | 22.90 | 16.10 | 8.26 | 0.36 | -2.51 | |
| 3S_1 | | 20.04 | 26.45 | 24.72 | 19.98 | 14.74 | 11.90 | 21.09 |
| ϵ_1 | | 0.12 | 0.70 | 1.73 | 3.13 | 5.03 | 8.86 | 17.63 |
| 3P_0 | | 0.13 | 0.68 | 1.22 | 0.9 | -0.72 | -3.56 | -4.99 |
| 1P_1 | | 0.15 | 1.07 | 3.10 | 6.12 | 9.84 | 14.32 | 16.76 |
| 3P_1 | | 0.01 | 0.08 | 0.18 | 0.06 | -0.37 | -0.77 | -0.43 |
| 3P_2 | | 0.18 | 1.26 | 3.48 | 6.21 | 8.59 | 10.08 | 10.43 |
| ϵ_2 | | -0.00 | -0.03 | -0.11 | -0.24 | -0.39 | -0.43 | -0.36 |
| 3D_1 | | 0.00 | 0.05 | 0.27 | 0.82 | 1.96 | 4.77 | 10.92 |
| 1D_2 | | 0.00 | 0.07 | 0.39 | 1.17 | 2.53 | 4.36 | 5.20 |
| 3D_2 | | 0.00 | 0.05 | 0.31 | 1.01 | 2.17 | 3.62 | 4.26 |
| 3D_3 | | 0.00 | 0.05 | 0.29 | 0.88 | 1.87 | 3.15 | 3.71 |
| ϵ_3 | | -0.00 | -0.00 | -0.00 | 0.01 | 0.06 | 0.17 | 0.23 |
| 3F_2 | | 0.00 | 0.00 | 0.02 | 0.09 | 0.25 | 0.56 | 0.81 |
| 1F_3 | | 0.00 | 0.00 | 0.02 | 0.05 | 0.14 | 0.30 | 0.38 |
| 3F_3 | | -0.00 | -0.00 | -0.00 | -0.01 | 0.06 | 0.17 | 0.24 |
| 3F_4 | | 0.00 | 0.00 | 0.02 | 0.09 | 0.26 | 0.58 | 0.76 |
| σ_{tot} (mb) | | 284.2 | 117.9 | 47.1 | 20.6 | 12.1 | 12.3 | 23.1 |

4.3 HYPERNUCLEAR DECAYS :

The decay properties of the hypernucleus are also studied to get the information on Λ - N interaction . There are three decay modes of hypernuclei :

(1) Strong decay (2) weak decay (3) electromagnetic decay

The lifetime of strong decay is very small and the detectors are not sensitive enough to record the spectrum of the outgoing particles in these decays. The electromagnetic decay studied is through the γ -ray transition of the excited hypernucleus which decays to the ground state. The weak hypernuclear decays have been more rigorously studied due to the longer lifetime and more limpid experimental interpretations.

A lambda hyperon bound to a nucleus decays with a life - time of weak processes $\tau \sim 10^{-10}$ sec. This life-time is longer than the normal strong and electromagnetic nuclear decay . In the weak decay process a hypernucleus formed in a (K^-, π^-) reaction is formed in an excited state with the Λ in one of its higher orbits . Through the electromagnetic gamma decay and/or nuclear Auger process, the hyperon comes to the lowest (1s) nuclear Auger process, the hyperon comes to the lowest (1s) nuclear shell model orbit⁽²²⁾ i.e. the ground state from where it decays through the weak processes.

4.3.1. Weak hypernuclear decays

These are described by the following decay modes :

(1) MESONIC DECAYS

$$\Gamma_m(\pi^-) : \Lambda \rightarrow p + \pi^- + 38 \text{ MeV} - (B_\Lambda - B_p)$$

$$\Gamma_m(\pi^0) : \Lambda \rightarrow n + \pi^0 + 41 \text{ MeV} - (B_\Lambda - B_n)$$

(2) NON-MESONIC DECAYS

$$\Gamma_{nm}(p) : \Lambda + p \rightarrow n + p + 177 \text{ MeV} - (B_\Lambda + B_p)$$

$$\Gamma_{nm}(n) : \Lambda + n \rightarrow n + n + 176 \text{ MeV} - (B_\Lambda + B_n) ,$$

where B_b is the binding energy for the baryon b ⁽³⁰⁾.

The schematic representation for the mesonic and non-mesonic decays has been shown in figure (8).

Cheston and Primakoff⁽³¹⁾ were the first who conceived the importance of studying the decay modes of hypernuclei. They stressed that the free space decay mode, $\Lambda \rightarrow N \pi$, would be stopped inside a hypernucleus due to the nuclear effects. Therefore, they pointed out that the two hadron $\Lambda N \rightarrow NN$ mode is more important. Based on their⁽³¹⁾ arguments a series of experiments (emulsion and bubble chamber) were performed to measure the ratio Γ_{nm} / Γ_π . They have also plotted it as a function of A , (shown in figure (9)), indicating that

$$(\Gamma_{nm} / \Gamma_\pi)^{\text{exp}} = 100 - 200 \quad \text{for } 40 < A \quad (1)$$

The total decay rate is the sum of the four partial decay rates :

$$\Gamma_{\text{total}} \left(\begin{smallmatrix} A \\ \Lambda Z \end{smallmatrix} \right) = 1/\tau = \Gamma_m(\pi) + \Gamma_{nm}(p) + \Gamma_{nm}(n) \quad (2)$$

The ratio of mesonic and non-mesonic decay rate varies with the hypernuclear mass. For the light hypernuclei e.g. $A = 3, 4$ the mesonic decay modes are favoured, whereas for the heavier hypernuclei the

non-mesonic decay modes dominates . The predominance of the non-mesonic decay rates at large A has been shown in figure (9) is due to the following⁽³²⁾

- (1) The increased binding energy of the lambda in heavier hypernuclei sharply restricts the phase space available to the mesonic decays .
- (2) The heavier nuclei have fewer available states for the slowly recoiling nucleon from the mesonic decay (Pauli blocking).
- (3) The increased nuclear density of the heavier hypernuclei increases the overlap of the lambda-nucleon wave functions and , therefore, increasing the non-mesonic rate.

The BNL group⁽³³⁾ the measurement of the mean life time τ , for the weak decay of ${}_{\Lambda}^{12}\text{C}$. They used the strangeness exchange reaction (SEX) reaction $K^- + {}^{12}\text{C} \rightarrow {}_{\Lambda}^{12} + \pi^-$ for hypernuclear production and tagging .The spectrum has been shown in figure (10).It is clear from the spectrum that the three hypernuclear states were observed in coincidence with the energetic proton from the non-mesonic decay : the hypernuclear states and two ground states. The explanations were that the ground state (region 1) has the particle shell model configuration $s(\Lambda); P_{(n)}^{-1}$ and is bound by 11 MeV (34) The first excited state (region 3) is bound ${}_{\Lambda}^{11}\text{B} + \text{low energy proton}$ (35) The third state (region 3) is bound by 10MeV and having the configuration $s(\Lambda) , s^{-1}_{(n)}$ (36)

The lifetime was measured by ascertaining the hypernuclear production time (t_p) , and hypernuclear decay time (t_d) for every individual event and the difference ($t_d - t_p$) . The results have been shown in table (6). The mesonic decay rates are near zero, therefore, the reaction $\Lambda + p \rightarrow n + \pi$

and $\Lambda + n \rightarrow n + n$, dominates. It was found that the neutron and proton stimulated decays are equally important.

TABLE - 6
HYPERNUCLEAR LIFETIME RESULTS

| <u>STATES</u> | <u>HYPERNUCLEUS</u> | <u>LIFETIME(τ)</u> | <u>$\Gamma_{\text{total}} / \Gamma_{\Lambda}$</u> |
|---------------|---------------------------|------------------------------------|--|
| 1 | $^{12}_{\Lambda}\text{C}$ | $211 \pm 31 \text{ ps}$ | 1.25 ± 0.18 |
| 2 | $^{11}_{\Lambda}\text{B}$ | $192 \pm 22 \text{ ps}$ | 1.37 ± 0.16 |
| 3 | $^A_{\Lambda}\text{Z}$ | $201 \pm 30 \text{ ps}$ | 1.31 ± 0.20 |

Bando et.al⁽³⁷⁾ have suggested about-10% depletion in the occupied nucleon orbits, which they proposed was due to NN short range and tensor correlations, leading to a saturation of the suppression of the π -mesonic decay, consistent with the emulsion data.

Kurihara et.al⁽³⁸⁾ have suggested that the repulsive core of Λ N interaction, continues in the Λ - nucleus potential, particularly in very light hypernuclei, and makes the Λ -wavefunction sizeably different from the nucleon ones, which in turn reduces the suppression of π -mesonic decay. However Oset et.al.⁽³⁹⁾ have found an enhancement of the π -mesonic decay, after incorporating the renormalization of the pion propagator in the nuclear medium within the framework of treating the π -mesonic and one pion exchange non-mesonic decay processes.

At BNL, Barnes et.al^(40,41) measured the partial decay rates of $^{12}_{\Lambda}\text{C}$, $^{11}_{\Lambda}\text{B}$, $^5_{\Lambda}\text{He}$, and an unknown species. Their data were consistent with the older data on $\Gamma_{\text{nm}}^{\text{n}} / \Gamma_{\text{nm}}^{\text{p}}$ but inconsistent with the data on $\Gamma_{\text{nm}} / \Gamma_{\pi^-}$.

Barnes quotes :

$$\Gamma_{\pi} / \Gamma_{\Lambda} = \begin{cases} 0.16 + 0.34 & \text{for } {}^5_{\Lambda}\text{He} \\ - 0.21 & \\ 0.06 + 0.8 & \text{for } {}^{12}_{\Lambda}\text{C} \\ - 0.05 & \end{cases}$$

$$\Gamma_{\pi^-} / \Gamma_{\Lambda} = \begin{cases} 0.43 + 0.10 & \text{for } {}^5_{\Lambda}\text{He} \\ - 0.10 & \\ 0.05 + 0.06 & \text{for } {}^{12}_{\Lambda}\text{C} \\ - 0.03 & \end{cases}$$

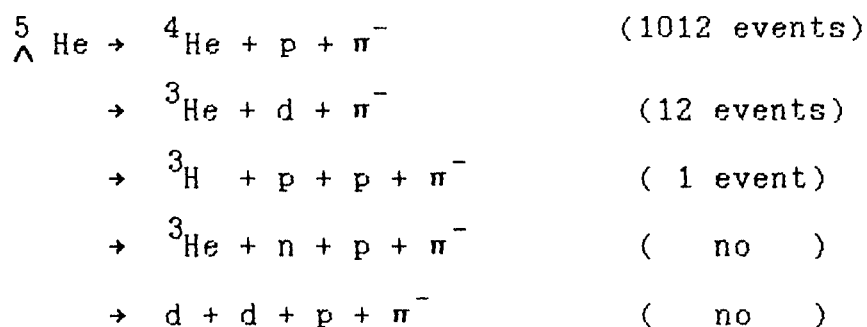
To show the consistency we compare Barnes's data with the prediction of Michigan State University (MSU) pion potential⁽⁴²⁾ or with undistorted plane wave (PW) for the pion⁽⁴³⁾,

$$\Gamma_{\pi} / \Gamma_{\Lambda} = \begin{cases} 0.15 \text{ (MSU)} , 0.09 \text{ (PW)} & \text{for } {}^5_{\Lambda}\text{He} \\ 0.17 \text{ (MSU)} , 0.08 \text{ (PW)} & \text{for } {}^{12}_{\Lambda}\text{C} \end{cases}$$

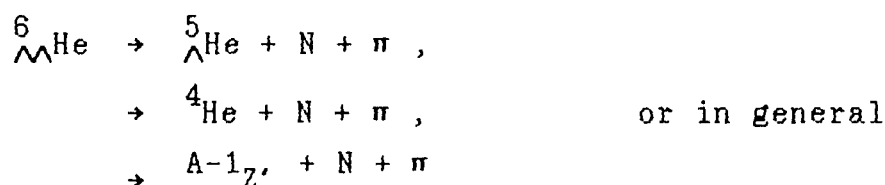
$$\Gamma_{\pi^-} / \Gamma_{\Lambda} = \begin{cases} 0.32 \text{ (MSU)} , 0.18 \text{ (PW)} & \text{for } {}^5_{\Lambda}\text{He} \\ 0.13 \text{ (MSU)} , 0.06 \text{ (PW)} & \text{for } {}^{12}_{\Lambda}\text{C} \end{cases}$$

In very light hypernuclear decays, the final nuclear states, most of the time comprise of the continuum states and a few (if any) bound states e.g. pion decay of ${}^4_{\Lambda}\text{H}$ leading to ${}^4\text{He} + \pi^-$ (914 events), ${}^3\text{H} + p + \pi^-$ (301 events), $d + d + \pi^-$ (12 events), etc., where only the first channel involves the discrete or definite pion energy. Therefore, it can be said that three-body final states is highly desirable. The confirmation of this comes from the reporting of Bohm et.al.,⁽⁴⁴⁾ where the experimental

observations for the decay of ${}^5_{\Lambda}\text{He}$ were :



Therefore, in the framework of Kapur-Peierls⁽⁴⁵⁾ method , a realistic treatment including the continuum three-body final states has been performed for the 3-body decay mode thus,



It has been found out that this method successfully applies to light Λ - and $\Lambda\Lambda$ -hypernuclear pionic decay. The calculated peaks reflect the low lying sharp resonances in the ${}^5_{\Lambda}\text{He} + p$ and $\alpha + p$ unbound states, respectively . They have got a discrete peak at pion kinetic energy $T_{\pi} = 32.7 \text{ MeV}$ in $\Gamma_{\pi}({}^6_{\Lambda\Lambda}\text{He})$ and a sharp peak at $T_{\pi} = 36.2 \text{ MeV}$ in $\Gamma_{\pi}({}^5_{\Lambda}\text{He})$. The pion spectrum from the weak decay of ${}^6_{\Lambda\Lambda}\text{He}$ has been found out to be almost monoenergetic. This can be utilized to identify light double Λ - hypernuclear productions⁽⁴⁶⁾.

The recent measurements ⁽⁴⁷⁾ imply that the lifetime of heavy hypernuclei are of the same order of magnitude as free τ_{Λ} :

$$\text{i.e. } \Gamma_{\pi} + \Gamma_{\pi} + \Gamma_{nm} = \Gamma_{\Lambda} , \quad \text{----- (3)}$$

which is clear from figure (11).

Therefore, the combination of equation (3) and (1) leads phenomenological indication as

$$\Gamma_{\pi^-}(\Lambda Z)^{\text{exp}} / \Gamma_{\Lambda} = 1/100 - 1/200 \quad \text{for} \quad 40 < A < 100 \quad \text{-----} \quad (4)$$

It has been found out that for no distortion case, $\Gamma_{\pi}(\Lambda Z)^{\text{PW}}$ decrease very fast with A as a direct consequence of the Pauli blocking, and the rate becomes even smaller than $10^{-4}\Gamma_{\Lambda}$ for $A > 100$ (48). Since the relation $\Gamma_{\pi^0}^{\text{PW}} = 2 \Gamma_{\pi^-}^{\text{PW}}$ holds approximately, therefore, this implies for π decay

$$\Gamma_{\pi}(\Lambda Z)^{\text{PW}} / \Gamma_{\Lambda} < 10^{-4} \quad \text{for } 100 < A$$

The experiment of equation (4) indicates the suppression of π -decay in hypernuclei but not as strong as this plane-wave estimates $\Gamma_{\pi}(\Lambda Z)^{\text{PW}}$. For the π decay, the Coulomb distortion alone gives rise to a great enhancement (π^- Coulomb), which is further enlarged by the strong interaction effect. This gives for heavier hypernuclei: $\Gamma_{\pi}(\Lambda Z)^{\text{cal}}/\Gamma_{\Lambda} = (0.5 - 1.0) \times 10^{-2}$ for $40 < A$.

The prediction is in fair agreement with experimental indication of equation (4).

Motoba et.al. (49) studied the π mesonic decay of p-shell and sd-shell hypernuclei, where they employed the shell model wavefunctions with the density dependent Hartree-Fock function. They found the summed decay ($\Gamma_{\pi^0} + \Gamma_{\pi^-}$) rate of π^0 and π^- decreases with the mass and each decay rate ($\Gamma_{\pi^0}, \Gamma_{\pi^-}$) shows a nontrivial and characteristic variation with A which reflects the shell structure effects. They have noticed a strong

transition strength e.g. π decay of ${}^9_{\Lambda}\text{Li}$, π decay of ${}^9_{\Lambda}\text{Be}$, and π decay of ${}^{12}_{\Lambda}\text{C}$. Further, they predicted in π^- decay, a large - assymmetric pion angular pattern from the polarized hypernuclei viz ${}^8_{\Lambda}\text{Li} (1^-)$, ${}^8_{\Lambda}\text{Be} (1^-)$, ${}^9_{\Lambda}\text{Be} (\frac{1}{2}^+)$.

The assymetry arises from the interference between the parity - conserving and parity- violating interactions, reflecting the structure of the parents and daughter nuclear states.

It is predicted that the π^0 / π^- ratio peaks periodically (exceeding 2) at $A = 22$ (for even Z), reflecting the four body correlation . This is a remarkable result due to the fact that the $\Delta I = 1/2$ rule realized in the elementary decay interaction ($\pi \rightarrow N + \pi$) leads to the ratio 0.5 , if there is no shell structure effect (50).

4.3.2. ELECTROMEGNETIC DECAYS

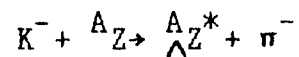
The gamma ray transitions can be grouped into two classes, relying the role of the Λ : (51)

(1) CORE TRANSITIONS :- In this type the gamma ray transition joins core states , and the Λ plays the role of a by-stander, however , the presence of Λ perturbs the core states .

(2) SPIN-FLIP DOUBLET TRANSITIONS :- These are $M - 1$ transitions joining the member of the hypernuclear doublets built on a core state. In this type the Λ - spin is flipped with respect to the core spin.

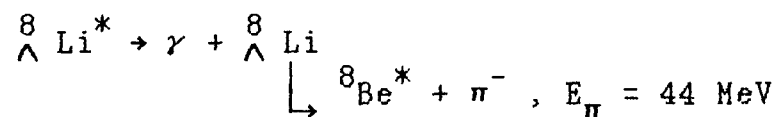
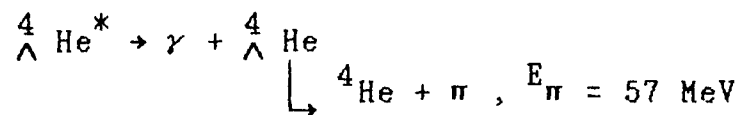
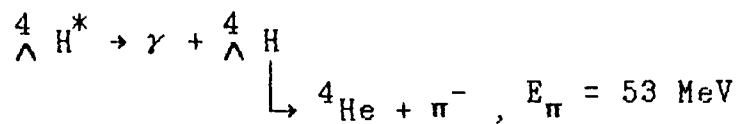
Both types of transitions have been observed in the experiments . The perception of hypernuclear γ rays is a method of determining the spin dependance of Λ - nucleon interaction (52). As it is well known that the

hypernucleus are formed using the strangeness exchange reaction on a nuclear target forming a hypernucleus in an excited state :



The first hypernuclear gamma ray spectra were observed at CERN⁵³⁻⁵⁵⁾ Using reaction of the K^- mesons on ${}^6\text{Li}$, ${}^7\text{Li}$, and ${}^9\text{Be}$ targets.

The ${}^4_{\Lambda}\text{H}$, ${}^4_{\Lambda}\text{He}$ and ${}^8_{\Lambda}\text{Li}$ γ -transitions were identified through the detection of π^- and π^0 mesons accompanying the two-body hypernuclear decays :



The CERN group⁵³⁻⁵⁵⁾ assigned the $(1.05 \pm 0.04) \text{ MeV}$ γ -ray to the $1^+ \rightarrow 0^+$ transitions in ${}^4_{\Lambda}\text{H}$, the $(1.15 \pm 0.04) \text{ MeV}$ γ -ray to the $1^+ \rightarrow 0^+$ transition in ${}^4_{\Lambda}\text{He}$, and $(1.22 \pm 0.04) \text{ MeV}$ γ -ray was tentatively identified as $1^- \rightarrow 1^-$ transition in ${}^8_{\Lambda}\text{Li}$ hypernucleus.

It has been found that the γ -ray transition occurs only in Λ -hypernuclei. The particle stable excited states are those in which the Λ is in s-state and the nuclear core is in its ground state or excited states. The states of the core give rise to doublets with small spin-dependant splittings (as shown in figure (12)). It has been found

out that the perception of γ - ray transitions between core excited state shows that the inter-doublet spacing closely follows the excitation energy of the core states . The spin dependence of the Λ - interaction is measured by the doublet splittings . The splitting in general decreases in magnitude if one goes from lighter to heavier system⁽⁵⁶⁾.

In general the hypernucleus decays by γ emission most of the times come before the weak decay . Since the electromagnetic life-time of the state varies inversely as the cube of the transition energy , therefore , for small splitting the weak decay of the Λ competes with the electromagnetic decay of the state.

Bagget et.al.⁽⁵⁷⁾ reported the radiative decay mode of $\Lambda \rightarrow p \pi^- \gamma$. From the 72 radiative Λ decays with stopping pion and proton , they have obtained the branching ratio :

$$\Gamma (\Lambda \rightarrow \pi^- \gamma , P_{\pi^-}^* < 95 \text{ MeV/c}) / \Gamma (\Lambda \rightarrow p \pi^-) \\ = (1.32 \pm 0.22) \times 10^{-3} ,$$

which was in good agreement with the theoretical predictions .

SPIN DEPENDENCE : Gal et.al.⁽⁵⁸⁾ have analyzed the interaction of the $s_{1/2}$ Λ - particle with the p nucleons . They considered the four two-body spin terms in their analysis . However , out of these four only three depend on Λ - spin :

- (1) the spin - spin term (Δ)
- (2) the spin - orbit term (s_{Λ})
- (3) the tensor term (T)

For the case where Λ is in p - orbit there is a one-body spin-orbit

interaction $\vec{\sigma}_\Lambda \cdot \vec{1}_\Lambda$ characterized by the energy splitting ϵ_p between $P_{1/2}$ and $P_{3/2}$. They found ϵ_p to be directly associated to the two-body spin-orbit term $S_\Lambda = \vec{\sigma}_\Lambda \cdot \vec{1}_{\Lambda N} = \frac{1}{6} S_\Lambda$

SPIN - SPIN INTERACTION : As we have mentioned earlier that Piekarczyk et al. identified the origin of γ - rays from the target as arising from mass hypernuclear system by recording the γ - rays in coincidence with the pionic decay modes of these hypernuclei which has been schematically shown here in figure (13):⁽⁵⁹⁾

$$E_\gamma \left({}^4_\Lambda \text{H} \right) = B \left({}^4_\Lambda \text{H} \right) - B \left({}^4_\Lambda \text{H}^* \right) = 1.04 \pm 0.004 \text{ MeV}$$

$$E_\gamma \left({}^4_\Lambda \text{He} \right) = B \left({}^4_\Lambda \text{He} \right) - B \left({}^4_\Lambda \text{He}^* \right) = 1.15 \pm 0.04 \text{ MeV}$$

Later their results were confirmed at Brookhaven where May et al.⁽⁶⁰⁾ observed a 1.1 MeV γ - ${}^7_\Lambda \text{Li} \rightarrow {}^2\text{H} + {}^5_\Lambda \text{He}$, $E_{\text{thres}} = 3.94 \text{ MeV}$ ray peak following fission of ${}^7_\Lambda \text{Li}$: ${}^7_\Lambda \text{Li} \rightarrow {}^2\text{H} + {}^5_\Lambda \text{He}$, $E_{\text{thres}} = 3.94 \text{ MeV}$.

The ground state spin for mass 4 hypernuclei is known from the analysis of the decay of hypernucleus in emulsion. Therefore, it appeared to them as if there is an attractive spin-spin force. However, Gibson et al.⁽⁶¹⁾ from the calculations of the spin-spin interaction in hypernuclei which was based on the free Λ - nucleon system, obtained the interaction term with an opposite sign. Therefore, it can be said that the interpretation of the splitting in mass 4 is not transparent i.e. it still requires many more experimental observations.

SPIN - ORBIT INTERACTIONS : Bruckner et al.⁽⁶²⁾ were the first who reported the ΛN spin - orbit interaction to be very small. However, the

most acceptable values to date is from Brookhaven (63), where the specimen was $^{13}_{\Lambda}\text{C}$. They took $^{13}_{\Lambda}\text{C}$ interactions into account due to the singlet nature of the ground state of the ^{12}C core. In figure (14), the spectrum of the hypernuclear states observed in $^{13}_{\Lambda}\text{C}$ using (K^-, π^-) reaction has been shown where the threshold for $^{13}_{\Lambda}\text{C} \rightarrow \Lambda + ^{12}\text{C}$ is at 11.6 ± 0.12 MeV excitation (64)

The peak 2 and 3 in figure (14) are the only excited bound states. Peak 2 lies at 4.4 ± 0.3 MeV excitation. The interpretation of this peak is as a core excited state; the ^{12}C is in its 4.44 MeV excited states and Λ is bound to the core in an s-state. The peak labelled 3 has dominant composition $(\text{P}_{1/2})_{\Lambda}$ with the ^{12}C core in its ground state. Another spectrum taken at 15° , which results in the momentum transfer near the maximum of the $L = 2$ transition amplitude, and another state with dominant composition $(\text{P}_{3/2})_{\Lambda}$ with the ^{12}C in its ground state (62). The difference in energy of these two states determines the Λ - nucleus spin orbit interaction:

$$\epsilon_P = \epsilon(\text{P}_{1/2})_{\Lambda} - \epsilon(\text{P}_{3/2})_{\Lambda} = 0.36 \pm 0.3 \text{ MeV}$$

The splittings of these two states is entirely due to the spin - orbit interactions.

(2) HYPERNUCLEAR GAMMA RAYS DUE TO LAMBDA SPIN FLIP :

May et.al (52) observed the γ -rays due to Λ spin flip, which they argued to be a direct source of measurement of the spin-dependence of the Λ - nucleon interaction. Their specimens were $^{10}_{\Lambda}\text{B}$ and $^{16}_{\Lambda}\text{O}$. They observed the gamma ray transition between the first excited state and the ground state of the hypernucleus. For $^{10}_{\Lambda}\text{B}$, the transition energy δ is due to

the interaction of a $P_{3/2}$ neutrons hole ($P_{3/2}^{-1} N$) with the $s_{1/2}^{\wedge}$ particle ($s_{1/2}^{\wedge}$). δ is a function of spin - orbit ($S_{1/2}$), spin - spin (Δ) and tensor (T) interactions and is $2/3 \Delta + 4/3 S_{\wedge} + 8/5 T$ (shown in figure (15a)). For $^{16}_{\wedge}O$, the transition energy δ' is due to the interaction of the $P_{1/2}$ neutron hole ($P_{1/2}^{-1} N$) with the $s_{1/2}^{\wedge}$ Particle ($s_{1/2}^{\wedge}$). The transition energy $\delta' = -1/3 \Delta + 4/3 S + 8 T$ (shown in figure (15b)). It has been suggested that due to the large coefficient of T , the \wedge - nucleon tensor interaction, may make a dominant contribution to the $^{16}_{\wedge}O$ doublet splitting (52). However, Bruckner et.al. (62) have estimated the spin - orbit parameter S_{\wedge} to be small and negative. Millener et. al. (15) have estimated T to be small and positive. For the value of Δ their estimation is $+ 0.4 \leq \Delta \leq 0.64$ MeV. (63-65)

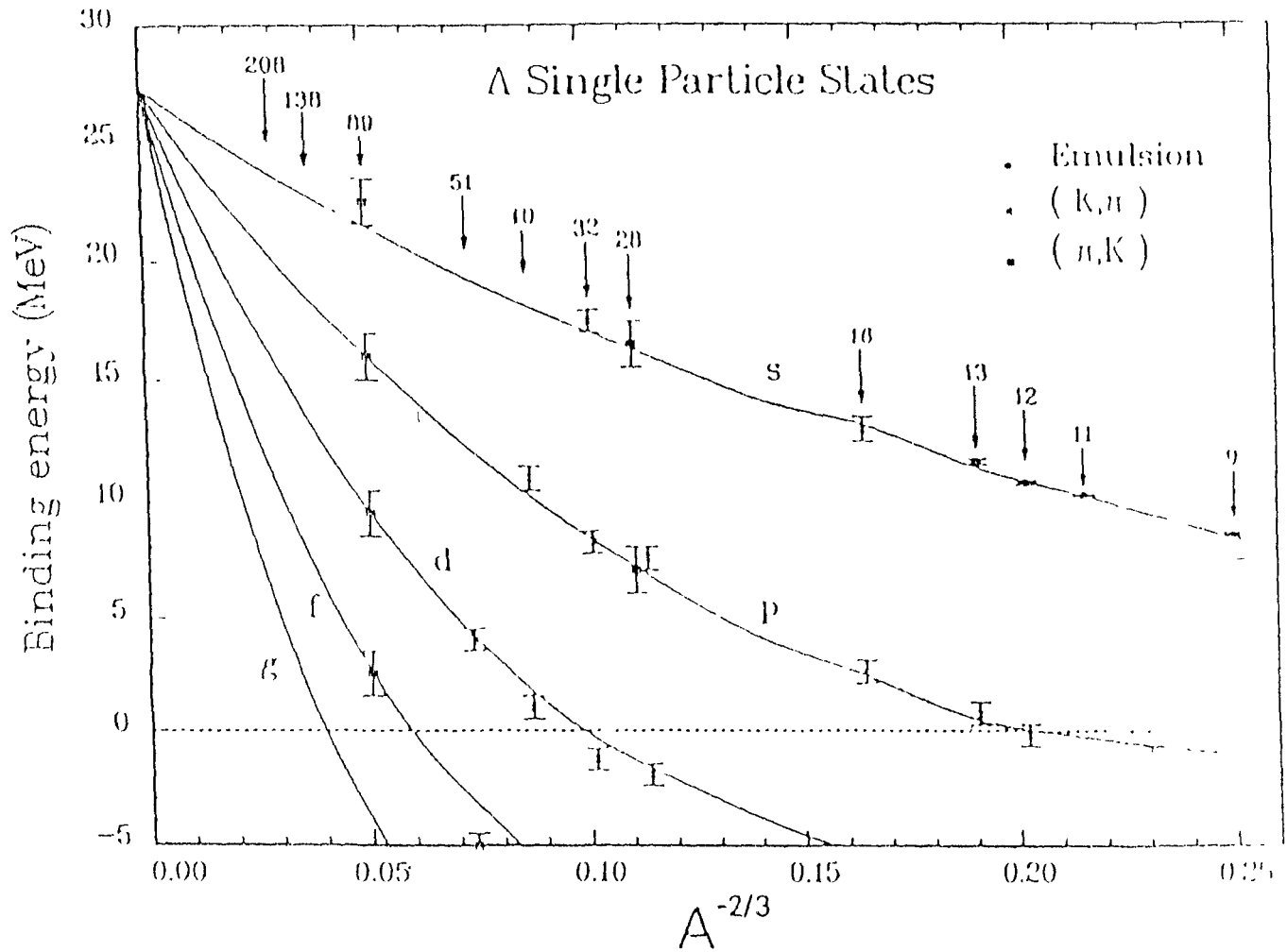


Figure 1: Experimental binding energies (dots, crosses, squares) for s,p,d,f single particle states of the Λ as a function of $A^{-2/3}$ (8)

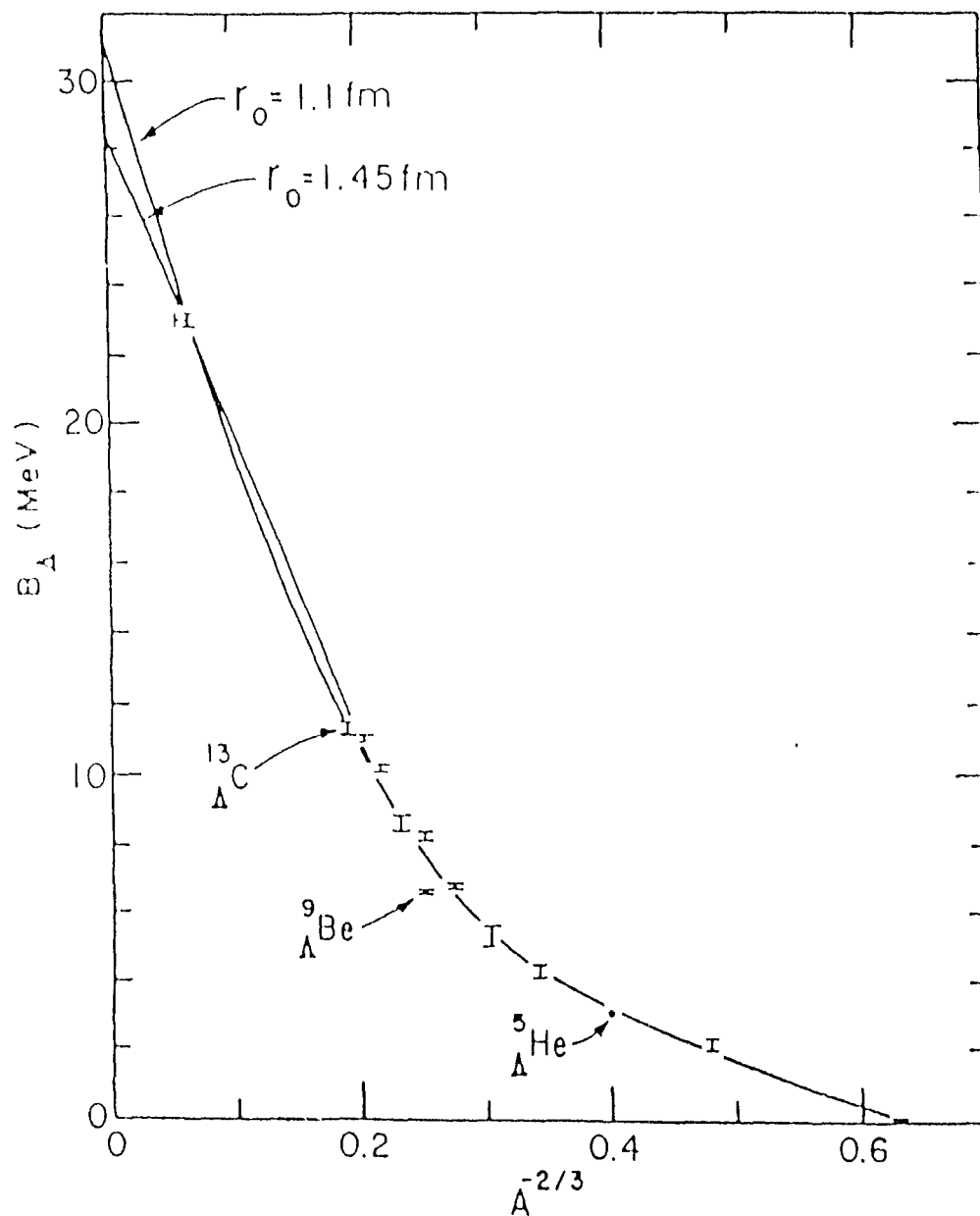


Figure 2: The binding energies B_A versus $A^{-2/3}$. The two curves are fitted to the values of B for the indicated values of r_0 , in order to correspond to a kinetic energy given by an infinitely deep square well of radius $R = r_0 A^{1/3}$.

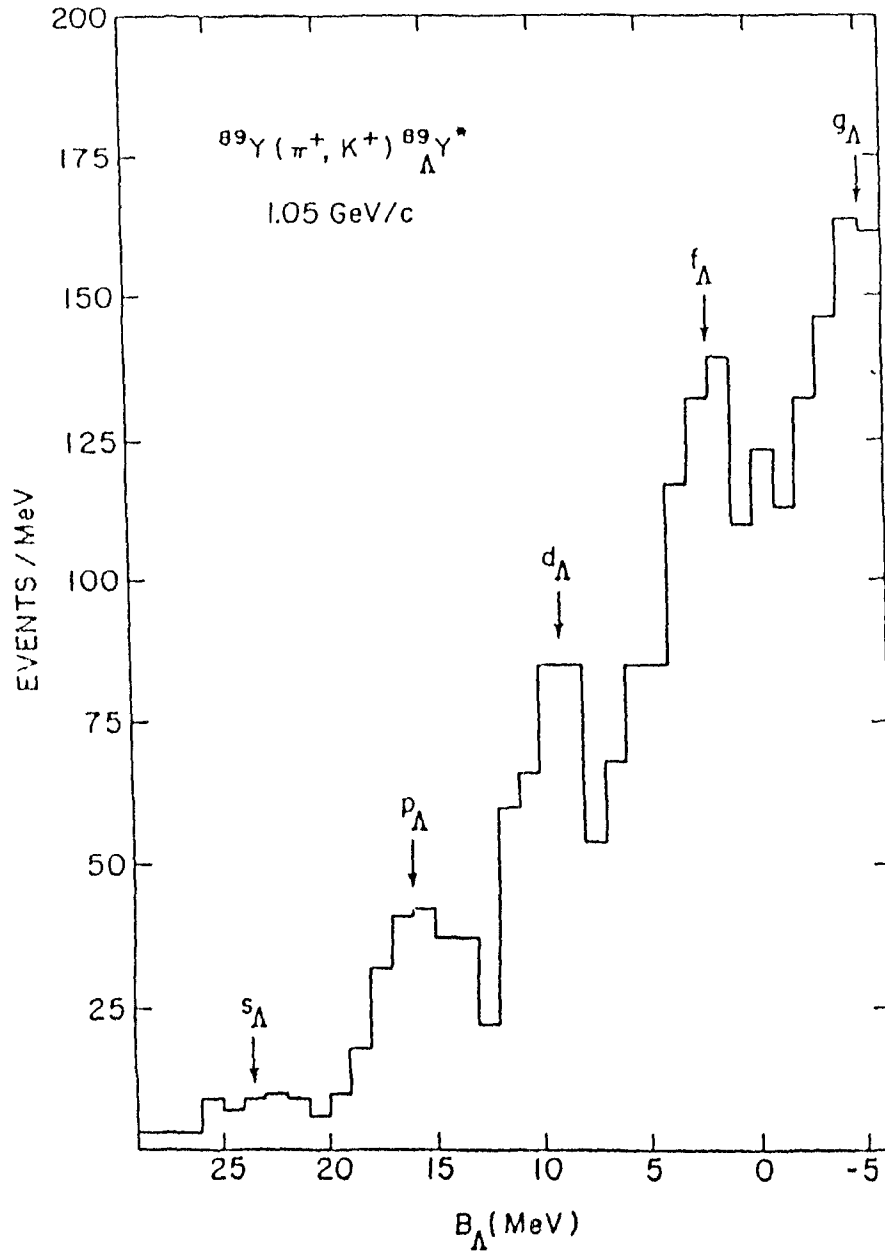


Figure 3: The excitation spectrum of the $^{89}_{\Lambda}\text{Y}$ hypernucleus as produced in the (π^+, K^+) reaction at 1.05 GeV/c. The labels $\{s_{\Lambda}, p_{\Lambda}, d_{\Lambda}, f_{\Lambda}, g_{\Lambda}\}$ identify the values of binding energy B predicted in Ref.7 based on a Woods-Saxon potential for the Λ .

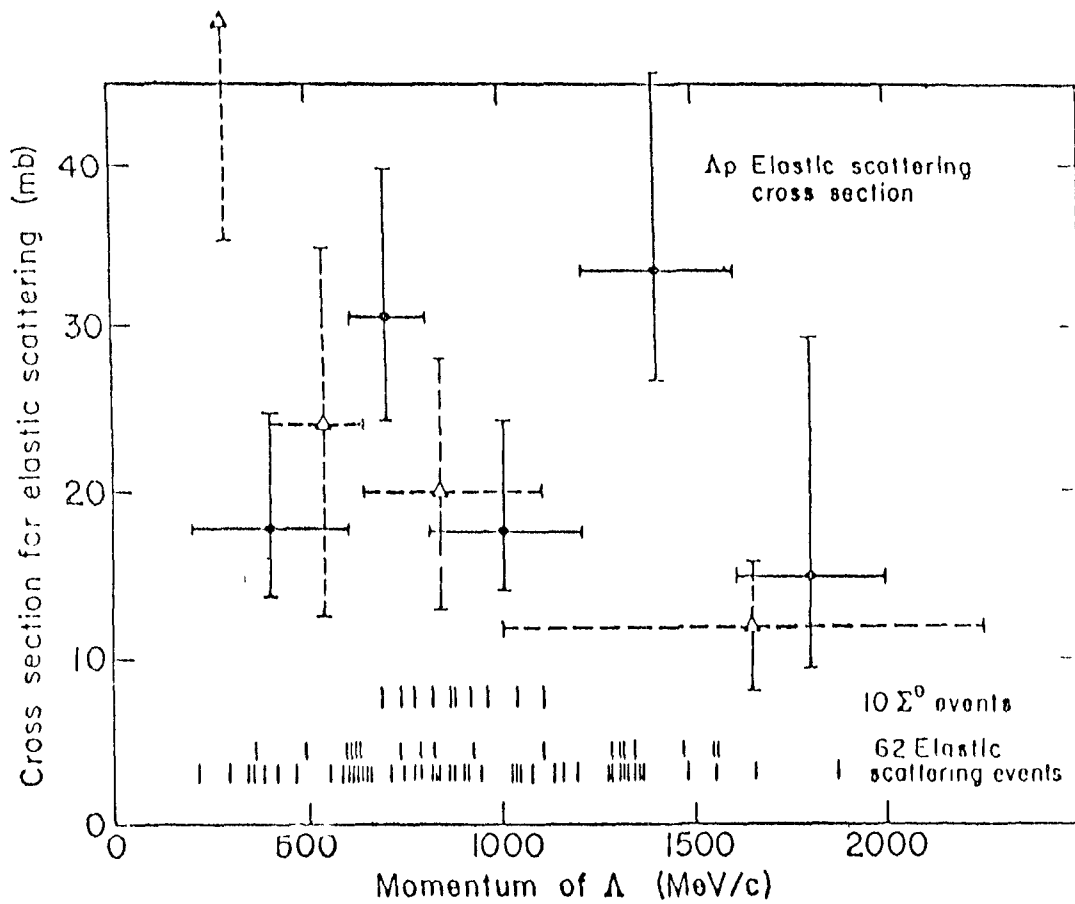


Figure 4: Λp total cross section. Closed circles correspond to data obtained in hydrogen bubble chambers, the triangles correspond to data obtained in heavy liquid chambers.

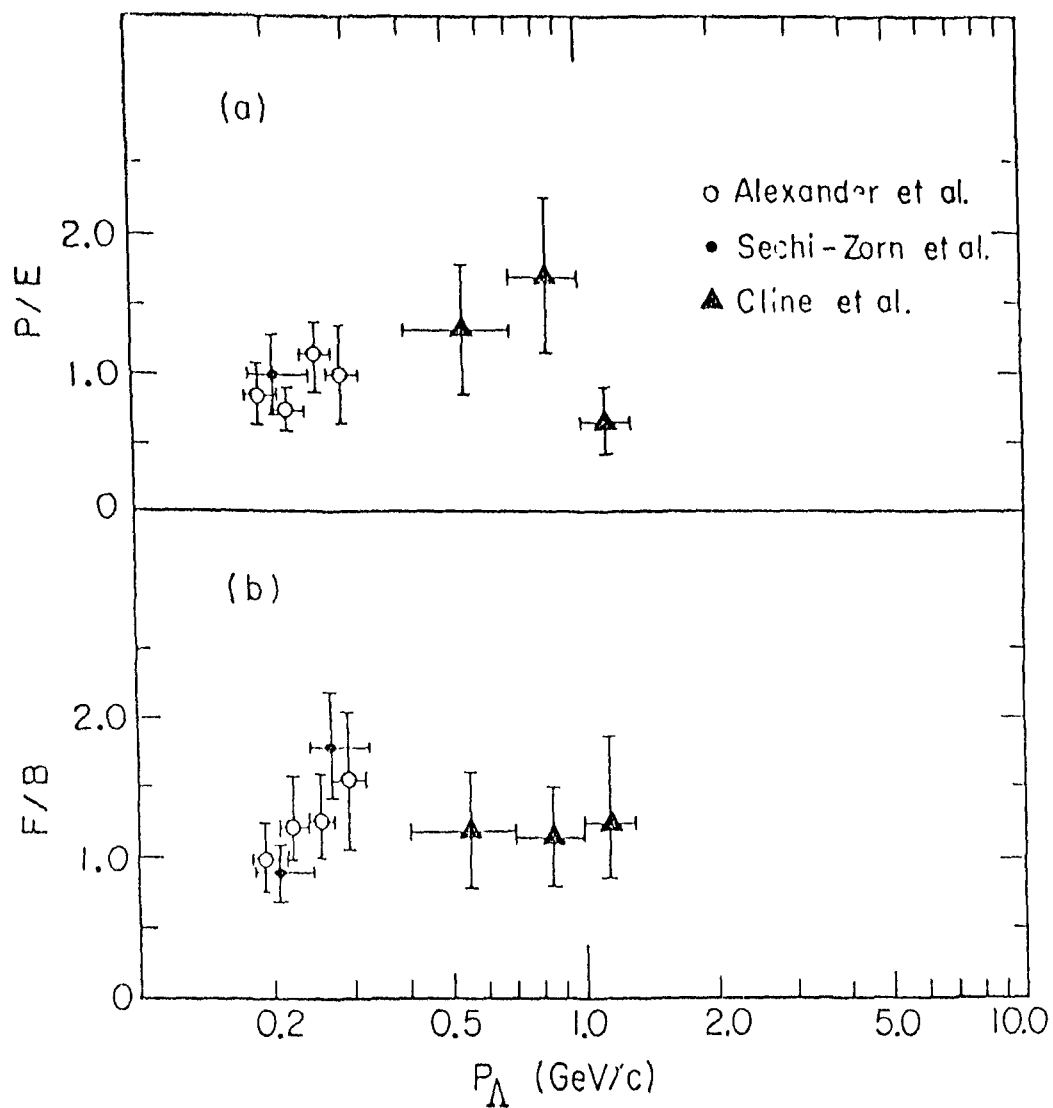


Figure 5: Polar to Equatorial (P/E) and forward to backward (F/B) ratios for Λ -p elastic scattering below incident momenta of 1 GeV/c.

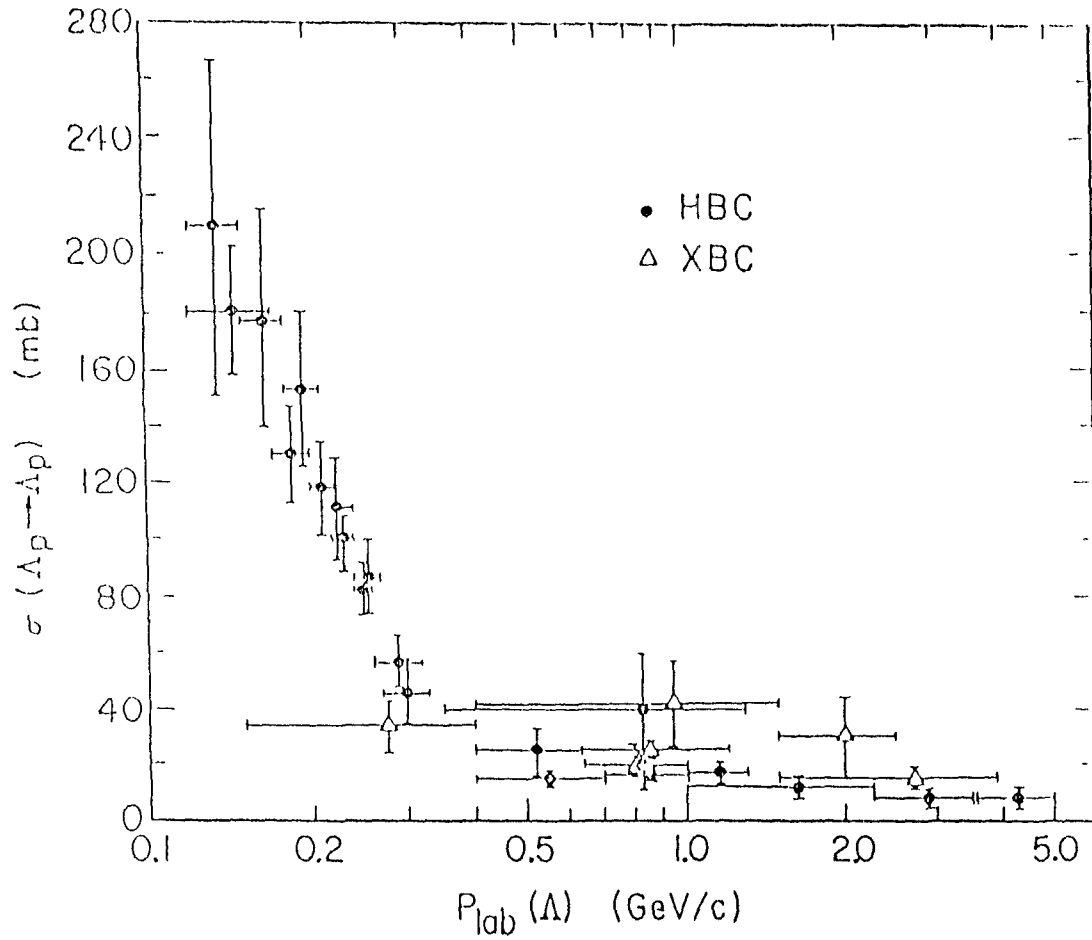


Figure 6: Preliminary Λp elastic cross sections (closed circles) from ref 22. The triangles correspond to previous reported cross-sections values obtained in hydrogen bubble chamber experiments.

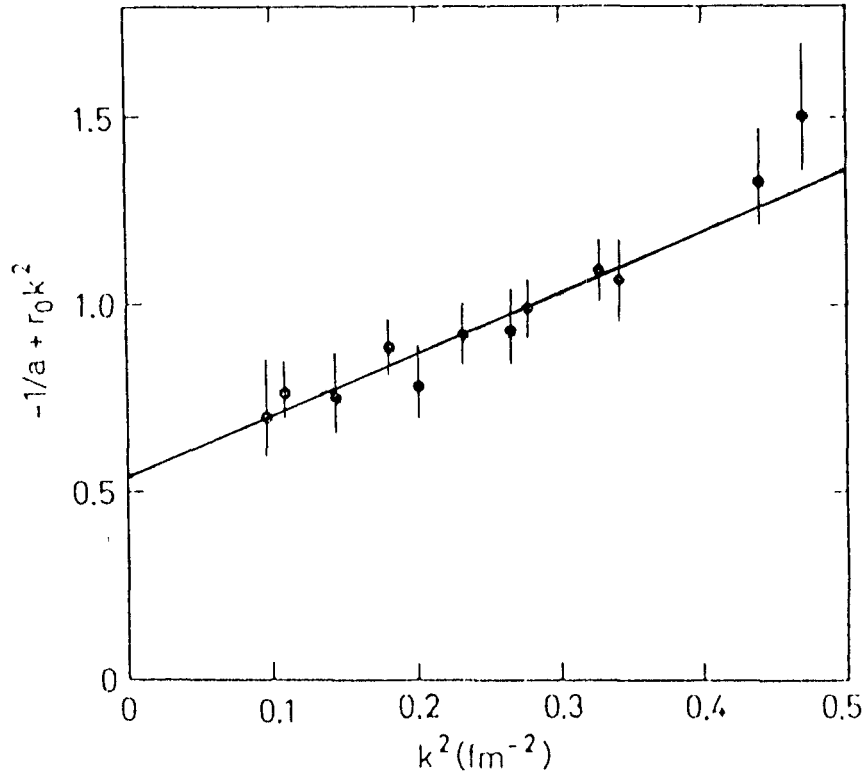


Figure 7: The quantity $-1/a + r_0 k^2$ is plotted against k^2 for the total p scattering cross sections. The line shows the best fit linear in k^2 .

NONLEPTONIC WEAK INTERACTIONS

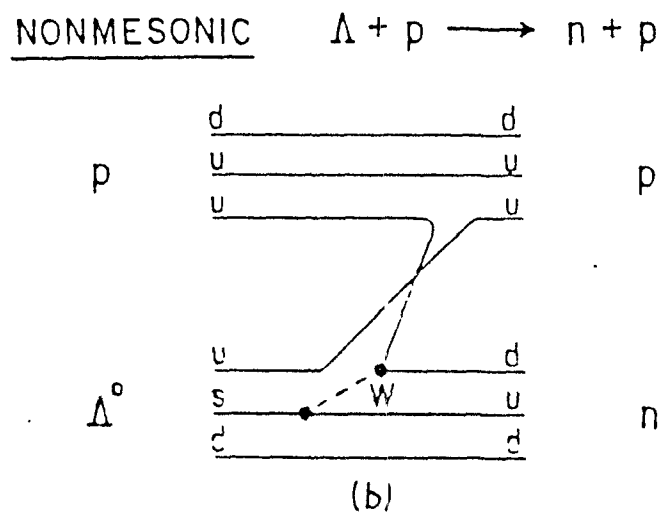
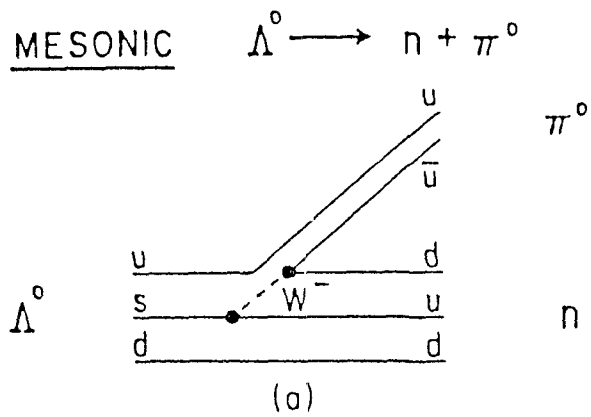
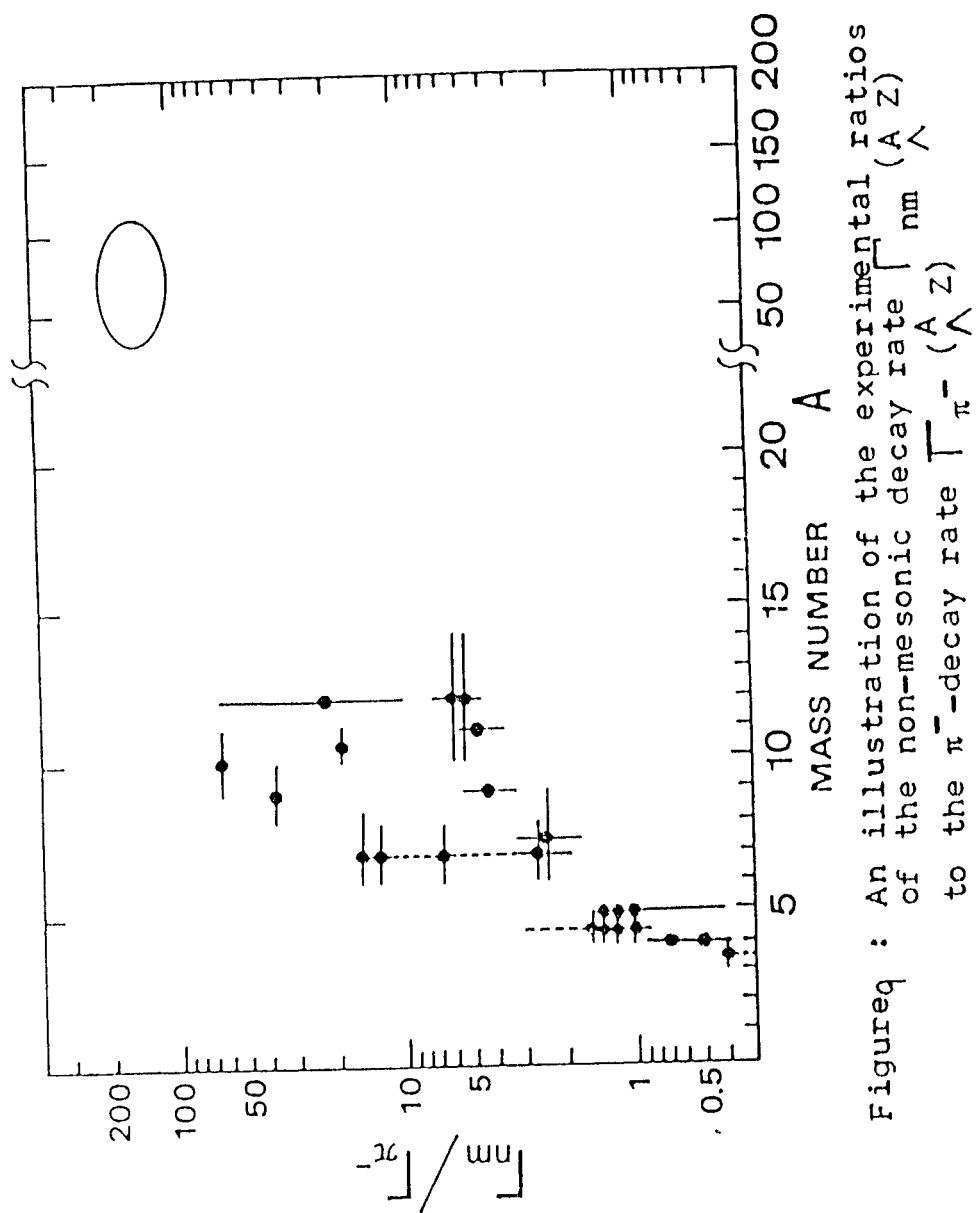


Figure 8: Quark diagrams for nonleptonic weak lambda interaction processes.



Figureq : An illustration of the experimental ratios
of the non-mesonic decay rate $\Gamma_{nm}(A, Z)$
to the π^- -decay rate $\Gamma_{\pi^-}(A, Z)$

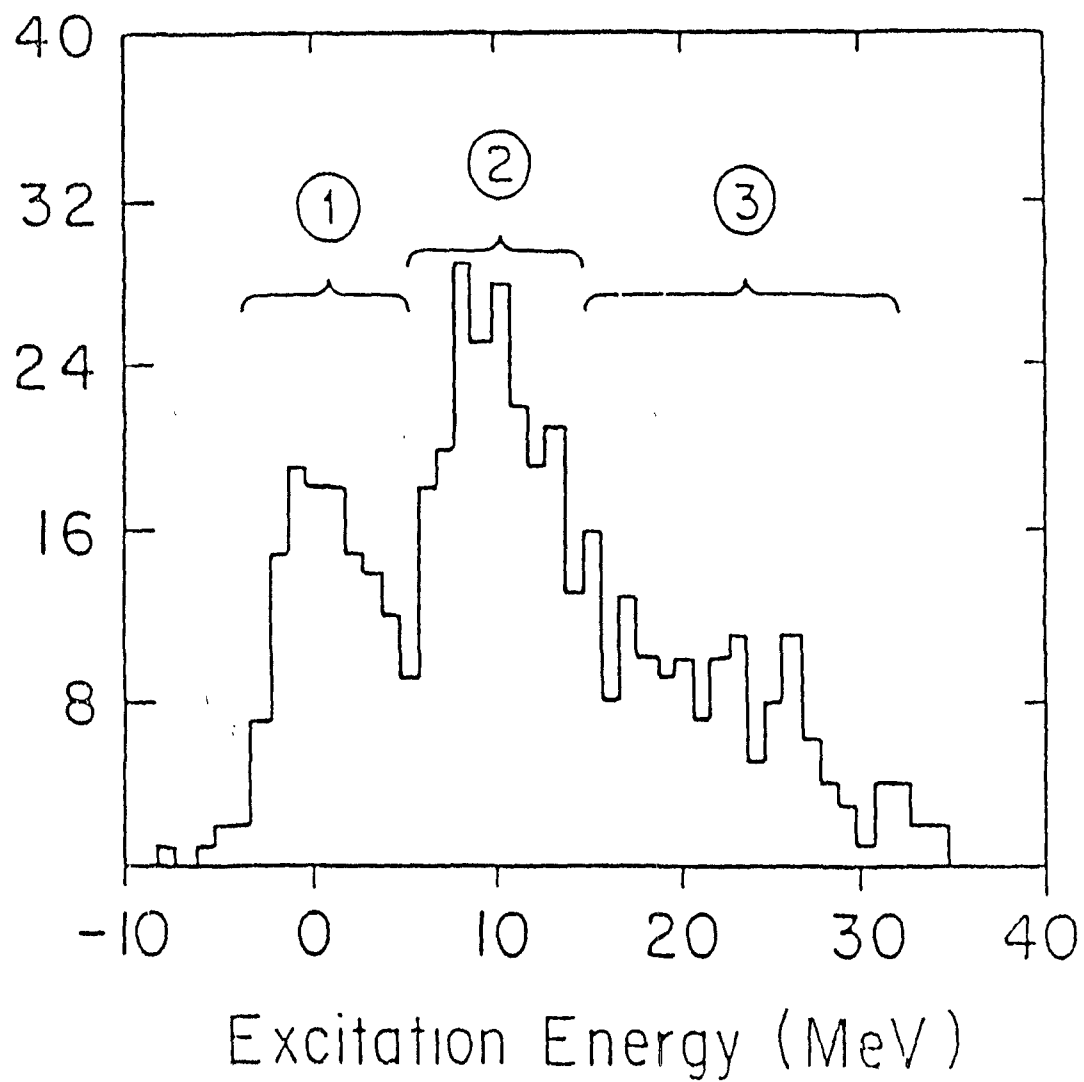


Figure 10: The $^{12}_{\Lambda}\text{C}$ hypernuclear excitation energy spectrum with experimental cuts shown for each of the three states discussed in our dissertation.

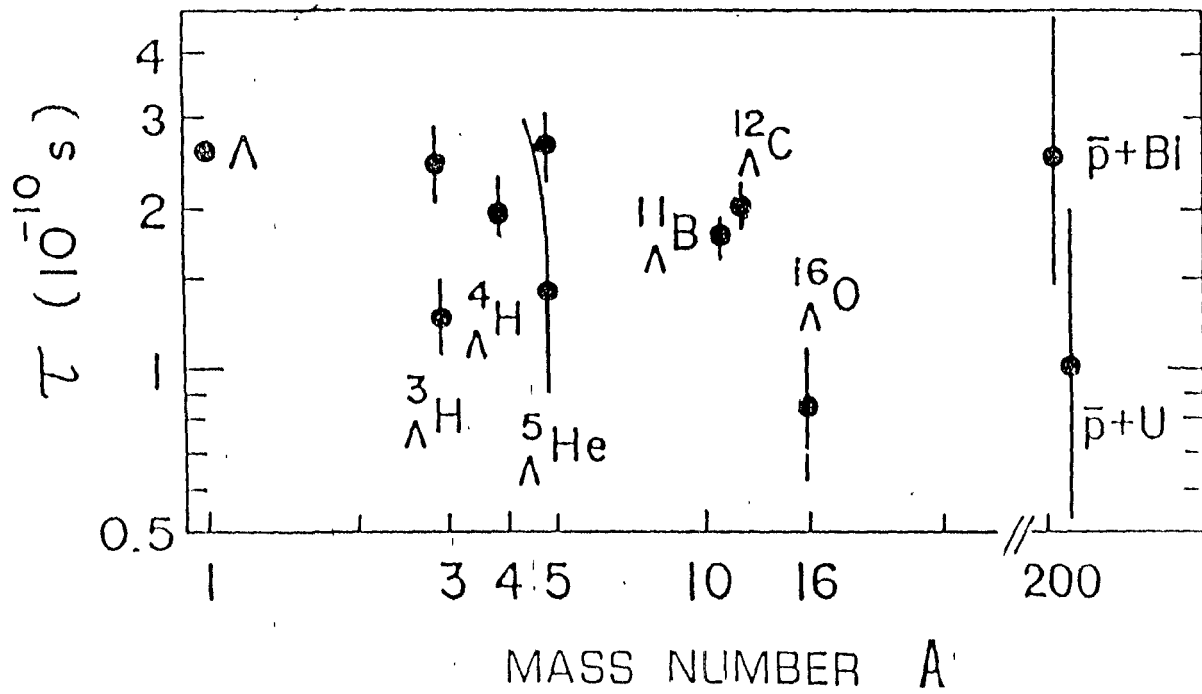


Figure 11: The observed life-times of $\tau(\Lambda^A Z)$ as a function of the mass number A .

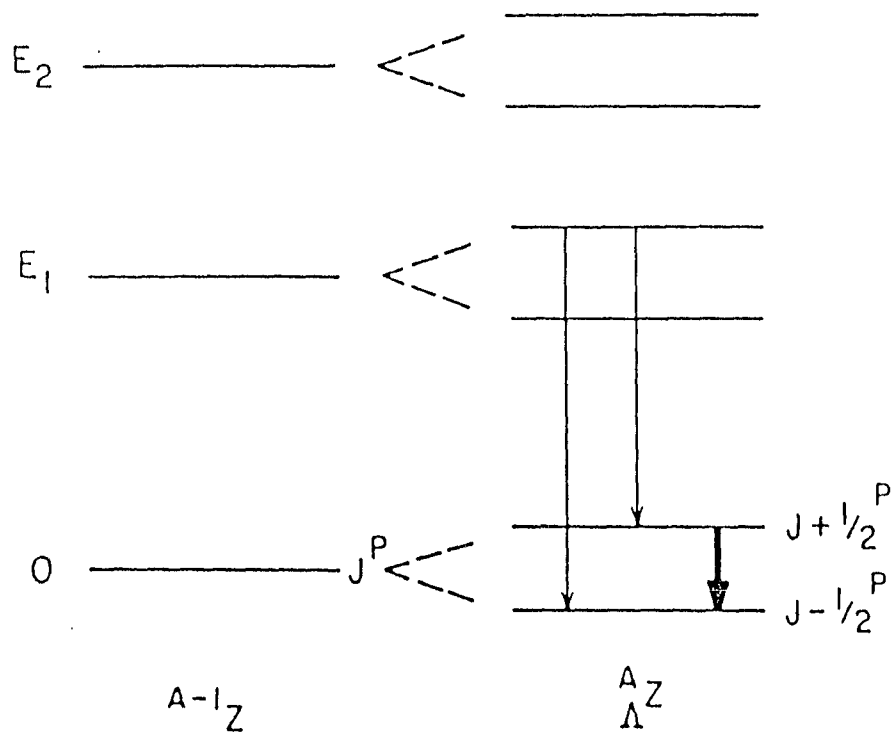


Figure 12: Schematic illustration of the doublet states of the Λ hypernuclei formed by coupling the S-shell Λ to the states of the core nucleus $A-1_Z$.

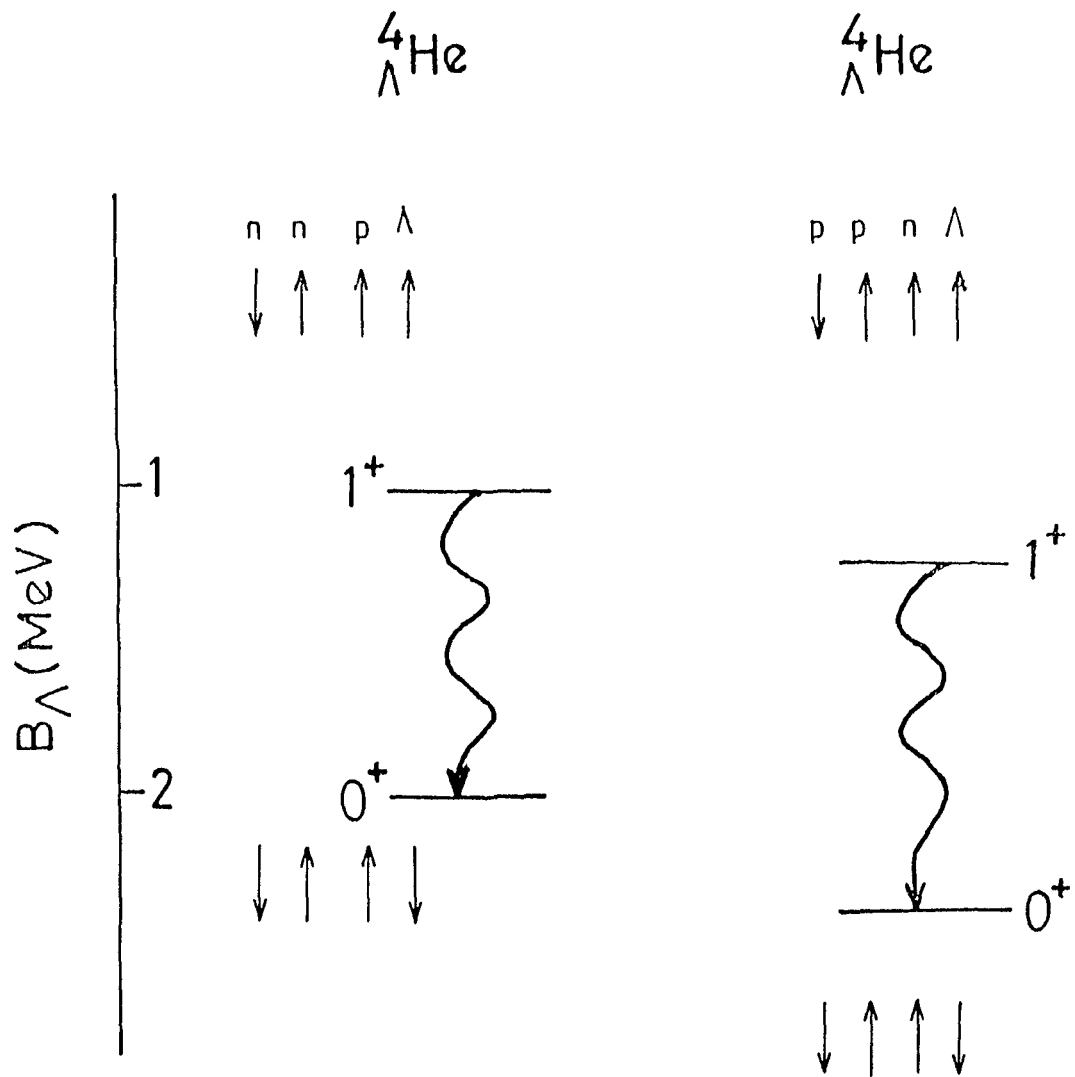


Figure 13: A schematic representation of the $A = 4$ hypernuclear systems.

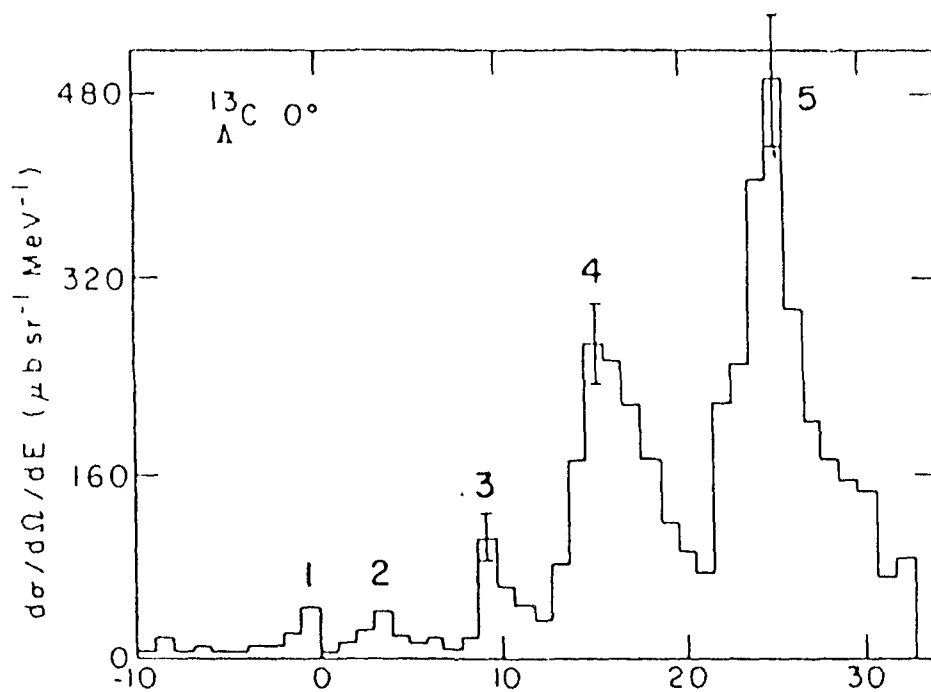


Figure 14: The excitation energy of ^{13}C observed in the $^{13}\text{C} (K^-, \pi^-) ^{13}\text{C}$ reaction, with $p_K = 800 \text{ MeV}/c$.

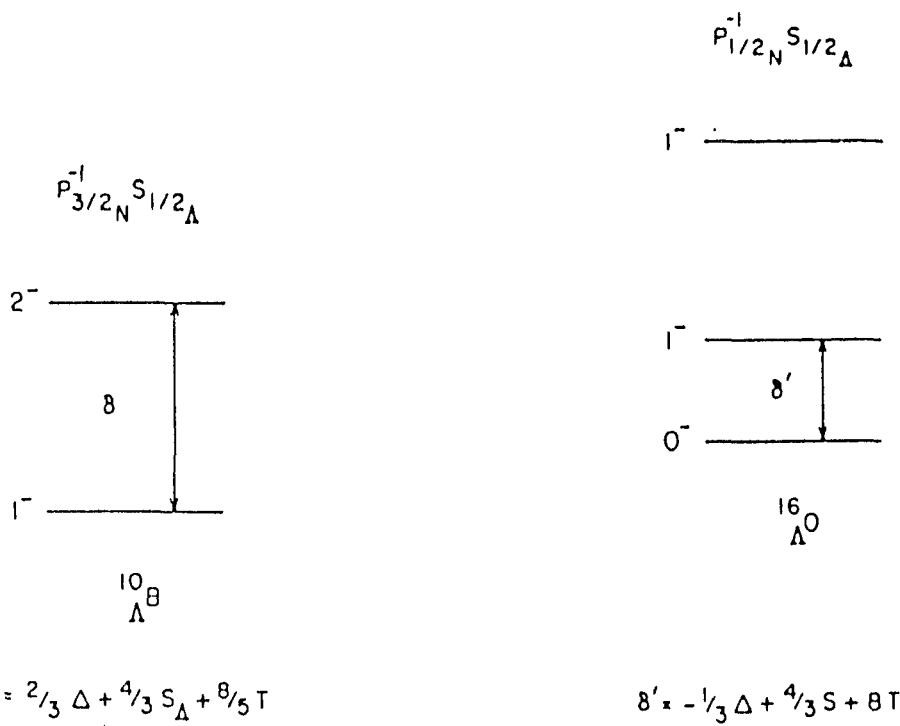


Figure 15a,b) The ground state doublets in ^{10}B and ^{16}O . The doublet-splittings are given in terms of the spin-dependent components of the π -nucleon interaction.

References

1. B.Povh , Progress in Part . and Nucl. Phys, Vol18, 183 (1987)
2. M.Phil.dissertation of N.Neelofer (1986) (Unpublished) (A.M.U.)
3. Ph.D. thesis of M.Shoeb (1984) (unpublished) (A.M.U.)
4. R.Chrien , Nucl.Phys . A478 , 705 C (1988)
5. C.B.Dover et.al., Phys. Rev. C22, 2073 (1988)
6. M.Juric et.al. , Nucl. Phys. B52 , 1 (1973)
7. J.Lemonne et.al. , Phys. Lett. 18, 354 (1965)
8. C.B. Dover , "Nuclear Physics with strange Particles " BNL-41894
,(1988)
9. D.M.Rote and A.R.Bodmer , Nucl. Phys. A148, 97 (1970)
10. A.Gal , Nucl. Phys. 8 , 1 (1975)
11. M.Shoeb and M.Z.Rahman Khan, J. Phys.. Soc. Japan 55, 3008 (1986)
12. I. Ahmad et.al. , Phys. Rev. C31, 1590 (1985)
13. N. Neelofar et.al . , Ind. J. Phys. 37, 5 , 419 (1991)
14. C.B.Dasakaloyannis et.al. , Prespective in Nucl. Phys.at Int. Energies
ICTP, Trieste , Italy Edited by Boffi,
Atti and Giannini World Scientific (1983)
15. A. Gal, Nucl. Phys. 8, 10 (1975)
16. C.G.Koutroulos , Few Body Systems Supplementum - 5 ,
Springer - Verlag. New York (1992)
17. " , Phys. Rev. C40, 275 (1989)
18. " , J. Phys. G : Nucl. Part. Phys. 17, 1069 (1991)
19. M.Grypeos etal , Nucl. Phys. A450 , 283c (1986)
20. B.Sechi-Zorn et.al , Phys. Rev. 17, 1735 (1968)

21. G.Alexander et.al. , Phys. Rev. 173, 1452 (1968)
22. D.Cline et.al. , Phys. Lett. 27B, 110 (1968)
23. J.T.Londergan and R.H.Dalitz, Phys. Rev.. C6, 76 (1992)
24. R.C.Herndon and Y.C.Tang, Phys. Rev. 165, 1093 (1968)
25. S.Ali et.al. , Phys. Lett. 24B, 11, 543 (1967)
26. G.Fast and De Swart, Int. Conf. on Hypernuclear Physics, ANL (edited by Bodmer and Hyman) Vol 2, May 5-7, 1969
27. M.Shueb and M.Z.Rahman Khan, Parmana Vol 26, No.5, (395), 1986
28. M.M.Nagels et.al. , Phys. Rev. D.15 , (1977) 2547 ; 20, 1633 (1979)
29. B.Povh, Prog. Part. Nucl. Phys. (ed.D.Wilkinson), Vol 8, 325 (1982)
30. P.D.Barnes, Nucl. Phys. A450 (1986) 43C
31. W.Cheston and H.Pirmakoff, Phys. Rev. 92 (1953) 1537
32. R.Grace et.al., DOE/ ER/ 03244-108
33. P.D.Barnes , CMU-DOE/ ER / 03244-121
Talk at the Int. Symposium on Hypernuclear and Kaon Phys, BNL (1985)
34. R.E.Chrien et.al., Phys. Lett. 89B, 31(1979)
35. T.Cantwell et.al., Nucl. Phys. A236, 445(1974)
36. R.Bertini et.al., Nucl. Phys. A360, 315(1981)
37. H.Bando et.al., Phys. Lett. B150 , 409(1985)
Prog. Th. Phys. 72 ,106(1984)
38. Y.Kurihara et.al., Phys. Rev. C31,971(1985)
39. E.Oset et.al., Nucl. Phys. A433 , 704(1985)
40. P.D.Barnes et.al., Nucl. Phys. A478,127c(1988)
41. P.D.Barnes et.al., Nucl. Phys. A479 ,89c(1988)

42. J.A.Carr et.al., Phys. Rev. C25, 952(1982)
43. R.Chrien et.al., Ann. Rev. Nucl. Proc. Sci 39,113(1989)
44. G.Bohm et.al., Nucl. Phys. B4 , 511(1968)
45. P.L.Kapur and R.E.Peierls, Proc. Roy. Soc. A166 , 277(1938)
46. Toshio Motoba , (π ,K) Hypernuclear production and Pionic decay
47. J.T.Bocquet et.al. Phys. Lett. B182, 146 (1986)
B192, 112 (1987)
48. H.Bando et.al. OECU-1991-10.
"Strangeness Nuclear Physics "
49. Toshio Motoba et.al., Nucl. Phys. A489 (1988) 683
50. Toshio Motoba , LAMF Workshop on (π , K) Physics
Los Alamos National Laboratory , New Mexico
October 11-13, 1990
51. Robert E.Chrien , BNL, New York, USA .
The gamma-ray spectroscopy of hypernuclei - 1984
52. M.May, Nucl. Phys. A450, 179c(1986)
53. A.bamberger et.al., Nucl. Phys. B60 ,1(1973)
54. M.Bedjidian et.al., Phys. Lett. 83B , 252(1979)
55. M.Bedjidian et.al., Phys. Letts. 94B ,480(1980)
56. J.D.Walecka , Annals. Phys. 63, 219(1971)
57. Bagett et.al., Phys. Lett 42B ,3,(1972)
58. A.Gal et.al., Ann. Phys. 113 (1980) 79
59. P.Piekarz et.al., Proceedings of the Int. Conf. on Hypernuclear and
Kaon Phys., Hiedelberg, Germany Max Planck-Institut fur
Kernphysik, MPIH-1982-V20.,Page 73-84.

60. M.May et.al. , (Ref9) page 63-72.
61. B.F.Gibson et.al., (Ref.9) page. 161-165.
62. W.Bruckner et.al,. Phys. Lett. 73B ,157(1978).
63. M.May et.al., Phys. Rev. Lett. 47 ,1106(1981).
64. T.Cantwell et.al. Nucl. Phys. A236 (1974) 445
65. D.J.Millener et.al. ,(in reference 1)

Chapter-5

Λ -N interaction

Introduction :

Theoretically the Λ - N interactions are studied through a phenomenological analysis of the available data. Herndon and Tang⁽¹⁾ made a detailed analysis of s-shell hypernuclei, using phenomenological hard-core two-body Λ N central potential constructed with Λ p scattering data. A good fit to B_Λ for ${}^3_\Lambda\text{H}$, ${}^4_\Lambda\text{H}$, and ${}^4_\Lambda\text{He}$ was obtained. The ${}^5_\Lambda\text{He}$ was found to be overbound by about 2.0 MeV.

The problem of overbinding of ${}^5_\Lambda\text{He}$ could not be resolved by the inclusion of central and non-central three-body Λ NN force. The inclusion of realistic NN interaction characterized by a tensor force in the analysis of Bando and Shimodaya⁽²⁾ could reduce the overbinding of ${}^5_\Lambda\text{He}$ by about half. Shinmura et.al.⁽³⁾ considered Λ N tensor force with a NN tensor force and found a good fit to the B_Λ of ${}^5_\Lambda\text{He}$. Bodmer et.al.⁽⁴⁾ with a central Urbana type Λ N interaction, consistent with Λ -N scattering analysed the binding energy of hypernuclei ${}^3_\Lambda\text{He}$, ${}^5_\Lambda\text{He}$, ${}^9_\Lambda\text{B}$, ${}^{13}_\Lambda\text{C}$ and Λ - binding to infinite nuclear matter. It was concluded that a repulsive Wigner type

three-body Λ NN force with the Λ NN potential is quite adequate to explain the overbinding of ${}^5_\Lambda\text{He}$. The detailed account of this analysis is given in the subsection 5.3.

Bedjidian et.al.⁽⁵⁾ found a weak spin dependence of the bare two-body Λ -N interaction. Boussy et.al.⁽⁶⁾ also found a weak spin - dependence in the Λ N -

force of δ - function form , based on the analysis of the spectroscopy data in the s-,d- and p- shell hypernuclei.

Gal et.al.⁽⁷⁾ made an analysis of p-shell hypernuclei within the uniform shell model framework using the intermediate coupled wavefunctions of Soper⁽⁸⁾ for the core - nuclei . It was found that a central two- body Λ - N potential is unable to give a satisfactory account of the data. Therefore , it was assumed that a non-central Λ N and three- body Λ NN forces are present.

Mujib etal.⁽⁹⁾ made an analysis of p-shell hypernuclei . A charge independent , central , strong spin-and state- dependent Λ N potential gives a satisfactory fit to the B_Λ data of p-shell hypernuclei, $^5_\Lambda\text{He}$ and $^7_\Lambda\text{Li}$ - binding to infinite nuclear matter , subsequently, Shoeb and Khan⁽⁹⁾ found that a charge independent , central , weakly spin and state -dependent effective two-body Λ -N potential along with a zero range three - body Λ NN force is adequate to explain the B_Λ data.

Straub etal.⁽¹⁸⁾ have studied the hyperon-nucleon scattering in the non-relativistic quark cluster model, where the medium and long range part of the hyperon-nucleon interaction is described by the one - boson - exchange and the short range part of the interaction by the gluon exchange between the quarks. However , the model is yet to take its final form.

Meson theoretical model has been widely studied and developed by Nijmegen group^(11,17) This model is based on the well known model of Nucleon-Nucleon interaction in One-Boson exchange potential.

In the following we shall discuss a few of these models in some detail.

5.1 Model of Gal , Soper and Dalitz

The information about the nuclear interaction of the Λ particle comes from the studies of Λ binding energies B_Λ , many of which are now known with considerable accuracy .The Λ hypernuclei with mass number $A \leq 5$ are known as s-shell hypernuclei and with the mass number $6 \leq A \leq 17$ are known as p-shell hypernuclei. The s-shell B_Λ values were well-fitted with a significant degree of spin dependence, with the notations U_s and U_t for the 1S_0 , and 3S_1 ΛN potential depths, the two potentials have been assumed to have the same shape and range and it was found out that $U_s > U_t$ ($\frac{U_t}{U_s} = 0.83 \pm 0.02$) . The values of the scattering parameters from these were :

singlet scattering length $a_s = -2.25 \pm 0.4$ fm

triplet " " $a_t = -0.77 \pm 0.06$ fm

Singlet effective range $r_s = 2.1 \pm 0.1$ fm

triplet " " $r_t = 3.5 \pm 0.2$ fm.

Later these parameters were determined through the $\Lambda - N$ scattering experiments which we have discussed in Chapter - 4.

Gal et al.⁽⁷⁾ made an extensive analysis of Λ binding energy of p-shell hypernuclei within the shell model framework using the intermediate coupled wavefunction . The main assumption were that of uniform single-particle wavefunction for the Λ particle and the nucleons , in the different nuclei throughout the p-shell . The core of the hypernucleus was considered to be rigid one i.e. the presence of the Λ does not polarize the core.

This in turn enables to have a relevant Λ -nucleon matrix element to be

parametrized in terms of relatively small number of reduced Λ -N matrix elements . On the basis of the calculation Gal et al.⁽⁷⁾ concluded that a simple assumption of a central two-body Λ -nucleon force is not adequate to explain the experimental B_Λ data. Therefore , the inclusion of the non-central Λ N and three -body Λ NN forces in the analysis was considered to be essential . The variation of Λ - wave function through the p-shell , the centre of mass effect on the core polarization were neglected throughout the calculation . It was concluded that the fit depends less on the strengths arising from the (Λ N) spin-orbit and (Λ NN) three-body interaction and requires a little mixing of the nuclear core states into the hypernuclear wave - function leaving only $^8_\Lambda\text{Li}$.

The fits were performed with some or all of the five $p_n s_\Lambda$ two-body matrix elements as parameters plus a single parameter characterizing a three-body Λ NN interaction which was assumed to be independent of σ_Λ . A wide variety of minima corresponding to different parameter sets were found . This was an indication of the limitation of the data set consisting only of the ground state spins.

-- Dalitz et al.⁽¹²⁾ considered the formation of low-lying excited state in p-shell hypernuclei ($p_n s_\Lambda$ configuration) via (K^- , π^-) reactions and the subsequent γ -decays of these levels . The conclusion was that the most direct information on the spin dependence of the Λ N effective interaction would come from the identification of s_Λ doublets based on core state with nonzero spin , and the doublet splitting depend mainly on combinations of three of the four-spin dependant Λ N matrix elements $-\Delta$ from the central spin -spin interaction , S_Λ from the Λ -spin

dependant spin-orbit interaction , and T from the tensor interaction

Millener et. al.⁽¹⁹⁾ based in a ΛN potential model and a phenomenological analysis of hypernuclear data, determined a set of four $p_n S_\Lambda$ two-body matrix elements which characterizes the spin dependence of the ΛN interaction in the p-shell.

We are mentioning the work of Gal et al.^(7,19) in some detail.

As it has been mentioned in Chapter - 1 one-pion exchange between Λ and N is forbidden due to the charge independence violation at $\Lambda\pi$ vertex (figure 11, Chapter 1) . Therefore , it is expected that the range of the ΛN force is shorter than the NN interaction. Two pion exchange (fig 12. Chap I) and higher exchange is allowed and in particular some of the multipion resonances are expected to contribute to the ΛN interaction . Isoscalar non - strange bosons, such as η (0^-) , ω (1^-) , σ (0^+) etc. have been used in the Gal et.al. calculations. The K (0^-) and $K^*(0^-)$ exchange does not contribute to the NN interaction , however, it does in the case of ΛN interaction (fig12 Chapter - 1)

The two pion exchange , K-exchange and π^0 -exchange contributes to the ΛN interaction .

A tensor force is not expected to show up strongly in the Λ and N system, since ρ and π exchanges are forbidden due to charge independence. The effective $\Lambda\omega$ vertex for tensor interaction is nearly equal to zero. Exchanges of η , K, and K^* give rise to a weak tensor component due to the medium and small values for the coupling constants . A strong component of spin-orbit force is expected from the exchanges of ω -, K^* , K - and σ - mesons, where K^* exchange contributes only to a symmetric force [$(\vec{S}_\Lambda - \vec{S}_N)$

. $\vec{1}_{\Lambda N}$] force and K exchange give rise to a significant antisymmetric force [$(\vec{s}_{\Lambda} - \vec{s}_N) \cdot \vec{1}_{\Lambda N}$] force.

The following coupling amplitudes (G_{BBM}) are used in the Gal's calculations. These have been expressed in terms of the VNN coupling amplitude G.

$$G_{\Lambda \Sigma V} = 2(1 - f) G / \sqrt{3}, \quad G_{\Sigma \Sigma V} = 2fG$$

$$G_{NN\bar{S}} = (4f - 1) G / \sqrt{3}, \quad G_{\Lambda\bar{S}} = -2(1 - f)G / \sqrt{3}$$

$$G_{\Lambda NK} = -(1 + 2f) G / \sqrt{3}, \quad G_{\Sigma NK} = (1 - 2f)G,$$

$$\text{where } f = \frac{F}{(F+D)}$$

5.1.1 Pseudoscalar Meson Exchange

The major contribution to the potential is from π^0 and K exchanges. The major term in these OBE potential is the tensor component.

$$V^T = C^T \left\{ \frac{m^3}{4M_{\Lambda}M_N} \right\} \left(\vec{\sigma}_{\Lambda} \cdot \hat{r} \vec{\sigma}_N \cdot \hat{r} - \frac{1}{3} \vec{\sigma}_{\Lambda} \cdot \vec{\sigma}_N \right) h(mr),$$

where $h(x)$ denotes the function

$$h(x) = \left(1 + \frac{3}{x} + \frac{3}{2} \right) \frac{e^{-x}}{x}$$

For η exchange, m denotes the mass m_{η} as

$$C_{\eta}^T = G_{\Lambda\eta} G_{NN\eta} / 4\pi = \left\{ -2(1-f)(4f-1)/3 \right\} \frac{G^2}{4\pi}$$

For K exchange , m denotes the mass $\sqrt{m_K^2 - (M_\Lambda - M_N)^2}$

$$\text{and } C_K^T = - P_{\Lambda N}^x \{ (1 + 2f)^2 / 3 \} G^2 / 4\pi$$

The K - exchange tensor force gives much the stronger contribution but due to the small range parameter the even V_K^T appears relatively ineffective in the p-shell hypernuclei $P_{\Lambda N}^x$ is the space -exchange operator which has the property

$$P^x \psi (\vec{r}_1, \vec{r}_2) = \psi (\vec{r}_2, \vec{r}_1)$$

\vec{r}_1 and \vec{r}_2 and the position coordinate of nucleon and Λ particle.

5.1.2 Scalar Meson Exchange

For σ energy gives a strong diagonal term in the ΛN channel which is the major part of the attraction in the ΛN potential.

For given mass m_σ , the magnitude of G_σ , the coupling constant between NN and the $I = 1$ member of the scalar octet , is determined for given f_σ by the central part of the ΛN potential.

$$V_\sigma^C = - \left[\frac{G_{\Lambda\sigma} G_{NN\sigma}}{4\pi} \right] m_\sigma y (m_\sigma r),$$

where $Y (x) = e^{-x}/x$

This σ -exchange also generates a spin -orbit potential of the form ,

$$V_\sigma = C_\sigma^{SO} m_\sigma^3 \left[\frac{\vec{\sigma}_\Lambda \cdot \vec{L}}{4M_\Lambda^2} + \frac{\vec{\sigma}_N \cdot \vec{L}}{4M_N^2} \right] g (m_\sigma r),$$

where m_σ denotes the σ -mass, and

$$g(x) = \left(1 + \frac{1}{x}\right) \frac{e^{-x}}{x^2}$$

$$C_\sigma^{so} = - \left\{ 2(1-f_\sigma)(1-4f_\sigma)/3 \right\} \frac{G_\sigma^2}{4\pi}$$

In terms of the symmetric and antisymmetric the spin-orbit potential :

$$V_\sigma^{so} = C_\sigma^{so} \left[\frac{1}{4M_\Lambda^2} + \frac{1}{4M_N^2} \right] \vec{S}_{\Lambda N}^+ \cdot \vec{L} g(m_\sigma r) \\ + C_\sigma^{so} m_\sigma^3 \left[\frac{1}{4M_\Lambda^2} - \frac{1}{4M_N^2} \right] \vec{S}_{\Lambda N} \cdot \vec{L} g(m_\sigma r),$$

where $\vec{S}_{\Lambda N}^\pm = \frac{1}{2} (\vec{\sigma}_\Lambda \pm \vec{\sigma}_N)$

For K_σ exchange, the spin-orbit potential takes the symmetrical form :

$$V_{k\sigma}^{so} = C_{k\sigma}^{so} \frac{m^3}{2M_\Lambda M_N} \vec{S}_{\Lambda N}^+ \cdot \vec{L} g(mr),$$

where

$$m = \left\{ m(K_\sigma)^2 - (M_\Lambda - M_N)^2 \right\}^{1/2}, \text{ and}$$

$$C_{k\sigma}^{so} = P_{\Lambda N}^x \left\{ (1 + 2f_\sigma)^{2/3} \right\} \frac{G_\sigma^2}{4\pi}$$

5.1.3 Vector Meson Exchange

The spin-orbit potential generated by the electric couplings is of the form

$$V_w^{so} (E'-E) = \left[\frac{G_{NNw}}{4\pi} \frac{G_{\Lambda w}^E}{\Lambda} \right] \frac{E}{2M^2} mg(mr) \left\{ \frac{M_N}{2M_\Lambda} \vec{\sigma}_\Lambda + \right.$$

$$\left. \frac{M_{\Lambda} \vec{\sigma}_N}{2M_N} \right\} \cdot \vec{L} ,$$

$$\text{where } g(x) = \left(1 + \frac{1}{x} \right) \frac{e^{-x}}{x^2} .$$

$$G_{NNW}^E = 3 G_{\rho}^E$$

$$\left(\frac{G_{\rho}^E}{4\pi} \right)^2 = (0.6 - 0.7)$$

$$M = M_{\Lambda} = M_N$$

The spin - orbit exchange force due to K^* exchange :

$$V_k^{so*} = -p_{\Lambda N}^x \left\{ \frac{(G_{\Lambda NK^*}^E)^2}{4\pi} \frac{(M_{\Lambda} + M_N)^2}{8M_{\Lambda}M_N} \left(\frac{m}{m^*} \right)^2 \right.$$

$$\left. - \frac{(G_{N\Lambda K^*}^E)(G_{N\Lambda K^*}^M)}{4\pi} \cdot \frac{M_{\Lambda} + M_N}{M} \right\} \left(\frac{m}{M} \right)^2 mg(mr) \vec{S}_{\Lambda N}^+ \cdot \vec{L}$$

where $m^* = m(K^*)$

$$m = \sqrt{m^{*2} - (M_{\Lambda} - M_N)^2}$$

$$G_{N\Lambda K^*}^E = -\sqrt{3} G_{\rho}^E$$

$$G_{N\Lambda K^*}^M = -\frac{3\sqrt{3}}{5} G_{\rho}^M$$

$$\frac{G_{\rho}^M}{G_{\rho}^E} = 4.65$$

$$\bar{M} = M_{\Lambda} = M_N$$

5.1.4 For ω -exchange

$$V_{\omega}^T = - \left(\frac{G_{NN\omega}^M}{4\pi} \right) \frac{M_{\Lambda} M_N}{4M^2} \left\{ \vec{\sigma}_{\Lambda} \cdot \hat{r} \vec{\sigma}_N \cdot \hat{r} - \frac{1}{3} \vec{\sigma}_{\Lambda} \cdot \vec{\sigma}_N \right\} \frac{m^3}{M^2} h(mr)$$

$$\text{where } h(x) = \left(1 + \frac{3}{x} + \frac{3}{x^2} \right) \frac{e^{-x}}{x}, \quad M_{\Lambda} = M_N = \bar{M} \quad \text{and } m = m^* = m_{\omega}$$

This expression vanishes due to $G_{\omega}^M = 0$.

There is also a tensor component in the K^* -exchange potential :

$$V_k^{T*} = P_{\Lambda N}^x \frac{(G_{N\Lambda K^*}^M)^2}{4\pi} \frac{(M_{\Lambda} + M_N)^2}{16\bar{M}^2} \left\{ \vec{\sigma}_N \cdot \hat{r} \vec{\sigma}_{\Lambda} \cdot \hat{r} - \frac{1}{3} \vec{\sigma}_{\Lambda} \cdot \vec{\sigma}_N \right\} \frac{m^3}{M^2} h(mr),$$

where $m^* = m(K^*)$

$$m = \sqrt{m^{*2} - (M_{\Lambda} - M_N)^2}$$

$$M_{\Lambda} = M_N = \bar{M}$$

This tensor interaction has about the same strength as SU (3) predicts for the K-exchange tensor interaction but a much shorter range parameter, therefore, it is expected that it will contribute a little in the p-shell hypernuclei.

5.1.5 The Λ NN interaction : The diagram 1a) corresponds to two-pion-exchange hypernuclear Λ NN interaction potential, where the two pions are exchanged between the Λ -particle and the different nucleons in the nucleus.

The intermediate hyperonic state has been represented by a blob in the fig 1b) which can be a Σ^* resonances. The first such resonance is a $\pi \Lambda_{p3/2}$ -resonance Σ^* (1385).

In fig 1b), each nucleon is localized with a distance of $\hbar/m_\pi c \approx 1.4$ fm from the Λ .

The Λ NN interaction is expressed in momentum space as

$$V(\Lambda N_1 N_2) = -\frac{3 C_P}{4\pi \mu^6} \vec{\tau}_1 \cdot \vec{\tau}_2 \int d^3p d^3q \vec{\sigma}_1 \cdot \vec{p} \vec{\sigma}_2 \cdot \vec{q} \frac{\vec{p} \cdot \vec{q}}{(p^2 + \mu^2)(q^2 + \mu^2)} e^{i\vec{q} \cdot (\vec{r}_1 - \vec{r}_\Lambda)}$$

where μ is two pion mass and ----- (1)

$$C_P = \frac{\mu^4}{6M_N^2} \cdot \frac{G_{NN\pi}^2}{4\pi} \left\{ \frac{\mu^2}{M_\Sigma - M_\Lambda} \left[\frac{M_\Sigma + M_\Lambda}{4M_\Sigma M_\Lambda} \right]^2 \frac{G_{\Lambda\Sigma\pi}^2}{4\pi} + \frac{\mu^2}{6\pi^2} \int_0^\infty dk \frac{\sigma_3(k)}{\mu^2 + k^2} \right\}$$

where $\sigma_3(k)$ denotes the $p_{3/2}$ cross-section for $\pi\Lambda$ scattering.

In coordinate space ,

$$V(\Lambda N_1 N_2) = -\frac{C_p}{6} \vec{r}_1 \cdot \vec{r}_2 \left\{ (\vec{\sigma}_1 \cdot \vec{\sigma}_\Lambda y(mr_{\Lambda 1}) + 3S_{\Lambda 1} h(mr_{\Lambda 1})) + (\vec{\sigma}_2 \cdot \vec{\sigma}_\Lambda y(mr_{\Lambda 2}) + 3S_{\Lambda 2} h(mr_{\Lambda 2})) \right\}_+,$$

$$\text{where } y(x) = \frac{e^{-x}}{x},$$

$$h(x) = \left[1 + \frac{3}{x} + \frac{3}{x^2} \right] \frac{e^{-x}}{x}$$

$$\vec{r}_{\Lambda N} = \vec{r}_N - \vec{r}_\Lambda, \quad \text{and}$$

$$\vec{S}_{\Lambda N} = (\vec{\sigma}_\Lambda \cdot \hat{r}_{\Lambda N} \vec{\sigma}_N \cdot \hat{r}_{\Lambda N} - \frac{1}{3} \vec{\sigma}_\Lambda \cdot \vec{\sigma}_N).$$

Physically, the inclusion of the two-pion exchange Λ NN force in a realistic Λ -nuclear calculation is significant because this force senses regions of the Λ N configuration which are almost asymptotic for any two-body Λ N interaction.

The coefficients for the Central Terms .

The central Λ N force gives rise to two spatial matrix elements V_t and V_s . V_t corresponds to the triplet and V_s to singlet Λ N configurations .

$$\frac{(3V_t + V_s)}{4} - (V_s - V_t) \vec{S}_\Lambda \cdot \vec{S}_N = \bar{V} - \Delta \vec{S}_\Lambda \cdot \vec{S}_N,$$

where Δ = spin dependence of the central forces $\vec{S} = \frac{1}{2} \vec{\sigma}$

\bar{V} = spin average matrix element

(7)

Gal et al. have found the effective central Λ N interactions in the singlet and triplet states to be of comparable magnitude. Therefore, the ratio of $\frac{\Delta}{V}$ is very small. This in turn implies that the effect of Δ is almost negligible in determining the binding energies of hypernuclei. The value of $C_p = 1.43$ MeV.

The Coefficient for Noncentral terms K , η , and K^*

contributes maximum to the tensor term T . The value of $f = 0.4$ for the pseudoscalar meson coupling with baryon, with $G_{NN\pi}^2 / 4\pi = 14.5$, as a cut of radius $d = 0.4$ fm in the Λ N interaction. For K^* exchange, the coupling constant $-(G_{\Lambda NK^*}^M)^2 / 4\pi \approx 15$ with $d = 0.4$ fm.

The following are the estimations for $T(K)$, $T(\eta)$ and $T(K^*)$,

$$\begin{array}{ccc} T(K) & T(\eta) & T(K^*) \\ + 0.120 & -0.021 & -0.050 \text{ MeV} = + 0.049 \text{ MeV} \end{array}$$

The contribution to spin-orbit terms S_+ and S_- comes mainly from σ , ω and K^* exchange.

The coupling constant for σ - meson is

$$\frac{G_{NN\sigma}^2}{4\pi} = \frac{G_{\Lambda\Lambda\sigma}^2}{4\pi} = 28 \quad \text{and} \quad f_\sigma = -0.5.$$

The contribution of σ , K^* and ω for the spin-orbit S_+ term

$$\begin{array}{ccc} S_+ (\sigma) & S_+ (K^*) & S_+ (\omega). \\ (-0.11) - (-0.17) & -0.108 & -0.029 \approx (-0.25) - (-0.31) \text{ MeV} \end{array}$$

The contribution of σ , K^* and ω for the spin-orbit S_- term

| | | |
|----------|---------------|---------------|
| $S_-(k)$ | $S_-(\sigma)$ | $S_-(\omega)$ |
| +0.040 | +0.029 | +0.062 |

The coefficient of the contribution of the terms Δ , S_- , T and S_+ to the total B_Λ value has been tabulated in table 1 for p-shell hypernuclei.]

5.2. Model of Nijmegen group :

Nagels et al.⁽¹¹⁾ made a detailed analysis of Λ N forces using meson theoretical model. There are various models viz. A, B, C, D, E, F, and soft core^(11,17). The basic idea of the model is the following :

The well studied nucleon-nucleon system is taken in the One - boson - exchange model. Assuming the SU (3) symmetry for coupling between the baryons and the bosons, the nucleon-nucleon system is then generalized to hyperon- nucleon system.

The results are fairly good to account for the properties of the Hyperon-Nucleon forces. There are two models (1) with hard core (2) with soft core. The spirit of Nijmegen group can be said to be an extension of the basic idea of Gal et.al. We are presenting here the chronological development of Nijmegen model. The analysis of nucleon - nucleon and hyperon-nucleon scattering with a one - boson- exchange potential model the NN results are obtained. The model was first evaluated in momentum space by solving the Lippmann - Schwinger equation, then by using Fourier transformation the potential model is obtained in configuration space. At first the model A (OBEP + TPEP model) was constructed, consisting of OBEP from the member of the pseudo-scalar and vector -meson nonets, and the Bruckner - Watson TPEP. Model A gave a reasonable account of the NN s

waves , but it failed to give a good quantitative description of the higher NN waves. To extend the NN calculations to YN channels Nagels et.al. included the SU(3) mesons in the study of pure OBEP models. The OBEP model was divided into two classes where the long-and medium -range forces were given by the sum of the pole contributions of the pseudo-scalar and vector -meson nonets.

The classes differed in the treatment of the scalar mesons. In the 1st class the existence of only one unitary singlet scalar meson , called ϵ was taken with a mass in the neighborhood of 700 MeV and a very large width. The models in the second class contained in addition an octet of scalar mesons. The first model in class I, called model B, have the pole parameter for ϵ : $m_\epsilon = 720$ MeV , $\Gamma_\epsilon = 400$ MeV which gave a reasonable description of NN with $\chi^2 / \text{data} = 5.9$ for the data upto 330 MeV. In model C (falling in class II) the different pole parameters for the ϵ were used with $m_\epsilon = 670$ MeV , $\Gamma_\epsilon = 500$ MeV, $\chi^2 / \text{data} = 4.0$. The results were better than the model B.

In the further continuation of class I, the model D was developed by considering the following mesons.

- (a) The pseudoscalar meson nonet π , η , K and X^0 with the singlet - octet mixing (η, X^0) angle from the Gell-Mann -Okubo mass formula , $\theta_p = -10.4^\circ$.
- (b) The vector meson nonet ρ , ϕ , K^* and ω with ideal ϕ - ω mixing angle $\tan \theta_v = 1/\sqrt{2}$.
- (c) The Scalar meson unitary singlet ϵ .
- (d) The effects of large widths of the ϵ and ρ meson were also included .

Then the model E was introduced . Model E differed from D in the respect that contributions of a nonet of scalar mesons were taken into account . The results were about the same as from model D.

A less favourable point of models D and E was that the breaking of $SU(3)$ was not only kinematical via the physical masses of the particles but also slightly dynamical via different hard cores in channels which belong to the same irreducible representation of $SU(3)$ e.g. 1S_0 (pp) and 1S_0 (Σ^+p) , which both belong to a 27 . Keeping these discrepancies into account an another model was required Therefore, the model F was introduced . It consists of local potentials due to exchange of member of the pseudoscalar, vector , and scalar -mesons nonets.

$SU(3)$ relations were assumed for the axial -vector couplings of the pseudoscalar mesons, for the electric and magnetic couplings of the vector mesons, for the direct coupling of the scalar mesons , and for the hard-core radii. In the fit to NN the non-strange meson-nucleon coupling— were determined. Simultaneously, the YN analysis determined the F/D ratios and the $SU(3)$ parameters of the scalar -mesons nonet . The NN data were reasonably agreeable with the experimental data upto pion production threshold.

The second phase of the Nijmegen model was started in 80s , where the soft - core baryon-baryon one-boson-exchange models "were introduced.

First of all, the Nucleon-Nucleon potential was obtained⁽¹⁷⁾. Recently, the hyperon-nucleon potential has been reported . Since, we are discussing in our dissertation the hyperon-nucleon potential , therefore, we shall discuss the soft - core model in detail⁽¹⁷⁾. We are outlining here the

concept of getting the Nucleon-Nucleon potential

An excellent fit of the NN data was obtained with the soft-core OBE model, based on Regge pole theory, where 13 parameters were used.

Most of the parameters are the coupling constants mixing angles or $F/(F+D)$ ratios.

For the hyperon-nucleon potential the interaction are described by the following exchange :⁽¹⁷⁾

(1) The pseudoscalar - meson nonet π, η, η', K with the mixing angle $\theta_p = -23.0^\circ$ from the Gell - Mann-Okubo mass formula

(2) The vector-meson nonet ρ, ϕ, K^*, ω with the $\phi - \omega$ idea mixing angle $\theta_v = 37.56^\circ$.

(3) The scalar - meson nonet σ, S^*, K, ϵ with a free $S^* - \epsilon$ mixing angle θ_s .

(4) The "diffractive" contribution from the Pomeron P, f, f' and A_2 .

To get the complete form of potential the following major steps are followed :

(1) The OBE potentials are defined for the Lippman -Schwinger equation.

(2) The OBE potential in momentum space for pseudoscalar vector, scalar, and diffractive exchanges are obtained.

(3) Fourier transformation is used to have the OBE potentials in coordinate space.

(4) The obtained potentials is then used to compare the YN data.

We are mentioning in some detail the major steps to obtain the hyperon-nucleon potential.

The considered hyperon-nucleon reaction are

$$Y(p_1, s_1) + N(p_2, s_2) \longrightarrow Y'(p'_1, s'_1) + N'(p'_2, s'_2),$$

where Y and Y' are particles 1 and 3, and N and N' are particles 2 and 4

The four momentum of the particle i is

$$p_i = (E_i, \vec{p}_i), \text{ where } E_i = \sqrt{\vec{p}_i^2 + M_i^2}$$

and M_i is the mass

The transition amplitude matrix M is related to the S matrix through

$$\langle f | S | i \rangle = \langle f | i \rangle - i(2\pi)^4 \delta^4(P_f - P_i) \langle f | M | i \rangle,$$

where $P_i = p_1 + p_2$ and $P_f = p'_1 + p'_2$ represent the total four momentum for the initial state $|i\rangle$ and the final state $|f\rangle$.

Three - dimensional integral equations for the amplitudes $\langle f | M | i \rangle$:

$$M_{fi}(\vec{q}_f, \vec{q}_i; s) = W_{fi}(\vec{q}_f, \vec{q}_i; s) +$$

$$\frac{1}{(2\pi)^3} \sum_n \int d^3k_n W_{fn}(\vec{q}_f, \vec{k}_n; s) G_o(\vec{k}, s) \times$$

$$M_{ni}(\vec{k}_n, \vec{q}_i; s),$$

where \vec{q}_i and \vec{q}_f denote the initial -and final -state momenta, and

$$G_o(\vec{k}; s) = \frac{1}{2} \frac{E_1(\vec{k}) + E_2(\vec{k})}{E_1(\vec{k}) E_2(\vec{k})} \times \left\{ s - ([E_1(\vec{k}) + E_2(\vec{k})]^2 + i\epsilon) \right\}^{-1}$$

with $s = [E_1(\vec{p}) + E_2(\vec{p})]^2$.

$\langle f | W | i \rangle$ is the pseudo-potential which corresponds to the pole approximation to the Feynman amplitudes for OBE with form factors at the baryon-baryon-meson (BBM) vertices.

Using the T-matrix definition as

$$(f|T|i) = [4M_{34}(E_3 + E_4)]^{-1/2} \langle f|M|i \rangle [4M_{12}(E_1 + E_2)]^{-1/2}$$

$$(\text{ where } M_{12} = (M_1 + M_2)/2, M_{34} = \frac{(M_3 + M_4)}{2})$$

and with some trivial steps the following form of Lippman - Schwinger equation is obtained .

$$(3,4|T|1,2) = (3,4|V|1,2) + \frac{1}{(2\pi)^3} \sum_n \int d^3 k_n (3,4|V|n_1, n_2) \times$$

$$\frac{2M_{n_1, n_2}}{\vec{q}_n^2 - \vec{k}_n^2 + i\epsilon} (n_1, n_2|T|1,2)$$

$$\text{where } (f|V|i) = [4M_{34}(E_3 + E_4)]^{-1/2} \langle f|W|i \rangle \times$$

$$[4M_{12}(E_1 + E_2)]^{-1/2}$$

The potential is then expanded as

$$V = \sum_{i=1}^6 v_i (\vec{k}^2, \vec{q}^2) P_i,$$

where

$$P_1 = 1$$

$$P_2 = \vec{\sigma}_1 \cdot \vec{\sigma}_2$$

$$P_3 = (\vec{\sigma}_1 \cdot \vec{k})(\vec{\sigma}_2 \cdot \vec{k}) - \frac{1}{3}(\vec{\sigma}_1 \cdot \vec{\sigma}_2)\vec{k}^2$$

$$P_4 = \frac{1}{2}(\vec{\sigma}_1 + \vec{\sigma}_2) \cdot \vec{n}$$

$$P_5 = (\vec{\sigma}_1 \cdot \vec{n})(\vec{\sigma}_2 \cdot \vec{n})$$

$$P_6 = \frac{1}{2}(\vec{\sigma}_1 - \vec{\sigma}_2) \cdot \vec{n},$$

$$\begin{aligned}
V_D(r) = & \frac{m_p}{4\pi} \left[g_{13}^D g_{24}^D \frac{4}{\sqrt{\pi}} \frac{m_p^2}{M^2} \cdot \left\{ \left\{ 1 + \frac{m_p^2}{2M_Y M_N} (3 - 2m_p^2 r^2) + \frac{m_p^2}{M_Y M_N} L \cdot S + \left(\frac{m_p}{2M_Y M_N} \right)^2 Q_{12} \right. \right. \right. \\
& + \frac{m_p^2}{M_Y M_N} \left[\frac{(M_N^2 - M_Y^2)}{4M_Y M_N} \right] \cdot \frac{1}{2} (\vec{\sigma}_1 - \vec{\sigma}_2) \cdot \vec{L} \left. \left. \right\} e^{-m_p^2 r^2} \right. \\
& \left. \left. + \frac{1}{4M_Y M_N} (\nabla^2 e^{-m_p^2 r^2} + e^{-m_p^2 r^2} \nabla^2) \right] \right] p,
\end{aligned}$$

(In these formulæ m is the average mass in the isospin multiplet.)

$$\text{where } \phi_c^n(r) = \frac{1}{\left(\frac{m}{4\pi} (-m^2)^n\right)} \left(\frac{1}{2\pi^2}\right) \int dk \cdot k^2 j_0(kr) (k^2)^n \Delta(k^2, m^2, \Lambda^2)$$

$$\begin{aligned}
\phi_T^n(r) = & \frac{1}{\left(\frac{-m^3}{4\pi} (-m^2)^n \phi_T^n(r)\right)} \left(-\frac{1}{6\pi^2}\right) \int dk \cdot k^4 j_2(kr) (k^2)^n x \\
& \Delta(k^2, m^2, \Lambda^2)
\end{aligned}$$

$$\begin{aligned}
\phi_{so}^r(r) = & \frac{1}{\left(\frac{m^3}{4\pi} (-m^2)^n\right)} \frac{1}{(2\pi^2 r)} \int dk \cdot k^3 j_1(kr) x \\
& (k^2)^n \Delta(k^2, m^2, \Lambda^2)
\end{aligned}$$

$$\text{with } \Delta(k^2, m^2, \Lambda^2) = \exp\left(-\frac{k^2}{\Lambda^2}\right) / (k^2 + m^2)$$

j_1 are the spherical Bessel function of the first kind and k runs from 0 to ∞ .

5.2.1. Form Factors and SU(3) The states of SU(3) irreducible representation for the ΛN channels have been tabulated in Table -1 . The SU(3) symmetry is broken via the physical masses of the mesons and baryons. The SU(3) irreducible representation in the BB channels form the basis for the parametrization of the short-range interaction with "hard cores". The role of the "hard cores" is taken over by the form factors. The behaviour of these form factors is controlled by Λ , the so called cutoff mass

$$\Delta^X (\vec{k}^2, m^2, \Lambda^2) = \frac{1}{\vec{k}^2 + m^2} e^{-\vec{k}^2/\Lambda^2}$$

where $X = \begin{matrix} P, & V, & S, & D \\ \downarrow & \downarrow & \downarrow & \downarrow \\ \text{pseudo scalar, vector, scalar, diffractive} \end{matrix}$

In case of ΛN , the two different form factors are used :

$$\Lambda_{27+8}^{\text{symmetric}} \quad \text{for } {}^1S_0 \quad (\Lambda N ; I = \frac{1}{2})$$

$$\Lambda_{10^*+8}^{\text{symmetric}} \quad \text{for } {}^3S_1 \quad (\Lambda N ; I = \frac{1}{2})$$

Table 1 : S-wave from factors mass used in this work
for ΛN case .

| | | | |
|-----------|-------------|--|---|
| 1S_0 | ΛN | $\{ 27 \} + \{ {}^8_{\text{symmetric}} \}$ | $\Lambda_{27+8}^{\text{symmetric}} = 820.0 \text{ MeV}$ |
| 3S_1 | ΛN | $\{ 10^* \} + \{ {}^8_{\text{antisymmetric}} \}$ | $\Lambda_{10^*+8}^{\text{an-sym}} = 1270.5 \text{ MeV}$ |

Coupling constants , F/(F+D) ratios and angles

Table 2 : Coupling constants for pseudoscalar and vector meson Λ -exchanges

| M | | $\Lambda \Lambda \Lambda$ |
|----------|-----|---------------------------|
| π | g | C S B |
| | f | C S B |
| η | g | -1.84905 |
| η' | g | 4.02537 |
| ρ | g | C S B |
| | f | C S B |
| ϕ | g | -1.53976 |
| | f | -3.09542 |
| ω | g | 2.00666 |

Table 3 : Coupling constants for scalar meson and "diffractive" $Y = o$ exchange

| M | $\Lambda \Lambda \Lambda$ |
|-------------|---------------------------|
| δ | C S B |
| S^* | -2.56308 |
| ϵ | 2.77698 |
| A_2 | C S B |
| f' | -2.05561 |
| $P \ O \ f$ | 2.70161 |

Table 4 : Coupling constant $F/(F+D)$ ratios, mixing angles, etc . The values with an asterisk have been determined in the fit to the YN data. The other parameters are theoretical input or determined by the fitted parameters and the constraint from the NN analysis.

| Mesons | | {1} | {8} | $F/(F+D)$ | angles |
|----------------|-----|---------|---------|-------------------------|---------------------------|
| Pseudoscalar | f | 0.18455 | 0.27204 | $\alpha_{PV} = 0.355^*$ | $\theta_P = -23.00^\circ$ |
| Vector | g | 2.52934 | 0.89147 | $\alpha_V^e = 1.0$ | $\theta_V = 37.50^\circ$ |
| | f | 0.97982 | 3.76255 | $\alpha_V^m = 0.275^*$ | |
| Scalar | g | 3.75548 | 1.27734 | $\alpha_s = 1.28555$ | $\theta_s = 40.895^{o*}$ |
| Diffractionive | g | 2.85507 | 0.44372 | $\alpha_D = 1.02267$ | $\psi_D = 15.50^{o*}$ |

Using the multichannel Schrodinger equation , and the form factors (table 1), coupling constant , $F/(F+D)$ ratios and mixing angles (table 2,3,4) the ΛN data have been analysed .The data for the total cross-sections have been tabulated in Table 5

Table 5: Comparison of the calculated and experimental values for the 12 Λ N data that were included in the fit. The superscript RH and M denote, respectively, the Rehovoth-Heidelberg and Maryland data. The laboratory momenta are MeV/c and the total cross sections in mb.

| P_{Λ} | $\Lambda p \rightarrow \Lambda p$ $\sigma_{\text{exp}}^{\text{RH}}$ | $\chi^2=1.0$ σ_{th} | P_{Λ} | $\Lambda p \rightarrow \Lambda p$ $\sigma_{\text{exp}}^{\text{M}}$ | $\chi^2=2.6$ σ_{th} |
|---------------|--|--------------------------------------|---------------|---|--------------------------------------|
| 145 | 180±22 | 192.8 | 135 | 209±58 | 209.2 |
| 185 | 130±17 | 138.8 | 165 | 177±38 | 163.6 |
| 210 | 118±16 | 113.2 | 195 | 153±27 | 127.9 |
| 230 | 101±12 | 96.4 | 225 | 111.0±18 | 100.4 |
| 250 | 83±9 | 82.4 | 255 | 87.0±13 | 79.2 |
| 290 | 57±9 | 60.8 | 300 | 46.0±11 | 56.6 |

5.2.2 Relativistic effects .

Recently, Koutroulos reported a phenomenological relativistic analysis of the ground and excited state binding energies of a Λ -particle in hypernuclei determined by recent (π^+, K^+) experiments by using various Λ -nucleus potentials . (13)

The motion of the Λ - particle in hypernuclei was assumed to be described by the Dirac equation :

$$(C \vec{\alpha} \cdot \vec{p} + \beta \mu C^2 + \beta U_s(r) + U_v(r)) \psi = E \psi ,$$

where the average Λ -nucleus potential is made up of an attractive component $U_s(r)$ and a repulsive component $U_v(r)$. μ is the Λ -core reduced mass. The combinations of $U_s(r)$ and $U_v(r)$ was used :

$$U_{\pm}(r) = U_s(r) \pm U_v(r)$$

The potential parameters for the different potentials were as follows :

(i) Square well potential :

$$U_+ = 30.57 \text{ MeV}, \quad U_- = 489.20 \text{ MeV}, \quad r_0 = 1.05 \text{ fm}$$

(ii) Wood-Saxon potential

$$U_t = 29.5 \text{ MeV}, \quad U_- = 416.9 \text{ MeV}, \quad r_0 = 1.153 \text{ fm}$$

$$a = 0.32 \text{ fm}$$

(where a is the diffuseness parameter)

(iii) Gaussian potential

$$U_t = 33.6 \text{ MeV}, \quad U_- = 427 \text{ MeV}, \quad r_0 = 1.27 \text{ fm}$$

(iv) Symmetrized Woods-Saxon potential

$$U_t = 29.9 \text{ MeV}, \quad U_- = 697.5 \text{ MeV},$$

$$r_0 = 1.178 \text{ fm}, \quad a = 0.31 \text{ fm}$$

(v) $U \pm(r) = -U \pm (\text{Cos } h^2(r/R))^{-1}$

$$U_t = 39.7 \text{ MeV}, \quad U_- = 201.6 \text{ MeV}, \quad r_0 = 0.98 \text{ fm}.$$

With the help of potential parameters , the binding energies and the root mean square radius of the orbits of the Λ - particle in hypernuclei was obtained . The best results were obtained for the Woods-Saxon potential , where the binding energies were in good agreement with the experimental results.

5.3 Model of Bodmer et. al.

To describe the overbinding problem of hypernuclei and Λ p scattering a consistent description has been obtained by Bodmer et al⁽⁴⁾ by incorporating strongly repulsive Wigner-type Λ NN forces. For nucleon with $A > 5$, a p-state Λ N interaction which is constant with Λ p scattering is also included. The effects of baryon structure are assumed to be of short range and the parametrised in the conventional way through repulsive cores and cutoff.

The charge symmetric central Λ N potential is taken to be

$$V_{\Lambda N} = V_{2\pi} = V_c - \left(\bar{V} - \frac{1}{4} V_{\sigma} \vec{\sigma}_{\Lambda} \cdot \vec{\sigma}_N \right) T_{\pi}^2,$$

where T_{π} is the one-pion-exchange tensor shape with cutoff ($c = 2 \text{ fm}^{-2}$) and T_{π}^2 corresponds to a TPE mechanism (fig 2) V_c is a Woods-Saxon repulsive core⁽⁶⁾ obtained from NN potential.

The spin-average and spin-dependant strengths \bar{V} , V_{σ} are given as

$$\bar{V} = \frac{1}{4} V_{\text{singlet}} + \frac{3}{4} V_{\text{triplet}}$$

$$V_{\sigma} = V_{\text{singlet}} - V_{\text{triplet}}$$

For Λ NN potential Bodmer et al⁽⁴⁾ took two types of Λ NN forces with Wigner-type potential.

(1) Dispersive Λ NN forces $V_{\Lambda NN}^D$

Two phenomenological forms are taken :

Spin independent : $V_{\Lambda NN}^D = W T_{\Lambda NN}^2 (r_1 \wedge) T_{\pi}^2 (r_2 \wedge)$

Spin dependant : $V_{\Lambda NN}^{DS} = V_{\Lambda NN}^D \left[1 + \frac{1}{6} \vec{\sigma}_{\Lambda} \cdot (\vec{\sigma}_1 + \vec{\sigma}_2) \right]$

where $V_{\Lambda NN}^D$ and $V_{\Lambda NN}^{DS}$ are equivalent for spin zero core nuclei (e.g. ${}^5_\Lambda\text{He}$, ${}^9_\Lambda\text{Be}$, D). $V_{\Lambda NN}^{DS}$ is obtained by assuming the dispersive modifications act only for triplet ΛN states (shown in fig 3)

(2) Two Pion Exchange ΛNN forces $V_{\Lambda NN}^{2\pi}$

The form is

$$V_{\Lambda NN}^{2\pi} = C_p \left[1 + (3\cos\theta - 1) T_\pi(r_1\Lambda) T_\pi(r_2\Lambda) \right] Y_\pi(r_1\Lambda) Y(r_2\Lambda),$$

where $Y(r)$ is the OPE Yukawa function and $\cos\theta = \hat{r}_1\Lambda \cdot \hat{r}_2\Lambda$ and $C_p = 1-2$ MeV. The two pion exchange ΛNN potential has been shown in figure (4) .

The following are the conclusions of the results referred above :-

- (1) The Λp scattering , the s-shell binding energies the well depth , and also ${}^9_\Lambda\text{Be}$ (representative of intermediate mass hypernuclei), can all be fitted with ΛN plus ΛNN forces consistent with meson exchange models . The ΛNN spin dependence reduces the spin dependence of the ΛN force by $\approx 1/3$, and corresponding contributes $\approx 1/3$ to the $0^+ - 1^+$ splitting of $A = 4$. ΛN tensor forces due to kaon exchange gives at most only a small reduction (≤ 4 MeV in the well depth D and (≈ 0.5 MeV) in $B_\Lambda ({}^5_\Lambda\text{He})$)
- (2) The TPE ΛNN forces $V_{\Lambda NN}^{2\pi}$) are not adequate for the overbinding of ${}^5_\Lambda\text{He}$. Therefore, for any value of C_p it is not possible to get an agreement with $B_\Lambda ({}^5_\Lambda\text{He})$.

- (3) The ${}^5_\Lambda\text{He}$ requires a strong repulsive ΛNN dispersive forces whose strength does not depend on C_p .

To have the appropriate fitting of all the s-shell B_Λ , the following constraints are considered :

The spin-independent (SI) and spin-dependant (SD) \wedge NN forces $V_{\wedge NN}^D$ and $V_{\wedge NN}^{DS}$ are considered whose solutions are given by SI(c) and SD(c) respectively with $c = 2$ or 3 fm^{-2} as the cutoff for $V_{\wedge NN}^{2\pi}$. Therefore, there are four solutions SI(c), SI(3), and SD(2), SD(3). The obtained s-shell acceptable solutions have been tabulated in Table (6).

Table 6 : Acceptable Interactions (MeV)

| | C_p | W | \bar{V} | V_σ | D | X_p |
|---|--------------|------------------|----------------|----------------|--------------|----------------|
| SI(2) | $3.5 \pm .9$ | $.02 \pm .01$ | $6.33 \pm .25$ | $.35 \pm .01$ | 25 ± 10 | $1.23 \pm .45$ |
| SI(3) | $2.3 \pm .3$ | $.016 \pm .02$ | $6.14 \pm .01$ | $.30 \pm .014$ | 29 ± 5 | $1.05 \pm .22$ |
| SD(2) | $2 \pm .7$ | $.010 \pm .004$ | $6.16 \pm .06$ | $.23 \pm .003$ | 41 ± 8.5 | $.40 \pm .43$ |
| SD(3) | $1.8 \pm .6$ | $.0195 \pm .006$ | $6.20 \pm .05$ | $.185 \pm .02$ | 31 ± 10 | $.89 \pm .50$ |
| s-shell + scattering acceptable solutions | | | | | | |
| SI(2) | 2.6-2.7 | .0115-.012 | 6.19-6.20 | | | .77-.8 |
| SI(3) | 2.0-2.6 | .014-.018 | 6.13-.15 | | | .83-1.3 |
| SI(2) | 1.3-2.4 | .0065-.012 | 6.11-6.20 | | | .25-.7 |
| SI(3) | 1.2-1.6 | .0135-.0175 | 6.16-6.20 | | | .40-.75 |

5.4. Model of Rahman Khan et . al. In the work of Gal etal.⁽⁷⁾ the following points were not taken into account :

- (a) The sensitivity of B_{Λ} to the size of the core nucleus .
- (b) The variation of the Λ -wavefunction as the core nucleus varies from ${}^4\text{He}$ to ${}^{14}\text{N}$.
- (c) the centre - of- mass motion .

In the light of these remarks Mujib etal.⁽⁹⁾ analysed the p-shell hypernuclei Λ -binding energy data by taking into account the variation of both the nuclear size and the Λ -wavefunction . Further, the centre of mass energy correction was also incorporated . The charged independent central, spin-and state -dependent two - body Λ N potential is of the form

$$U_{i\Lambda} = \left[\frac{1}{4} (U_s^1 + 3U_t^1) - \frac{1}{4} (U_s^1 - U_t^1) \vec{\sigma}_i \cdot \vec{\sigma}_{\Lambda} \right] f(r),$$

where i is for a nucleon, $f(r)$ is shape function normalised to unity, U_s^1 and U_t^1 are volume integral of the Λ N potential in the singlet and triplet state corresponding to the relative angular momentum state 1, and r is the relative Λ -nucleon distance .

$f(r)$ is of the form

- (a) Gaussian shape

$$f(r) = \exp \left(- \frac{r^2}{\alpha^2} \right) / \pi^{3/2} \alpha^3 ,$$

where α is range parameter

- (b) Skryme type

$$f(r) = \delta(\vec{r}) - \left[\frac{I_2}{3I_1} \right] \frac{1}{h^2} \left[p^2 \delta(\vec{r}) + \delta(\vec{r}) p^2 - 2\vec{p} \cdot \delta(\vec{r}) \vec{p} \right] ,$$

where $I_n = \int_0^\infty r^{2n} f(r) dr$ (for $n = 1, 2, 3$)

are the moments of $f(r)$

The binding energy (B_Λ) data as well depth (D_Λ) have been found either with the Skryme or with the Gaussian potentials. The state dependence of the ΛN effective interaction has been found to be essential feature of the analysis .

Shoeb and Khan ⁽⁹⁾ have included a three-body ΛNN force of the form :

$$W_3 (r_i , r_j , \Lambda) = t_3 (\vec{\tau}_i \cdot \vec{\tau}_j) (\vec{\sigma}_i \cdot \vec{\sigma}_j) g (r_i \Lambda) g (r_j \Lambda)$$

where t_3 is the volume integral of the force , g 's are the radial form factors .

The weakly spin-and state - dependent ΛN potential with Skryme - type gaussian , Yukawa and exponential shpes along with a zero -range three-body ΛNN force fit the B_Λ data equally well.

Ahamd etal ⁽¹⁴⁾ showed that the folding model with a density dependent effective ΛN interaction satisfactorily explain the available binding energy data of p-shell and heavier hypernuclei .

The Λ -nucleus potential has been based on the following assumptions :

—(1) The range of ΛN interaction has been assumed to be the same as the finite size of the nucleon .

Therefore , the experimental charge densities have been taken in the calculations.

(2) The second assumption is of short - range .

Therefore, $(1 - \beta \rho^{2/3})$ has been assumed to be constant .

The Λ -nucleus potential is of the form

$$V_{\Lambda}(r) = \bar{V}_0 \tilde{\rho}(r) \left[1 - \beta \rho^{2/3}(r) \right] \quad , \quad \text{--- (1)}$$

$$\text{where } \tilde{\rho}(r) = \frac{1}{(\pi d^2)^{2/3}} \int e^{-(r-r')^2/d^2} \rho(r') d\vec{r}'$$

\bar{V}_0 is the strength parameter in MeV fm³

ρ is the nuclear mass density of the target nucleus

β is a density dependent parameter

and d is the range parameter .

By assuming the proton and neutron distribution to be the same , the folded density $\tilde{\rho}_{(r)}$ has been assumed to be the same as the charge density distributions of the core nucleus .

Therefore, the modified form of (1) is

$$V_{\Lambda}(r) = \bar{V}_0 \tilde{\rho}(r) \left[1 - \beta \rho^{(2/3)}(r) \right]$$

Mian et al⁽¹⁵⁾ made an explicit treatment Λ N force by assuming its form as :

$$V_{\Lambda}(r) = \frac{\bar{V}_0}{2\pi^2} \int F(q) \exp \left[-\frac{q^2 d^2}{4} \right] q^2 j_0(qr) dq \quad ,$$

$$\text{where } F(q) = \int e^{i \vec{q} \cdot \vec{r}} \rho(r) \left[1 - \beta \rho^{2/3}(r) \right] d\vec{r} \quad ,$$

$j_0(qr)$ is the spherical Bessel function of order zero, \bar{V}_0 , d and β are the strength, range and density dependent parameter . The best fit (χ^2 - fitting) has been found with the following values :

$$\bar{V}_0 = 297.86 \text{ MeV} \cdot \text{fm}^3$$

$$\beta = 1.92 \text{ fm}^2$$

$$d = 0.72 \text{ fm}$$

$$\kappa^2 = 6.6.$$

The following conclusions can be obtained analysis :

(1) The folding model with a density dependent ΛN interaction is quite reasonable for interpreting the ground state hypernuclear binding energy data .

(2) The value of the density dependent parameter β is almost the same as the value obtained from the optical method studies of the scattering of light nuclear projectiles .

(3) The value of d indicates that long-range ΛN interaction is due to 2π -exchange .

Since from the theoretical considerations the presence of a three-body component in the Λ -nucleus interaction potential is important, therefore, Mison et al.⁽¹⁶⁾ made the analysis of Λ binding energy data of light hypernuclei with effective two body ΛN plus three body $\Lambda N N$ interaction. The expression for the total (spin and isospin average) potential for the interaction of particle described by the coordinate \vec{r} with a core nucleus of mass number A is of the form :

$$V(\vec{r}, \vec{r}_1, \vec{r}_2, \dots, \vec{r}_A) = \sum_{i=1}^A V_{\Lambda N}(\vec{r} - \vec{r}_i) + \sum_{i < j} V_{\Lambda NN}(\vec{r}; \vec{r}_i, \vec{r}_j) ,$$

Where \vec{r}_i are the nucleon coordinates and $V_{\Lambda N}$ and $V_{\Lambda NN}$ are the two-body and three-body potential, respectively .

The potential is of the form

$$V_{\Lambda A}(\mathbf{r}) = V_2(\mathbf{r}) + V_3(\mathbf{r}) ,$$

where

$$V_2(\mathbf{r}) = A \int V_{\Lambda N}(\mathbf{r} - \mathbf{r}') \rho(\mathbf{r}') d\mathbf{r}' ,$$

$$V_3(\mathbf{r}) = \frac{A(A-1)}{2} \int V_{\Lambda NN}(\mathbf{r}; \mathbf{r}_1 - \mathbf{r}_2) \rho^{(2)}(\mathbf{r}_1, \mathbf{r}_2) d\mathbf{r}_1 d\mathbf{r}_2 ,$$

where $\rho(\mathbf{r})$ and $\rho^{(2)}(\mathbf{r}_1, \mathbf{r}_2)$ are the one-body and two-body densities of the core nucleus respectively later on the two-body $V_2(\mathbf{r})$ and three body interaction $V_{\Lambda NN}$ have been taken of the Gaussian form.

It has been found that for all the Λ -hypernuclei (leaving only ${}^5_{\Lambda}\text{He}$) the binding energy data (B_{Λ}) are well explainable by the potential. The three-body force seems to account for the dependence of the effective two-body ΛN interaction .

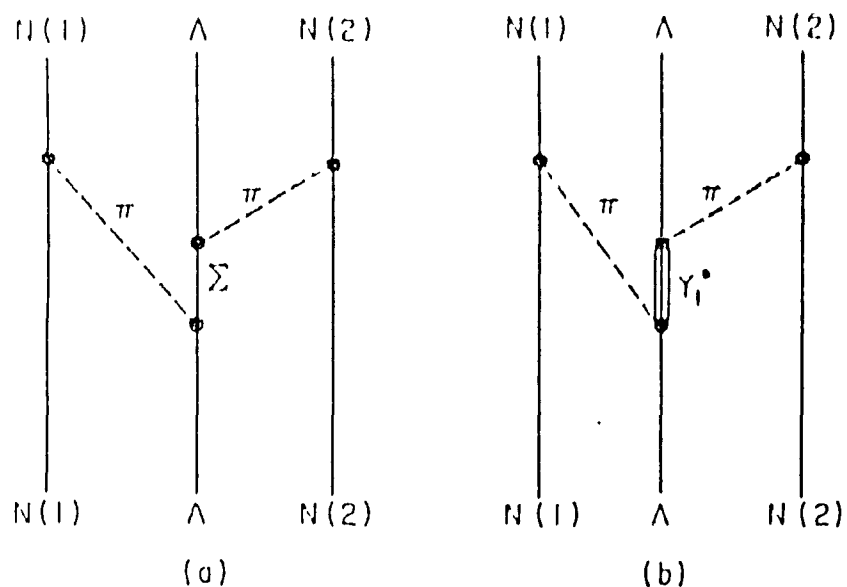


Figure 1: Contributions to the NN interaction arising from the exchange of two pions between a Λ particle and two neighbouring nucleons. The two figures illustrate two classes of graph:

- (a) Those where the intermediate hyperon is a Σ particle;
- (b) Those where intermediate Y_1^* resonance states are excited.

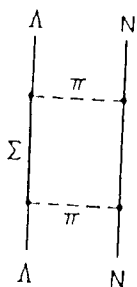


Figure 2: Representative diagram for TPE N potential

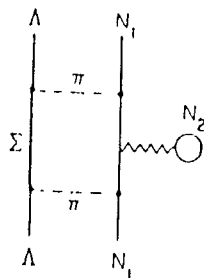


Figure 3: Representative diagram for dispersive NN potential

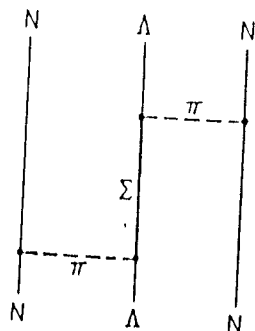


Figure 4: Diagram for TPE NN potential

References

1. R.C. Herndon and Y.C. Tang , Phys. Rev. 159, 853 (1967) ;
Phys. Rev. 165, 1093 (1968)
2. H.Bando and I. Shimodaya , Prog.Theo. Phys. 63,1812(1980)
3. S.Shinmura et.al. , Prog. Theo. Phys. 65, 1290 (1981)
4. A.R.Bodmer et.al. , Phys. Rev. C29, 684 (1985)
A.R.Bodmer and Q.N. Usmani , Nucl. Phys.A450,257c(1986)
5. M.Bedijian et.al. , Phys. Lett. 83B , 252 (1979)
6. A.Boussy , Phys. Lett. 84B, 41 (1979); Phys. Lett. 91B , 15 (1980)
7. A.Gal et.al. , Ann. Phys. (NY) 63, 53 (1971) ;
72, 445 (1972) .
8. J.M.Soper (Reference in 7)
9. F.Mujib , Nucl. Phys. 5, 541 (1979)
10. M.Shoeib and M.Z.Rahman Khan, J. Phys. G:Nucl. Phys.10,1047(1984)
11. M.Nagels et.al. , Phys. Rev. D 12, 744 (1975) ; 15, 2547 (1977) ;
20 , 1633 (1979) ;
Nucl. Phys. B147, 189 (1979)
12. R.H.Dalitz and B.Downs, Phys. Rev. 111, 967 (1958) ;
R.H.Dalitz et.al. , Nucl. Phys. B47, 109 (1972)
13. C.G.Koutroutos Phys. Rev. C40, 275 (1989) ; Nucl. Part. Phys. 17, 1069
(1991) ; Few-Body Systems supplementum -5, Springer-Verlag (N.Y.) 1992
14. I.Ahmad et.al. , Phys. Rev. C31, 1590 (1985)
15. M.Mian , Phys. Rev. C35, 1463 (1987)
16. M.Mian et.al. , IC / 88 / 48
17. P.M.M.Maessen et.al. , Phys. Rev. C 40, 5, 2226 (1989)

18. Straub et.al. (reference in 17)
19. D.J.Millener , Phys. Rev. C 386, 2700 (1988)

Chapter - 6

$\Sigma - N$, $\Xi - N$ and $\Lambda - \Lambda$ Potentials

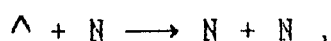
Introduction :

The previous chapter has been devoted to a detailed discussions of the various models of Λ -nucleon interaction . The data on other hypernuclei involving particles like Σ , Ξ , etc. are sparse and there are a very few analyses of these data using phenomenological potentials .

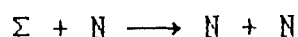
In this chapter we present a brief description of the available data and various attempts to analyse them . We shall discuss firstly Σ -Nucleon interaction followed by Ξ -Nucleon and $\Lambda - \Lambda$ interaction. We are excluding other hyperon-nucleon interaction such as the interaction of charmed hyperon nuclei with the nucleon from our discussion due to lack of data .

6.1 Σ - Nucleon Interaction

Bertini et.al⁽¹⁾ were the first who discovered Σ -hypernucleus in 1979 at CERN . The reaction was (K^-, π^-) on ${}^9\text{Be}$ at $p_K \sim 720$ MeV/c and $\theta_\pi = 0^\circ$. Approximatley , 80 MeV above the ${}^9_\Lambda\text{Be}$ peak, two peaks of width < 8 MeV were found. Those peaks were assigned due to the production of ${}^9_{\Sigma^0}\text{Be}$. It is well established that in the nuclear matter Λ decay can proceed through a weak interacting process ($\Delta S = 0$) :



whereas the Σ hyperon can decay through a strong interacting process ($\Delta S = 0$) :



Therefore, the Λ escape width is small and it was expected on these

theoretical grounds that Σ escape width should be large (as broad as $\Gamma \sim 25 \text{ MeV}$ ⁽²⁾) .

At BNL , Piekarczyk et.al.⁽³⁾ have observed the spectra of (K^-, π^+) on ${}^6\text{Li}$ and ${}^{16}\text{O}$ at $p_\pi \sim 713 \text{ MeV}/c$. In the experiment of ${}^6\text{Li} (K^-, \pi^+) {}^6_\Sigma\text{H}$ distinct peaks, at roughly 10 and 22 MeV of excitation energy were observed . The upper peak was found to be narrower , with a width of 3MeV. This was consistent with the experimental resolution . Dover et.al.⁽⁴⁾ have interpreted it in terms of $P_N \rightarrow P_\Sigma$ and $P_N \rightarrow S_\Sigma$ transitions (lower peak) and the $S_N \rightarrow S_\Sigma$ transition (upper peak) .

Maijling et.al.⁽⁵⁾ interpreted it in terms of cluster model . Since the S_N^{-1} hole strength in ${}^6\text{Li}$ is known to be dominated by a very narrow ($\Gamma \approx 100 \text{ keV}$) ${}^5\text{He} \frac{3}{2}^+$ excited state at 16.76 MeV, coupling a Σ in the 1S to this core state to form 1^+ produces a narrow state , in analogy to a similar $S_N \rightarrow S_\Lambda$ transition observed in ${}^6_\Lambda\text{Li}$.

The cluster decomposition expected to this state is

$$\left[\frac{4}{\Sigma} n \left(I = \frac{3}{2} , I_3 = -\frac{3}{2} , S = 0 \right) \otimes d \right]_{1^+}$$

The interpretation was that since $\frac{4}{\Sigma}$ has the structure $\frac{4}{\Sigma} n = (\Sigma^- p)_{S=0} (nn)_{S=0}$, Σ^- can only convert to Λ on the proton in the deuteron cluster and the width remains small.

At CERN , a very short Kaon beam line called K26 was constructed to study Σ hypernuclei near recoilless condition . On the (K^-, π^+) spectrum on ${}^{12}\text{C}$

a single excitation at $\Delta M = 278 \text{ MeV}$ was observed (which corresponds to about - 3MeV in the binding energy of Σ^-) , and was assigned as a

$$\left[(p_{3/2})_p^{-1} (p_{3/2})_{\Sigma^-} \right] 0^+ \quad \text{substitutional state,}$$

In the (K^-, π^+) spectrum on ^{16}O , two excitations at $\Delta M \approx 277$ MeV and $\Delta M \approx 284$ MeV were observed ^(6,7) They were assigned as a

$$\left[(p_{3/2})_p^{-1} (p_{3/2})_{\Sigma^-} \right] 0^+ \quad \text{and} \quad \left[(p_{1/2})_p^{-1} (p_{1/2})_{\Sigma^-} \right] 0^+ \quad \text{substitutional state,}$$

respectively .

$$\text{Since, the} \quad \left[(p_{1/2})_p^{-1} (p_{1/2})_{\Sigma^-} \right] 0^+ \quad \text{peak}$$

appears about 6 MeV above the $\left[(p_{3/2})_p^{-1} (p_{3/2})_{\Sigma^-} \right] 0^+$ peak. It was concluded that the Σ spin-orbit strength in the p-shell was about 12 MeV, or twice that of the nucleon .

Yamazaki et.al^(8,9) had performed an experiment at KEK of (K^-, π^+) on ^{12}C . This method was developed to 'tag' Σ hypernuclei, where the idea was that the Σ^- trapped in a Σ nucleus will, ultimately, convert into Λ and by detecting the Λ decay products ($p \pi^-$ or $n\pi^0$), the continuum, due to the Σ^- quasi-free production (Σ^- escaping), can be suppressed. In the π^0 -tagged spectrum a narrow excitation at $\Delta M \approx 278$ MeV was found. Other than these two excitations were suggested at $\Delta M \approx 282$ MeV and at $\Delta M \approx 287$ MeV.

The peaks at 278 MeV and at 287 MeV were assigned as due to

$$\left[(p_{3/2})_p^{-1} (p_{3/2})_{\Sigma^-} \right] 0^+, 2^+ \quad \text{and to} \quad \left[(p_{3/2})_p^{-1} (p_{1/2})_{\Sigma^-} \right] 2^+,$$

respectively.

From this spacing, they have deduced the spin-orbit splitting of $\epsilon_{\Sigma} = 5 \pm 0.5$ MeV. However, the third peak was not explained. R.S. Hyano ⁽¹⁰⁾ at KEK, performed the experiment with stopped kaons. The results have been plotted in fig (1).

The interpretation of fig (1) was that the prominent peak at $p_{\pi} = 185$ MeV/c, and tails on both sides of the peak were due to $\Sigma^+ \rightarrow \pi^+ n$, where Σ^+ was produced in the quasi-free (stopped K^-, π^-) reaction. The tails were due to Σ^+ decay in flight, while the peak was due to the Σ^+ decay at rest after slowing down in the target. The broad bump below $p_{\pi} \sim 170$ MeV/c corresponds to the production of Σ^- on ^{12}C .

To describe the Σ -nucleus strong interaction, an optical potential with imaginary part was used.

The potential was of the form

$$U_{\Sigma}(r) = \left[V_{\Sigma}^0 + i W_{\Sigma}^0 \right] \rho(r) / \rho_0,$$

where $\rho_0 (=0.17 \text{ fm}^{-3})$ is the nuclear matter density, $\rho(r)$ is of the Woods-Saxon form and the imaginary part of the potential takes care of the $\Sigma \rightarrow \Lambda$ conversion. Then the best fit to the existing Σ^- atomic X-ray data were obtained with an effective scattering length $a = 0.35 \pm i 0.19$ fm, and an empirical potential

$$V(r) = - \left[28 + i 15 \right] \text{ MeV } \frac{\rho(r)}{\rho_0}$$

This suggests a large width $\Gamma_{\Sigma} \sim -2W_{\Sigma} = 30 \text{ MeV}$.

However, the fit's results depend strongly on the choice of the radius parameter.

The potential depth for the radius parameter $r_0 = 1.27 \text{ A}^{1/3} \text{ fm}$ and

diffuseness $a = 0.73$ fm was obtained by fitting the Σ atomic X ray data⁽¹⁰⁾. The obtained value was $V_{\Sigma}^0 \approx -10$ MeV and $W_{\Sigma}^0 \approx -9$ MeV. The following conclusions were drawn on $^{12}_{\Sigma^-}$ Be in the framework of above mentioned model (10)

(i) The Σ^- - nuclear interaction is weak

(ii) The stopped K data seem to favour non-negligible $\Sigma \rightarrow \Lambda$ conversion strength.

(iii) The potential parameter derived from the analysis of Σ atomic X ray data can reproduce both the inflight and the stopped K data fairly well.

Harada et.al^(11,12) showed theoretically the possible existence of $^4_{\Sigma}$ He and $^4_{\Sigma}$ He below the Σ -emission threshold on the basis of four-body calculations with the realistic Σ N potential which simulate the Nijmegen - D potential. The $^4_{\Sigma}$ He - hypernucleus is in bound state with $J^{\pi} = 0^+$ and $T \sim 1/2$.

The results are in agreement with the experimental observation at KEK^(11,12). The binding energy and width came to be $B(^4_{\Sigma}) = 3.7 \sim 4.6$ MeV. and $\Gamma = 4.5 \sim 7.9$ MeV.

Hayano et.al⁽¹³⁾ at KEK have reported the existence of Σ -nucleus bound state formed in (K^-, π^-) reaction at rest on a 4 He target. A peak was found which was attributed to the formation of the $^4_{\Sigma}$ He ground state corresponding to $\Delta M = M(^4_{\Sigma} \text{He}) - M(^4\text{He})$.

Yamada et.al⁽¹⁴⁾, have performed the combined analysis of Σ^- atoms and $^4_{\Sigma}$ He with the use of Nijmegen OBE potentials. The conclusion was that the model D can reproduce both - the binding energy and width of $^4_{\Sigma}$ He, which F and NSC cannot. Further the conclusion was that the systematic reproduction of the Σ^- atom data cannot be obtained with the existing OBE

potentials .

Akaishi et.al.⁽¹⁵⁾ , have reported the form of nucleus - Σ potential as

$$\bar{U}_{\text{nucl-}\Sigma} = U^0 + U^T \vec{T}_c \cdot \vec{t}_\Sigma$$

The first term is repulsive at short distances .

The second is the strong Lane term which plays an essential role to make the Σ -nucleus potential bound . The Lane term is given by

$U^T = \sqrt{2} U_{h\Sigma} - t_{\Sigma^0}$. The Lane term also recovers the isospin symmetry broken due to the threshold difference . Due to this the bound $^4_\Sigma \text{He}$ becomes a $T \sim 1/2$ good isospin state .

Khin Swe Myint et.al.⁽¹⁶⁾ have reported that there exists a possibility of the formation of Σ - hypernucleus states with narrow widths in heavy nuclei like ^{208}Pb under the cooperation of the strong interaction, the Coulomb interaction and the centrifugal potential.

6.2 Ξ - Nucleon Interaction

From the emulsion technique , the binding energy (B_Ξ) data of Ξ - hypernuclei¹⁷⁻²⁰ is available which we list in table 1. It may be mentioned here that the existence of Ξ -hypernucleus is doubtful and accuracy of the data is poor and that is why much work has not been done in this and field . The B_Ξ of all the Ξ -hypernuclei (except $^{29,30}_\Xi \text{Mg}$), shows a smooth mass dependence which can be reproduced with a phenomenological single particle Ξ nucleus potential of the form

$$V_\Xi(r) = -V_{0\Xi} (1 + \exp(r-R)/a)^{-1} ,$$

where $R = r_0 A^{1/3}$ with A is the mass number , $V_{0\Xi}$ is Ξ -well depth, r_0 is

in fermi and the surfare diffuseness is 0.65 fm .

Dover and Gal⁽²¹⁾ have estimated $V_{o\equiv}$, the \equiv - well depth to be 24 ± 4 MeV for $r_o = 1.1$ fm and 21 ± 4 MeV for $r_o = 1.25$ fm.

Shoeb and Rahman Khan⁽²²⁾ have analysed the binding energy data $(B_{\equiv})_{\text{Nucl}}$ by solving the two - body \equiv -nucleus Schrodinger equation in each case . The single - particle \equiv -nucleus potential was assumed to follow the form of the realistic charge density of the relevant core nucleus , or the density of the neighbouring core nuclei for the case where the charge density of the relevant core nucleus is not known. The Coulomb part of binding energy was calculated to fair degree of accuracy by assuming the spherical uniform nuclear charge distribution . In each case the depth of the single particle potential ($V_{o\equiv}$) is calculated and found to be weaker than the \wedge -single particle well depth .

An analysis of the binding energy data of p-shell hypernuclei using two parameter \equiv N potential of gaussian and Skryme type was also made by Shoeb and Rahman Khan⁽²²⁾ . Then it was compared with the effective \wedge N potential of Boussy⁽⁷⁾ . Again the \equiv N potential turned out to be weaker than the \wedge N potential .

Following the frame work of Shoeb and Rahman Khan⁽²²⁾ Lalazissis etal⁽²³⁾ have solved the Schrodinger equation analytically for the ground state binding energies $(B_{\equiv})_{\text{nucl}}$, by assumming a \equiv - nucleus single particle potential.

The \equiv -nucleus potential was of the form

$$V_{\equiv}^{-A}(r) = - \frac{D}{\cosh^2(r/R)} , \quad 0 \leq r < \infty$$

where $D > 0$ is the potential depth , $R = r_0 A^{1/3}$

with $r_0 = \frac{1}{\pi} \left[\frac{3 |\bar{V}_{\equiv N}|}{D} \right]^{1/3}$ and A is

the mass number of the core nucleus . The nuclear part of the ground state binding energy $(B_{\equiv})_{\text{nucl}}$ has been expressed in the form .

$$(B_{\equiv})_{\text{nucl}} = D \left[\left(1 + \frac{\hbar^2}{8\mu D r_0^2} A^{-2/3} \right)^{1/2} - 3 \left(\frac{\hbar^2}{8\mu D r_0^2} \right)^{1/2} A^{-1/3} \right]^2$$

where

$$\mu = \mu_{\equiv} A = \frac{m_{\equiv}}{\left[1 + \left(\frac{m_{\equiv}}{m_N} \right) \frac{1}{A} \right]}$$

$$\lambda = \frac{1}{4} \left[\left(1 + \frac{8\mu D R^2}{\hbar^2} \right)^{1/2} - 1 \right]$$

The kinetic energy of $(B_{\equiv})_{\text{nucl}}$

$$\langle T_{\equiv} \rangle = \frac{\hbar^2}{2\mu R^2} \times \frac{3(4\lambda - 2)(4\lambda + \frac{2}{3})}{4(4\lambda + 1)}$$

The potential energy of $(B_{\equiv})_{\text{nucleus}}$

$$\langle V_{\equiv} \rangle = -D + \frac{3D}{(4\lambda + 1)}$$

In the calculations of the Coulomb part of the \equiv -Nucleus interaction

$$E_c = - \frac{6e^2}{5} \cdot \frac{Z_*}{c} \left[1 - \frac{7\pi^2}{6(4\ln 3)^2} \left(\frac{t}{c} \right)^2 \right]$$

(where Z_c is the atomic number of the core nucleus , t is the skin thickness , c is the half density radius) , the diffuseness of the nuclear surface was taken into account .

However , this improvement in calculation of E_c over that of Shoeb and Rahman Khan⁽⁶⁾ does not make any quantitative changes in the conclusion The⁽¹⁷⁾ results of the $(B_{\equiv})_{\text{nucl}}$ has been tabulated .

Notice from Table 2 that the values of these quantities viz . E_c , $(B_{\equiv})_{\text{nucl}}$, $\langle V_{\equiv} \rangle$ and $\langle T_{\equiv} \rangle$ differ considerably in most of the cases . Therefore , there is a need of more reliable method for their determination and for these more experimental work is required .

Table 1 : Binding energy of the different \equiv -hypernuclei

| Hypernuclei | | Binding energy |
|---------------------|----------------|----------------------|
| He | : B_{\equiv} | = 5.9 ± 1.2 MeV |
| ¹¹ B | : B_{\equiv} | = 9.2 ± 2.2 MeV |
| ¹³ C | : B_{\equiv} | = 18.1 ± 3.2 MeV |
| ¹⁵ C | : B_{\equiv} | = 16.0 ± 4.7 MeV |
| ¹⁷ O | : B_{\equiv} | = 16.0 ± 5.5 MeV |
| ²⁸ Al | : B_{\equiv} | = 23.2 ± 6.8 MeV |
| ^{29,30} Mg | : B_{\equiv} | = 2.4 ± 6.3 MeV |

Table 2 : The values of the Coulomb E_c the nuclear part of the binding energy $(B_{\Xi^-})_{\text{nucl}}$, the total binding energy B_{Ξ^-} , the nuclear part of the potential energy $\langle V_{\Xi^-} \rangle$, the kinetic energy $\langle T_{\Xi^-} \rangle$ and of the RMS radius for a number of Ξ^- hypernuclei . The (GS) energies are in MeV and the RMS radii in femtometres (fermi) .

| A_c | E_c | $(B_{\Xi^-})_{\text{nucl}}$ | B_{Ξ^-} | $\langle V_{\Xi^-} \rangle$ | $\langle T_{\Xi^-} \rangle$ | $\langle r_{\Xi^-}^2 \rangle^{1/2}$ |
|--|-------|-----------------------------|-------------|-----------------------------|-----------------------------|-------------------------------------|
| Case 1 : $D= 55.2$ MeV, $r_0 = 0.59$ fm | | | | | | |
| 8 | 1.7 | 5.5 | 7.2 | -16.9 | 11.4 | 2.061 |
| 12 | 3.4 | 9.4 | 12.8 | -22.4 | 12.9 | 1.799 |
| 16 | 3.7 | 12.3 | 16.0 | -25.6 | 13.3 | 1.716 |
| 20 | 4.0 | 14.5 | 18.5 | -27.9 | 13.4 | 1.682 |
| 24 | 4.3 | 16.3 | 20.6 | -29.6 | 13.3 | 1.667 |
| 28 | 4.7 | 17.8 | 22.5 | -31.0 | 13.2 | 1.662 |
| 32 | 5.2 | 19.0 | 24.2 | -32.1 | 13.1 | 1.661 |
| 40 | 6.9 | 21.0 | 27.9 | -33.8 | 12.8 | 1.668 |
| Case 2 : $D = 40.7$ MeV , $r_0 = 0.754$ fm | | | | | | |
| | | 5.7 | 7.4 | -14.9 | 9.2 | 2.225 |
| | | 8.8 | 12.2 | -18.6 | 9.8 | 2.033 |
| | | 10.9 | 14.6 | -20.8 | 9.9 | 1.973 |
| | | 12.6 | 16.6 | -22.3 | 9.8 | 1.953 |
| | | 13.8 | 18.1 | -23.5 | 9.7 | 1.947 |
| | | 14.9 | 19.6 | -24.4 | 9.5 | 1.949 |
| | | 15.8 | 21.0 | -25.1 | 9.3 | 1.955 |

| | | | | |
|--|------|-------|-----|-------|
| 17.2 | 24.1 | -26.3 | 9.1 | 1.972 |
| Case 3 : D = 30 MeV , $r_o = 0.986$ fm | | | | |
| 5.8 | 7.5 | -13.0 | 7.2 | 2.458 |
| 8.1 | 11.5 | -15.4 | 7.3 | 2.327 |
| 9.7 | 13.4 | -16.9 | 7.2 | 2.294 |
| 10.9 | 14.9 | -17.9 | 7.0 | 2.289 |
| 11.8 | 16.1 | -18.7 | 6.9 | 2.296 |
| 12.6 | 17.3 | -19.3 | 6.7 | 2.308 |
| 13.2 | 18.4 | -19.8 | 6.6 | 2.322 |
| 14.2 | 21.1 | -20.6 | 6.3 | 2.352 |

6.3 Λ - Λ Interaction

Danysz et.al.⁽²⁴⁾ were the first to observe the $^{10}_{\Lambda\Lambda}$ Be and later Prowse et.al.⁽²⁵⁾ reported the existence $^6_{\Lambda\Lambda}$ He. Recently at KEK , Imai et.al.⁽²⁶⁾ have reported a third candidate as $^{13}_{\Lambda\Lambda}$ B .

The separation energy $B_{\Lambda\Lambda}$ of two Λ s' from the core nucleus is given by 10.92 ± 0.6 MeV for $^6_{\Lambda\Lambda}$ He and $17.7 \cong 0.08$ MeV for $^{10}_{\Lambda\Lambda}$ Be. It can be given in the form as

$$\Delta B_{\Lambda\Lambda} = B_{\Lambda\Lambda} - 2B_{\Lambda} = \begin{cases} 4.6 \pm 0.6 \text{ MeV } (^6_{\Lambda\Lambda} \text{ He }) \\ 4.29 \pm 0.1 \text{ MeV } (^{10}_{\Lambda\Lambda} \text{ Be }) \end{cases}$$

where B_{Λ} is the separation energy of a single Λ particle .

Bodmer et.al.⁽²⁷⁾ and Wang et.al.⁽²⁸⁾ have independently , obtained a linear relationship between $^6_{\Lambda\Lambda}$ He and $^{10}_{\Lambda\Lambda}$ Be binding energies based on the cluster calculations. The relationship

$$B_{\Lambda} ({}^6_{\Lambda}\text{He}) \approx -\alpha + \beta_{\Lambda} ({}^{10}_{\Lambda}\text{Be})$$

with the different sets of α and β .

However , when the data of ${}^6_{\Lambda}\text{He}$ was fitted , the ${}^{10}_{\Lambda}\text{Be}$ was found to be overbound by several MeV , while when ${}^{10}_{\Lambda}\text{Be}$ was fitted the ${}^6_{\Lambda}\text{He}$ was underbound by several MeV . We are mentioning the work of Bodmer et al.⁽²⁷⁾ in a little detail .

A 3-body $\alpha+2\Lambda$ model was used with $\alpha-\Lambda$ potential obtained from effective ΛN and ΛNN interaction for ${}^6_{\Lambda}\text{He}$ and a 4-body $2\alpha+2\Lambda$ model for ${}^{10}_{\Lambda}\text{Be}$. For $V_{\Lambda\Lambda}$ a variety of shapes and ranges were used both for the repulsive core V_c and for the attractive part V_A .

For the $\alpha+2\Lambda$ model of ${}^6_{\Lambda}\text{He}$ the Hamiltonian was

$$H = T_{\alpha} (1) + \sum_{i=2}^3 \left[T_{\Lambda} (i) + V_{\alpha\Lambda} (r_{ij}) \right] + V_{\Lambda\Lambda} (r_{23})$$

and for the $2\alpha + 2\Lambda$ model of ${}^{10}_{\Lambda}\text{Be}$ this was

$$H = \sum_{i=1}^2 \left[T_{\alpha} (i) + T_{\Lambda} (i+2) \right] + V_{\alpha\alpha} (r_{12}) + \sum_{\substack{i < j \\ i=1,2 \\ j=3,4}} V_{\alpha\Lambda} (r_{ij}) \\ + \sum_{i=3}^4 V_{\alpha\alpha\Lambda} (r_{1i}, r_{2i}) + V_{\Lambda\Lambda} (r_{34}) \quad ,$$

where T_{α} and T_{Λ} are the α and Λ kinetic energy operators , respectively. The potential $V_{\alpha\alpha}$, $V_{\alpha\Lambda}$ and $V_{\alpha\alpha\Lambda}$ were the inputs in the calculations⁽²⁹⁾. With a reasonable $V_{\Lambda\Lambda}$ (repulsive core V_c comparable to that for $V_{\Lambda N}$, reasonable ranges for $V_{\Lambda\Lambda}$) the obtained value of $a_{\Lambda} \approx -(2.5-3.5) \text{ fm } r_0^{\Lambda}$

$\approx 2.6 - 3.1 \text{ fm}$.

It was conjectured that the Λ interaction is strongly attractive , comparable to or even more attractive than the Λ N force, and is not far from giving a bound Λ state ⁽³⁰⁾ However , meson -exchange model obtained by the Nijmegen group predicted $a_{\Lambda} \approx - 0.26 \text{ fm}$ ⁽³¹⁾.

By calculating B_{Λ} for ${}^6_{\Lambda}\text{He}$ and ${}^{10}_{\Lambda}\text{Be}$ with a large number of different V_{Λ} having different shapes, ranges and strengths, Bodmer et.al. ⁽³⁷⁾ obtained a linear relationship between the calculated values.

The relationship is given as

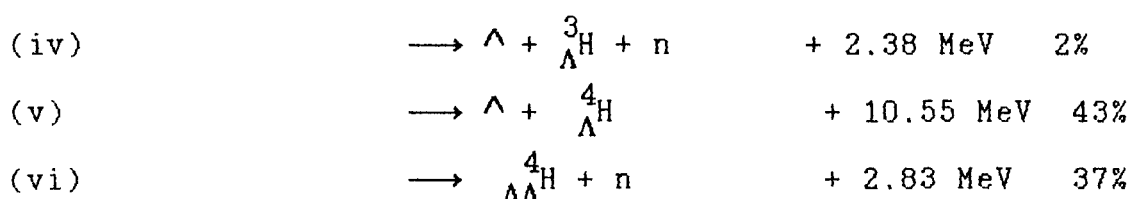
$$B_{\Lambda} ({}^6_{\Lambda}\text{He}) \approx - 5.0 + 0.83 B_{\Lambda} ({}^{10}_{\Lambda}\text{Be}) .$$

However , for the experimental value of $B_{\Lambda} ({}^{10}_{\Lambda}\text{Be})$ this relation predicts significantly too small values of $B_{\Lambda} ({}^6_{\Lambda}\text{He}) = 9.7 \text{ MeV}$, whereas the experimental value is $10.9 \pm 0.6 \text{ MeV}$.

May et al ⁽³²⁾ have suggested that when a stopped K^- is targeted on ${}^4\text{He}$ then due to the large branching ratio ($\sim 37\%$) there exist a greater probability of a double Λ hypernucleus formation (${}^4_{\Lambda\Lambda}\text{H}$) and it can be observed iff a neutron is detected in such type of reaction .

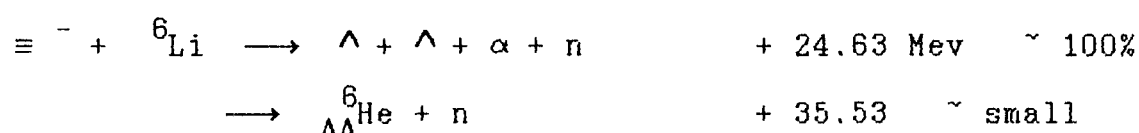
Akaishi et.al ⁽³³⁾ and Kumagai et.al ⁽³⁴⁾ have independently , calculated the branching ratio of double Λ -hypernucleus formation from a $\Xi^- + {}^4\text{He}$ atom where the possible proposed processes are

- (1) $\Xi^- + {}^4\text{He} \longrightarrow \Lambda + \Lambda + p + n + n + 0.03 \text{ MeV}$ Negligible
- (ii) $\longrightarrow \Lambda + \Lambda + d + n + 2.25 \text{ MeV}$ "
- (iii) $\longrightarrow \Lambda + \Lambda + t + 8.51 \text{ MeV}$ 18%



The small Q values from two-body processes increases the probability of double hypernucleus very much .

In the case of ${}^6\text{Li}$, the Q values are large as compared with those of the ${}^4\text{He}$ case e.g.



The large Q value suggests a four body decay .

Baltz et.al.⁽³⁵⁾ have predicted the forward cross-section of the order of 2-10 nb/st for the excitation of high spin 3^- and 4^+ states and the ${}^{16}\text{O} (K^-, K^+)$ reaction at 1.1 GeV /c .

Yamamoto et.al.^(36,37) derived the G-matrix interaction for $\Lambda\Lambda$ using the Nijmegen model D ⁽⁸⁾ , F ⁽⁸⁾ and soft core version ⁽³⁸⁾ (NSC) and calculated $B_{\Lambda\Lambda}$ ($\Delta B_{\Lambda\Lambda}$) values for ${}^{10}_{\Lambda\Lambda}\text{Be}$, ${}^{13}_{\Lambda\Lambda}\text{B}$ and other double $\Lambda\Lambda$ hypernuclei . They have taken the wave function contribution mainly from core + $\Lambda + \Lambda$ + three body and partially from $\alpha + x + \Lambda + \Lambda$ four body contribution, where $x = n, d, t, \alpha$.

The D2 model was used with hard core radii $r_0 = 0.532 \text{ fm}$, the value of $B_{\Lambda\Lambda}$ (three body binding energy of nuclear core and two Λ particle) , $\Delta B_{\Lambda\Lambda}$ (interaction energy given by $B_{\Lambda\Lambda} - 2B_{\Lambda}$ (in MeV) , \sqrt{r}^2 (the r.m.s. ratio of $\Lambda - \Lambda$ distances in fm) and $\sqrt{R^2}$ (the r.m.s. radii of $\Lambda\Lambda$ -core distance in fm) were obtained . The results for ${}^{13}_{\Lambda\Lambda}\text{B}$ and ${}^{10}_{\Lambda\Lambda}\text{Be}$ are

quite apporeciabls . However, more consistent work is required in this regard .

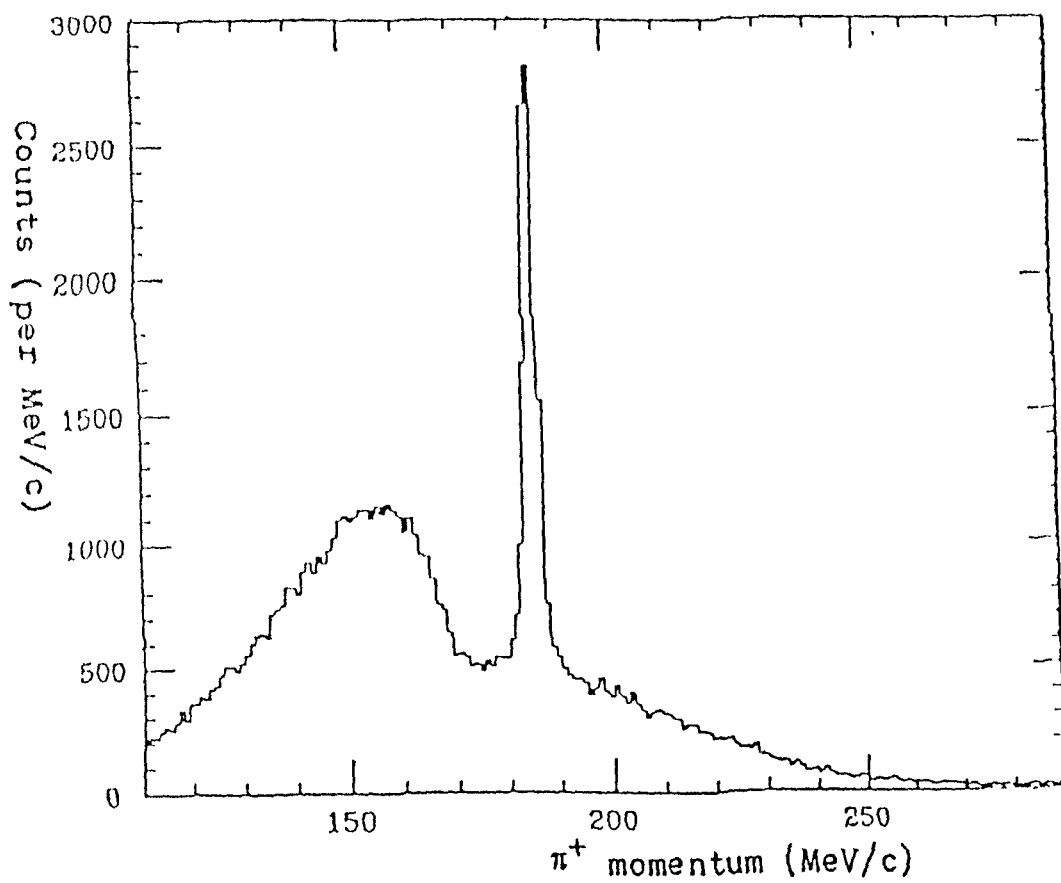


Figure 1: Inclusive (Stopped K^- , π^+) data on ^{12}C .

References

1. R. Bertini et.al ., Phys . Lett. 90B , 375 (1980)
2. A. Gal et.al ., Phys . Rev. Lett 44, 379 (1980)
3. H. Piekarz et.al., Phys. Lett. 110B , 428 (1982)
4. C.B.Dover et.al., Phys. Lett 110B , 433 (1982)
5. L.Majling et.al. , Phys. Lett. 92B , 256 (1980)
6. R. Bertini et.al., Phys. Lett. 136B , 29 (1984)
7. R. Bertini et.al., Phys. Lett. 158B , 19 (1985)
8. T.Yamaziki et.al ., Phys. Rev.Lett. 54, 102 (1985)
9. T.Yamaziki et.al. . , Phys. Nucl.Phys. A450 , 1c (1986)
10. R.S.Hayano , Nucl. Phys. A478 , 113c (1988)
11. T.Harada , Few Body System , Supplementum -5, Springer Verlag
New York (1992)
12. T.Harada et.al. , Nucl.Phys. A507 , 715 (1991)
13. R.S.Hayano et.al. , Phys.Lett. B231 , 255 (1989)
14. T.Yamada same as ref 11.
15. Y.Akashi , same as ref 11.
16. Khin Swe Myint et al. , Prog. Theor. Phys. 82 112(1989).
17. D.H.Wilkinson et al ., Phys.Rev.Lett 3 , 397 (1959)
18. A.Bechdolff et.al. , Phys. Lett. 26B , 174 (1959)
19. J.Catala et.al. . , "Proceedings of the Int.Conf. on
Hypernuclear Phys ," Vol 2, p758 , Argonne , Illinois (1969)
20. A.S.Mondal et.al., Nuovo Cim. 54A , 333 (1979)
21. C.B.Dover and A.Gal, Ann.of Phys. 146, 309 (1983)
22. M.Shueb and M.Z.Rahman Khan , J.Phys. Soc. Japan 55, 3008 (1986)

23. G.A.Lalazissis et.al., J.Phys. G : Nucl. Part. Phys. 15, 303 (1989)
24. M.Danysz et.al., Phys. Rev. Lett. 11 , 29 (1963)
25. D.J.Prowse et.al ., Phys. Rev. Lett 17, 782 (1966)
26. K.Imai et.al . , Nucl. Phys. A527 , 181c (1991)
27. A.R.Bodmer et.al . , Nucl. Phys. A468 , 653 (1987)
28. Wang et.al . , Prog. Theor. Phys., 76 , 865 (1986)
29. A.R.Brodmer et.al . , Nucl. Phys. A422, 510 (1984)
30. A.R.Bodmer and Q.N.Usmani . , Nucl. Phys. A450 , 257c (1986)
31. M.M.Nagels et.al . , Phys. Rev. D15 , 2547 (1977) ;
Phys. Rev. D20 , 1633 (1979)
32. M.May et.al. , Nuovo Cimento 102A , 401 (1989)
33. Y.Akaishi et.al. Few Body Systems Supplemented 5 355-364 (1992)
34. I.Kumagai et.al. Soryusiron-Kenkyn, 82, 42 (1990)
- 35.Baltz et.al. Phys. Lett. 123B : 9(1983)
36. Y.Yamamoto et.al. Prog. Theor. Phys. 73 (1985), 805; 83(1990),254
37. Y.Yamamoto et.al. Few Body System , Supp 5 , 365-371 (1992)
38. P.M.M.Maessen et.al. Phys. Rev. C40 (1989), 2226

Chapter - 7

Summary and Conclusions

In this dissertation we have presented an up-dated review of the baryon-baryon potentials for nucleons and hyperons . After a brief introduction to the subject in chapter one ,a discussion of the nucleon-nucleon potential is given in chapter 2 and 3. The discussion is extended to include the strange particles and a description of Λ -N, Σ -N, Ξ -N and Λ - Λ potentials is given in chapters 4,5 and 6. Main results are summarized below.

(1) In the case of nucleon-nucleon interactions various phenomenological potentials (viz Hamada-Johnston, Reid Hard and Soft Core, Paris and Argonne) and field theoretic potential (viz full Bonn potential) are discussed . The complete data on the low energy N-N scattering parameters are not described in the most of these models (Table-2 and 6, Chapter 2). Presently Paris and Bonn potentials are widely used in the analysis of available data on nucleon-nucleon processes . The long range NN interaction is known to be dominated by one-pion-exchange, which also gives a strong spin-spin and tensor force. The spin-orbit force comes from the exchange of vector bosons i.e. the iso-singlet ω , and isovector ρ -mesons the strong repulsive core being due to ω -exchange . Bonn group has considered multipion exchanges and exchange of heavy mesons of various kinds. They have shown how multiple exchanges of mesons can lead to interactions, which have reasonable strengths and ranges . The intermediate isobar states do give , at least, a fraction of the strength in the scalar, isoscalar channel previously occupied by the σ -meson. The

2π -exchange model is useful in describing the intermediate range of the nuclear force and it takes, nuclear resonances (isobars) and direct $\pi\pi$ interaction, into account.⁽¹⁾

The "full Bonn potential" gives a quantitative description of the deuteron data, NN scattering phase-shifts (Table -2, Figure-8, Chapter 3,).

The tensor force turns out to be weak in "full Bonn model" which is seen in a low percentage D state of the deuteron, whereas the quadrupole moment and the asymptotic D/S state of the deuteron are large and in very good agreement with the experimental results.

The Paris group has shown that dispersion relations may provide a mechanism to evaluate the two-pion exchange term from observables in the $N + \bar{N} \rightarrow \pi + \pi$ and π -N channels.

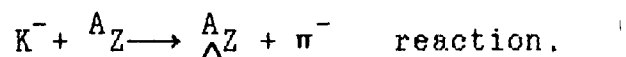
The deuteron properties and NN scattering phase shifts are obtained (Table 2, fig 1, Chapter 2). The results are in good agreement with the experimental values.⁽²⁾

However, "the full Bonn model" is found to be more reasonable.

The problem of describing the NN interaction in the core region is still persisting. Actually, nucleons are composite systems with a rich resonance structure, which are attributed to constituent quarks interacting by gluon exchange. Ideally, a model of the NN interaction would start with a field theoretic description of interactions. However, the quarks (flavour and colour), the fundamental building blocks of the theory, have not, yet, been seen experimentally despite repeated searches. No satisfactory theory has yet been developed.

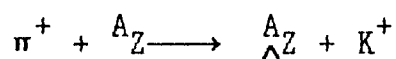
Our understanding is only based on certain mathematical structure of quarks and their interaction. Therefore at first there is need to understand the q-q interaction theoretically while one needs more accurate experimental data on N-N systems in order to get a clear picture of the core region from a microscopic theory based on quarks and gluons. (3)

(ii) The history of Λ hypernuclei can be divided into three periods (4). The "early period" opened with the discovery of the first hypernucleus in a nuclear emulsion in 1952, and included the studies of Λ hypernuclei carried out in emulsions in the decade following this discovery. The "middle ages" period contains the work done in the 60's 70's and early 80's with the (K^-, π^-) reaction. (5) Kaons with a momentum ~ 550 MeV/c transfers a little momentum to the nucleon in the



However, since both K^- and π^- are strongly absorbed in the nucleus, this reaction populates specially the less strongly bound levels. The "modern era" would be signaled by the introduction of the associated production reaction (π^+, K^+) and the electromagnetic production to produce Λ hypernuclei. This era will also benefit by the start of Kaon factories which will produce intense kaon beams.

The associated production is



This reaction has the advantage that the K^+ is not much distorted in the nucleus and, therefore, the reaction offers more possibilities to populate deeply bound states of the nucleus.

The cross-section for the elementary reaction

$$\pi^+ + n \longrightarrow \Lambda + K^+ \quad \text{peaks near 1050 MeV/c}$$

The proposed electromagnetic productions of hypernuclei (γ, K^+) and (e, e', K^+) reactions is useful as an attractive alternative reaction for the study of hypernuclei at the new generation of electron accelerators. It excites both the natural and un-natural parity, low and high spin hypernuclear states with the comparable strengths.

There is no strong reaction through which a Λ bound in the nucleus could decay. Energetically, the $\Lambda N \longrightarrow N N$ reaction is possible due to the reason that $\Delta S = 1$, it proceeds via the weak interaction. For Λ , both the $\Lambda \longrightarrow N \pi$ and the $\Lambda N \longrightarrow N N$ decay modes involve weak interactions and nearly of the comparable strength. A study of decay can provide useful information about Λ -N forces.

The binding energy of the nuclei in the s-shell and p-shell have been compared with predictions of the various phenomenological potentials. Following this procedure Gal et.al.⁽⁶⁾, Nagels et.al.⁽⁷⁾, Bodmer et al.⁽⁸⁾ and Rahman Khan et.al.⁽⁹⁾ have given Λ -Nucleon potentials.

Gal et.al.⁽⁶⁾ made a direct analysis of p-shell hypernuclei within the shell model framework using intermediate coupled wave functions of Soper.⁽¹⁰⁾ In these calculations a uniform single-particle shell model wave function for the Λ particle and nucleons in different hypernuclei is considered. Later they included the non-central two-body Λ -N, central and non-central three-body Λ NN is forces.

The meson theory of Λ N interaction is given by Gal et.al. The following exchanges are considered

(a) Scalar meson exchange : σ exchange

the NN channel and recently they have constructed a potential model (soft core) in the YN channels.

Again in this case, the YN version of the model is obtained by extension of the NN model through the application of SU (3) .

The potentials are due to the dominant parts of the π , η , η' , ϕ , ρ , ω , δ , ϵ , and S^* Regge trajectories. In addition to these, the $J=0$ contributions from the tensor f , f' , A_2 and Pomeron trajectories are included in the potentials. The calculations are nearly the same as in hard core model. The different potentials models for YN scattering with their χ^2/data have been tabulated below

| Model | χ^2 / data |
|-----------|------------------------|
| A | 0.71 |
| B | 0.68 |
| C | 0.62 |
| D | 0.65 |
| E | 0.61 |
| F | 0.89 |
| Soft core | 0.58 |

It has been found that various ΛN potential when applied to light hypernuclei like ${}^5_{\Lambda}\text{He}$ give too much binding as compared with the experimental results.

Bodmer et.al.⁽⁸⁾ have considered this overbinding problem of hypernuclei and Λp scattering by incorporating Wigner-type ΛNN forces with a p-state ΛN interaction. A reasonable good fit to B_{Λ} data have been obtained.

Shoeb et.al.⁽⁹⁾ have considered a weakly spin-and state- dependent Λ N potential with Skyrme type gaussian ,Yukawa and experimental shapes along with zero-range three body Λ NN force. Fits were performed for the B_Λ data of p-shell hypernuclei .Also a skyrme-type Λ N potential along with a zero-range three-body force fits, the B_Λ of p-shell hypernuclei and also reproduces B_Λ of ${}^5_\Lambda\text{He}$ and gives a value to the binding energy in infinite nuclear matter consistent with empirical estimate .

Following conclusions can be drawn on the Λ -N interaction based on experimental and phenomenological descriptions :

(1) Λ N interaction is stronger in the singlet state than the triplet state. Λ particle has isospin 0, therefore , the exchange of isovector bosons e.g. π, ρ , etc. mesons are not allowed . The lowest order contribution comes from 2π and K exchange .

(2) The Λ N interaction is dominated by the central potential and that the contributions of spin-spin and tensor force are very less in the long range Λ N interaction.

(3) Λ N interaction has a hard core comparable to NN interaction . Because the long one-pion -exchange is absent from the Λ N interaction and Λ N - Σ N coupling is strong, three-body Λ NN forces are predicted to play a crucial role in hypernuclei.

(4) The spin-orbit interaction is weaker in Λ -N interaction than the nucleon-nucleon interaction .

(5) Tensor force is also weak in the Λ -N interaction

(6) The spin - spin interaction is weaker than the N-N interaction .

(7) Pauli blocking is very effective in reducing the Λ mesonic width, which is considerably reduced in heavy hypernuclei with respect to free Λ width. Still the direct measurements of decay rates are difficult, therefore, there is a need of more intense K π beams and improved experimental techniques.

(iii) Σp interaction at low momenta has been studied similar to Λp system. The existing data on Σp is more scarce than for Λp interaction due to its short lifetime and more ionisation losses in bubble chamber.

The average potential, Σ -particle feels in the nucleus is slightly shallower than the potential for the Λ particle. The estimation of $V_{\Sigma} \approx 24 \pm 4$ Mev. From the analysis of Σ -hypernuclei, a reasonable fit to all data give preference to large spin-orbit coupling, larger than the nucleon one and a weak residual interaction comparable to that of Λ particle. A recent measurement suggesting the presence of a Σ -bound state resulting from the (K^-, π^-) reaction on ${}^4\text{He}$ has been reported. This is a great break through in the field of Σ -hypernucleus because till 80's the existence of stability of Σ -hypernuclei has been a subject of intense investigation and still a challenging problem.

The Pauli blocking effect has been found to play almost non-significant role in reducing the Σ widths. Narrow width in Σ hypernuclei has been attributed due to the polarization of the medium by spin-isospin interaction responsible for the $\Sigma N \rightarrow \Lambda N$ transition. In very light hypernuclei a strong ΣN repulsion at short distances is also a reason for narrow ΣN width. (11)

Central potential V_{NB} for $B = N, \Lambda, \Sigma$ are determined from the

analysis of nuclear and hypernuclear data. The results are tabulated below. The measured values of the spin-orbit potentials are also mentioned .

Table

| System | Nucleus + | | |
|-------------------------------------|-----------|-----------|----------|
| | N | Λ | Σ |
| Central potential V_c (in MeV) | 50 | 30 | 25 |
| Spin-orbit | 1 | 0 | 0.8-1.8 |

(iv) The properties of the Ξ -nucleus interaction have been studied from the OBE approach ⁽¹²⁾ By comparing the Ξ -nucleus single particle potential with the experimental values of Ξ -binding energy , the value of

$$V_{o\Xi} = 24 \pm 4 \text{ MeV for } r_o = 1.1 \text{ fm}$$

$$(\Xi \text{-well depth}) \quad 21 \pm 4 \text{ MeV for } r_o = 1.25 \text{ fm.}$$

In model D ⁽⁷⁾ of Nagels et.al. the value of $V_{o\Xi} = 23 \text{ MeV}$ with the predictions that the spin-orbit and isospin - dependent potential for Ξ would be very small. From model F ⁽⁶⁾ with repulsive Ξ potential the value of $V_{o\Xi} = -28 \text{ MeV}$.

Still , the existence of long lived Ξ -state in nuclei is yet to be established. The prediction of the long lived Ξ -states has been made on the basis of narrow Σ - states.

(v) For the case of Λ hypernuclei , the Λ well depth D_Λ can be

understood by considering Λ N force which are consistent with free-space scattering and a repulsive Λ NN interaction.

The Λ N and Λ Λ potentials are parametrized in terms of short - range repulsive core of Woods-Saxon form and an attractive piece with a range characteristic of two pion exchange.

The Λ interaction obtained from the $^{10}_{\Lambda}$ Be is strongly attractive, corresponding to a 1S_0 scattering length in the range $-5 \leq a_{\Lambda\Lambda} \leq -2\text{fm}$. This is comparable to the 1S_0 Λ N and NN interaction for which $a_{\Lambda N} \approx -3\text{fm}$ and NN $a_{NN} \approx -4\text{fm}$. However, the attraction is not sufficient to form a 1S_0 Λ bound state. (8)

In conclusion we would like to say that a study of the various aspects of hypernuclear data like binding energy of hypernuclei, weak and electromagnetic decays and other reaction data on hypernuclei with pion and kaon beams will provide useful information on hyperon nucleon interactions. These are supplemented by the data on Λ p scattering.

These data on hypernuclei and Λ p scattering taken together can help to determine various parameters used in the theoretical formulation of hyperon-nucleon potentials.

References

1. R. Machleidt et.al. , Phys. Reports 149 , 1 (1987)
2. M. Lacombe et. al. , Phys. Rev. C21, 861 (1980)
3. R.E.Chrien , Nucl. Phys. A478 , 705c (1988)
4. M.Donysz and J.Pniewski , Philos Mag. 44, 348 (1953)
5. V.L.Telegdi , Sci . Am . 206, 50 (1962)
6. A.Gal et.al. , Ann. Phys. (N.Y.) 63 , 53 (1971) ;
72, 445 (1972)
7. M.M.Nagels et.al. , Phys. Rev. D15, 2547 (1977) ;
D20 , 1633 (1979)
8. A.R.Bodmer et.al., Phys.Rev.C29, 684(1984)
- 9.M.Z.Rahman Khan and M.Shueb ,J.Phys.Soc. of Japan
55, 3008(1986)
- 10.J.Soper ,Phil.Mag. 2, 1219(1957)
- 11.T.Yamazaki et.al.,Phys. Rev.Letts.54 ,102(1985)
- 12.E.Oset et.al.,Phys.Letts. 188,Vol.2,79(1990)